Characterisation of Phytoalexin Accumulation in Maize Inoculated with *Cercospora zeina*, the causal organism of Grey Leaf Spot Disease

Jean Felistas Ntuli

Thesis submitted in fulfilment of the requirements for the Degree of

Master of Science

Department of Molecular and Cell Biology

Faculty of Science

University of Cape Town

February 2016

Supervisors: Dr Shane Murray and Dr Robert Ingle

PLAGIARISM DECLARATION

I **Jean Ntuli** know the meaning of plagiarism and declare that all of the work in this thesis, save for that which is properly acknowledged, is my own. This thesis is my own work and has not been previously submitted in its entirety or part thereof at any university for another degree.

Signed: 

Date: 12/02/2016

ACKNOWLEDGEMENTS

I would like to thank the Equity Development Programme (EDP) in the department of Molecular and Cell Biology and the National Research Fund (NRF) Thutuka for providing financial support that made this research project possible.

I thank my supervisors Dr Shane Murray and Dr Robert Ingle for making designing and facilitating this research project and for their guidance, technical advice and patience. Shane, you nurtured me and I always felt at home with you.

Acknowledgements to the Crampton Lab at the University of Pretoria for growing and inoculating the maize plants. Acknowledgements to the Centre for Proteomic and Genomic research (CPGR) for use of some of their facilities i.e. bio-analyser and qPCR light cycler. I also acknowledge the central analytical facility (CAF) at Stellenbosch University and the United States Department of Agriculture (USDA) for Gas Chromatography Mass Spectrometry (GC: MS) analysis.

Special thanks to my fellow researchers in lab 430; Delroy, Tyronne, Emang, Tia, Edmund and Angus and lab 227 Sara, Jonathan, Jeanne and Amy. We always encouraged each other and had fun times both in the lab and outside. Dr Jacqueline Meyer you taught me good work ethic and gladly helped me when I had any problems with my research. Thank you to my fellow postgraduate research committee (PRC) members and the entire MCB family, I learnt a lot about confidence and event planning through all our extra-curricular activities, from the game-of-thrones themed soccer tournaments to chatties and research day presentations.

To my husband Dr Herbert Ntuli, thank you for inspiring me and for providing practical support and having patience despite being a PhD student yourself. I thank my parents and my family for believing in me. To my father Irvine Mapfumo, you always encouraged me to pursue academic excellence despite not having the opportunity to do so yourself. You are my solid rock, unwavering in your support through this entire journey. “Mukanya ndini Chinamhora, nemwenje wamakandipa, ndajekesa nzira kune vachatevera mumashure”.

ABSTRACT

Grey Leaf Spot (GLS) is a fungal disease of *Zea mays* (maize) that is caused by *Cercospora zeina.* It thrives in sub-tropical climates and causes devastating crop losses of up to 60% in southern Africa where maize is grown as a staple food source. Phytoalexins are low molecular weight anti-microbial bio-chemicals that are synthesised *in planta* in response to biotic stress. Related studies have characterised many phytoalexins produced in various plants against several diseases. In maize, phytoalexins fall into to two terpenoid groups: kauralexins and zealexins. To date no studies have been carried out that examine the accumulation in maize of phytoalexins in response to *C. zeina*. This research project found that in maize samples inoculated with *C. zeina*, kauralexin accumulation significantly increased with disease development stages (T0 – 0 days post inoculation, T1 – 17 dpi, T2 – 18 dpi and T3 – 24 dpi) while zealexins did not change. Gene expression of the phytoalexin biosynthesis genes *TPS6* and *TPS11* (both encoding the protein terpene synthase 6/11, specific for zealexins) and *CPPS2* (encoding *ent*-copalyl diphosphate synthase 2, specific for kauralexins) increased significantly at each time point, reaching a maximum level at T2. Infiltration of maize leaves with a chitosan elicitor to mimic fungal pathogen associated molecular pattern (PAMP), and a subsequent callose assay showed positive induction of a callose defence response. However, gene expression and phytoalexin accumulation did not change following chitosan treatment, although zealexin accumulation was higher than kauralexins. Previous studies have shown that phytoalexins accumulate transiently in seedlings. Six diverse Southern African maize lines were compared for phytoalexin accumulation at seedling stage. Zealexin accumulation was generally higher than kauralexins and there were significant differences in both zealexin and kauralexin accumulation in different lines. Gene expression analysis using Genevestigator looked at microarray files and found that expression of *TPS6/11* (zealexin biosynthesis) and *CPPS2* (kauralexin biosynthesis) genes to be largely co-regulated and highly expressed in response to fungal pathogens, nematodes, insect pests and abiotic stresses; *Ustilago maydis*, *Phytophthora cinnamomi*, *Fusarium moniliforme*, *Colletotrichum graminicola*, *Sporisorium reilianum*, *Meloidogyne incognita*, *Ostrinia nubilalis*, waterlogging and drought stress. Finally promoter region analysis showed similar *cis*-acting regulatory elements in the 1kb region upstream of the promoter of both genes and defence specific elements. Thus kauralexin phytoalexins are produced in response to *C. zeina* inoculation, chitin is not likely to be the key PAMP leading to phytoalexin accumulation, phytoalexin accumulation in seedlings is genotype-dependent and phytoalexin biosynthesis genes are expressed under different conditions suggesting a wider range of action beyond repelling fungal pathogens.

LIST OF ABBREVIATIONS

°C	degrees celcious
µg	microgram
µl	microlitre
µM	micro molar
ANOVA	analysis of variance
bp	base pair
Bx	benzoxazinoid
BLAST	basic logarithmic alignment search tool
CAF	Central Analytical Facility
cDNA	complementary deoxyribonucleic acid
Chit	chitosan
cm	centimetre
CPPS2	*ent*-copalyl diphosphate synthase 2
cpr1	cytochrome P450 reductase 1
Cq	cycle threshold
DEPC	diethylpyrocarbonate
df	degrees of freedom
dpi	days post inoculation
DNA	deoxyribonucleic acid
ETI	effector triggered immunity
EtBr	ethidium bromide
EtOH	ethanol
FPP	farnesyl pyrophosphate

FW	fresh weight
g	grams
g	gravity constant (9.81m.s^{-1})
GB	golden bantam
GC: MS	gas chromatography mass spectrometry
GDB	genome data base
GLS	grey leaf spot
GOI	gene of interest
GPP	geranyl pyrophosphate
GGPP	geranyl geranyl pyrophosphate
gst3	glutathione S-transferase III
h	hours
HAc	acetic acid
HCl	hydrochloric acid
IPP	isopentyl pyrophosphate
kb	kilo base
KEP	Kalahari early pearl
l	litre
LSD	least significant differences
M	molar
mM	millimolar
MIQE	minimum information required for quantitative experiments
ml	millilitre

MS	mean of squares
MVA	mevalonic acid
MW	molecular weight
NaOH	sodium hydroxide
NCBI	National Centre for Biological Information
ng	nanogram
nM	nanomolar
NT	no treatment
p	probability
PAMP	pathogen associated molecular pattern
PCR	polymerase chain reaction
pg	picograms
PR	pathogenesis related
PLACE	Plant cis-acting elements
PLANTCARE	Plant cis-acting regulatory DNA elements
QDR	quantitative disease resistance
qPCR	quantitative polymerase chain reaction
QTL	quantitative trait loci
RNA	ribonucleic acid
RFU	relative fluorescence units
RG	reference gene
RT	reverse transcriptase
s	seconds

SD	standard deviation
SEM	standard error of the mean
SNP	single nucleotide polymorphism
TPS	terpene synthase
TSS	transcription start site
UV	ultraviolet
V1	vegetative stage leaf one fully developed
V2	vegetative stage leaf two fully developed
v/v	volume per volume
VE	vegetative stage emergence
VIGS	virus induced gene silencing
w/v	weight per volume

TABLE OF CONTENTS

LIST OF FIGURES

LIST OF TABLES

Chapter 1 : Introduction and Literature Review

INTRODUCTION

The study of the biochemical defence mechanisms that are involved in the protection of crops, is of increasing importance as the human population increases and thus the need for food also rises. While the demand for food is expected to increase, the food production systems are likely to be lagging behind due to limited arable land area, abiotic stresses, and the continued presence of pests and diseases.

Zea mays (maize) is an important crop because it is easily grown, adapted to different growing conditions and has a high energy nutritional value. It was ranked as the second most important food source in the world for 2012 by the food and agriculture organisation (FAO), with sugar cane in first place and rice, wheat, milk and potatoes behind it[1]. Over 870 million metric tonnes of maize were grown worldwide in 2012 with just over 20 million metric tonnes grown in southern Africa. Maize is consumed as a basic food in the developing countries of southern Africa where it is the staple food and it is also important in the more developed countries where it has more diversified uses, for example it is used in the manufacture of biofuels and animal feeds.

Fungal pathogens such as the *Cercospora* species which cause grey leaf spot (GLS) disease in maize), are an example of a plant disease that cause a threat to food security. GLS is a fungal foliar disease that naturally occurs in the warm sub-tropical climatic region of southern Africa. This disease is specific to maize and can cause losses of up to 60% of potential yield in a maize field (Latterell & Rossi, 1983; Ward et al., 1999). GLS is transmitted from plant to plant through the air via spore inoculum. Both *C. zeina* and *C. zea-maydis* are two similar species of *Cercospora*, responsible for GLS outbreaks. In Southern Africa *C. zeina* is predominant (Meisel et al., 2009) and therefore was selected as the focus of this research.

New ways of increasing the production of maize by reducing potential yield losses caused by plant diseases need to be developed in order to combat food security. One way of achieving this is by reducing losses due to plant diseases through bio-engineering of crop plants with

[1] http://faostat.fao.org/site/339/default.aspx

resistance to the disease. Phytoalexins are a large and diverse group of secondary metabolites of plants with antimicrobial properties that may be used as a mechanism of resistance. Recent literature on phytoalexin characterisation has demonstrated that these biochemicals are produced in the maize plant in response to a number of fungal diseases (Ahuja et al., 2012). Phytoalexin production and function have not been characterised in response to *Cercospora zeina,* and it is therefore of interest to investigate whether phytoalexins also play a role in defence of GLS caused by *C. zeina* infection.

Phytoalexins have been characterised in maize in response to the following fungal diseases of maize *Colletotrichum graminicola*, *Rhizopus microsporus*, *Fusarium graminearum* (Schmelz et al., 2011) *Cochliobolus heterostrophus*, *Colletotrichum sublineolum* and *Aspergillus flavus* (Huffaker et al., 2011) In this project we aim to characterise phytoalexins in maize in response to *Cercospora zeina* the causal organism of grey leaf spot disease.

Disease resistance mechanisms

Plants are sessile organisms and therefore in order to survive they evolved various ways to mitigate unfavourable biotic and abiotic stresses. Each plant has multiple layers of protection mechanisms that work together to influence the overall resistance and therefore survival of the plant (Agrios, 2004). Disease resistance mechanisms can be broadly divided into defences that are constitutive or basal (pre-formed) and defences that are induced only in the event of an infection or active immunity (Agrios, 2004; Jones & Dangl, 2006).

In order to gain entry into the interior of the plant, pathogens use various methods to overcome the natural barriers. The outermost layer on a maize leaf is the cuticle and it repels water and prevents adhesion of any water borne pathogens. This waxy layer covers the external surfaces of the entire plant particularly the young parts. The cuticle deposited by the outermost cells and it is made up of cutin, various waxes, pectin and cellulose in different proportions (Agrios, 2004) and its location is shown in Figure 1.1 below.

Fungal pathogens gain entry through stomata, hydathodes, direct piercing of the epidermal cells or through wounds (Jones & Dangl, 2006). They grow between and through plant cells with the aim of extracting nutrition away from the plant to maximise their own growth and reproduction. There are two types of pathogens based on the mode of attack, firstly the necrotrophs kill the host plant typically releasing toxins and the biotrophs need a living host to complete their life cycle (Dangl & Jones, 2001). *C. zeina* is a facultative necrotroph that invades a living maize plant and eventually kills the host (Beckman & Payne, 1982) and its main entry point is through open stomata on the underside of maize leaves (Beckman & Payne, 1982)

Once the pathogen has successfully gained entry, there are physical barriers that prevent entry into tissues and cells. Plant tissues are held together by pectin which acts like cement between bricks if plant tissues were analogous to a brick wall. Pectin takes up the space between adjacent cell walls known as the middle lamella. Pectin consists of long chains of polysaccharides mainly consisting of galacturonan molecules combined with fewer rhamnose molecules that form a physical barrier. However certain pathogens can release various types of pectinase enzymes that break down pectin into smaller chains (Agrios, 2004).

The plant cell is protected by the cellulose cell wall forming another physical barrier. Cellulose consists of glucose polysaccharide chains that are bound together by hydrogen bonds into microfibrils (Agrios, 2004). Pathogens can use cellulase enzymes to disintegrate this layer to gain entry into cells and cause further disease progression. Figure 1.1 shows the cross section of an epidermal leaf surface and the constituent protective layers (Agrios, 2004).

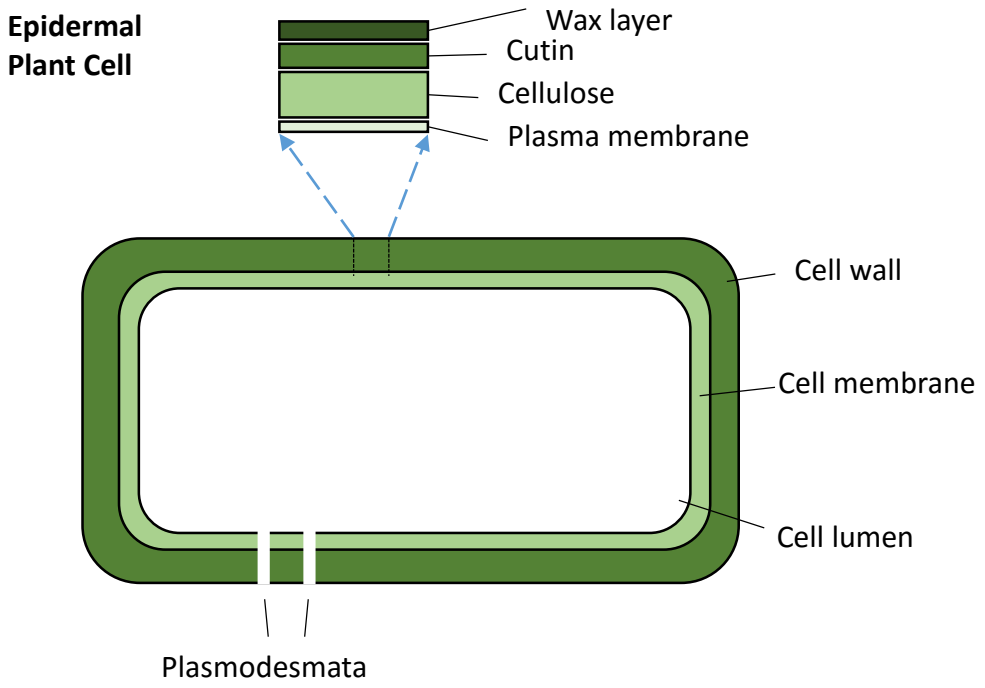

Figure 1.1: Plant Epidermal leaf cross section. The outer protective layer on a plant consists of layers of waxes, cutin, cellulose and the cell (plasma) membrane. The Plasmodesmata are openings used for direct communication by directly adjacent plant cells (Agrios 2005).

Plant immunity is based on the ability of a plant to recognise a pathogen and turn this recognition into a defence response that results in overall resistance (Dangl & Jones, 2001). Pathogen associated molecular patterns (PAMPs) are molecular motifs that are highly conserved within a group of related microbes, and perform essential functions for example chitin, flagellin or lipopolysaccharides (Sessa, 2013). The plant identifies these PAMPs when proteins called pattern recognition receptors (PRR's) that are embedded in the cell

membranes interact with them. Detection of a PAMP results in PAMP Triggered Immunity (PTI) where signal transduction leads to the activation of defence mechanisms resulting in halting of the pathogen and subsequent disease resistance. These defences include production of reactive oxygen species (ROS), activation of mitogen activated protein kinase (MAPK) signalling and expression of defence genes including pathogenesis related (PR) proteins and phytoalexin biosynthetic genes (Ahuja et al., 2012). Reactive oxygen species are highly reactive molecules that contain oxygen, for example hydrogen peroxide (H_2O_2) and superoxide anion (O_2^-). They are normally formed in the mitochondria as by-products of oxidative phosphorylation reactions and also as a response to bacterial invasions (Ray, Huang, & Tsuji, 2013). The resultant oxidative stress causes damage to nucleic acids, proteins and lipids of invading pathogens (Ray et al., 2013). The MAPK signalling cascades form internal communication links that regulate plant growth and development processes (Tena, Asai, Chiu, & Sheen, 2001). This type of signalling is also found in the defence response from perception of a pathogen to pathways that mount a defence response (Tena et al., 2001).

Due to the co-evolution of plants and their pathogens, the pathogens are able to evade PTI by neutralising the PRR's through the production of effectors (Jones & Dangl, 2006). Plants have countered this by recognising effectors and this is known as Effector Triggered Immunity (ETI) (Jones & Dangl, 2006; Sessa, 2013). Effectors are molecules produced by the pathogen to increase its virulence and they can selectively bind to specific proteins (often components of PTI) in the host plant to modify its biological activity (Dangl & Jones, 2001). ETI uses resistance (*R*) proteins to recognise effectors that are now known as avirulence (*Avr*) factors (Sessa, 2013). ETI leads to a stronger PTI response (Jones & Dangl, 2006).

Maize immunity to necrotrophic pathogens can be classified as quantitative disease resistance (QDR) (Poland et al., 2009). QDR is genetically controlled by one or several genes located on the same region of a chromosome and they are transmitted together (Benson et al., 2015). These regions are known as quantitative trait loci (QTL). Maize QDR is not well understood (Poland et al., 2009) however it is made up of many genes which each contribute a small amount to the overall resistance phenotype (Poland et al., 2009). The advantage of QDR over single gene resistance is its robustness in that the plant can survive being overcome by the pathogen due to evolution of new effectors (Poland et al., 2009). Phytoalexin-mediated defence response may be contributing to the QDR (Poland et al., 2009).

Chitin is a β-1, 4-linked polymer of N-acetylglucosamine and chitosan is a β-1,4-linked polymer of D-glucosamide and acetylglucosamine (Hadwiger, 2013; Luna et al., 2011). Chitosan is a deacetylated version of chitin as shown in Figure 1.2 (Agrawal et al., 2002; Hadwiger, 2013) Chitosan has exposed amino groups as shown in Figure 1.2 below that may bind with protein groups. Polymers of either are relatively insoluble except when broken down to units of less than seven sugar groups (Hadwiger, 2013). Chitin and chitosan are both PAMPs that induce callose formation and are important constituents of many fungal cell walls including fungal pathogens (Agrawal et al., 2002). Besides triggering callose deposition, they also induce increase in hydrogen (H_2O_2) production, transcription and translation of PR proteins, phytoalexin production (Agrawal et al., 2002) and regulate plant growth (Hadwiger, 2013).

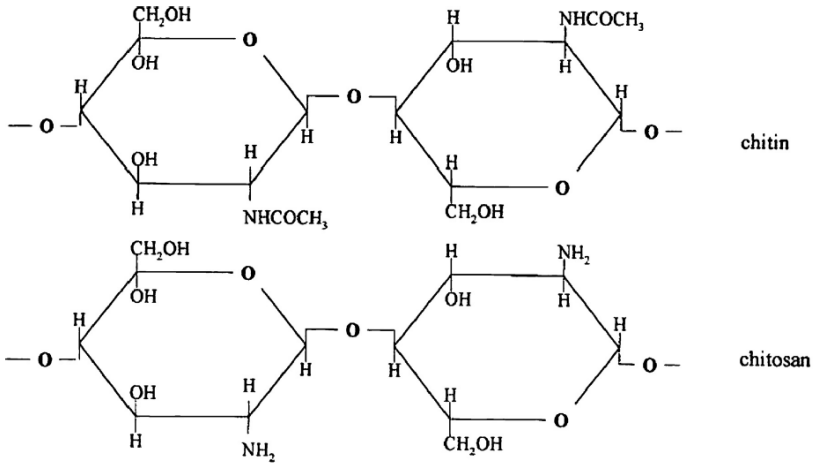

Figure 1.2: Biochemical structure of Chitin and Chitosan

Source: Agrawal et al 2013

Most studies on chitosan elicitor and callose deposition have been done on dicotyledonous plants and less on monocotyledonous plants like *Oryza sativa* (rice) and maize (Agrawal et al., 2002). Callose deposition is a method to measure the activity of a plants immune system (Agrawal et al., 2002; Luna et al., 2011). Callose deposition is triggered by PAMPs such as chitin and chitosan and damage associated molecular patterns (DAMPs) such as oligogalacturonides. DAMPs are endogenous elicitors from damaged plants either due to a pathogen or herbivore (Luna et al., 2011). Synthetic chitosan is similar enough to chitin so it can be used as a trigger to measure PTI. The chitosan response can be measured indirectly by

doing a callose assay. Plants are equipped with β-glucanase and chitinases enzymes that break down chitin and chitosan as a defence mechanism (Hadwiger, 2013).

Chemical defence responses in plants: Phytoanticipins vs Phytoalexins

Biochemical defence responses are part of the last line of defence that interacts directly with a pathogen and reduces its growth. The biochemical defences of all plants, including maize, are made up of a broad array of biochemicals according to their types and functions. This diversity and specialisation of biochemicals is thought to be a result of the short lived nature of the compounds, because they are produced locally around the area of infection and are made in specialised organelles of a plant cell (Frey et al., 2009).

There are two major groups of biocidal defence chemicals in plants and these are phytoanticipins and phytoalexins (Meyer et al., 2015). The phytoanticipins are constitutively present and are always available in the plant while the phytoalexins are synthesised *de novo* upon infection (Ahmad et al., 2011; Meyer et al., 2015). The amount of phytoanticipins may also increase at the time of infection and this means it is difficult to always get a clear cut separation of the two groups (Meyer et al., 2015; Pedras et al., 2011).

Benzoxazinoids are a large, well-studied group of phytoanticipins found in the grass family (Poaceae/ Gramineae) – including maize, and some isolated species of dicots (Ahmad et al., 2011; Frey et al., 2009). In addition to protecting the plant against biotic factors (diseases and pests), the benzoxazinoid phytoanticipins are allelopathic whereby they supress the growth of nearby competitive plant species. An example this is the release of root exudations in *Secale cereale* (Rye) that contain benzoxazinoids and acts to inhibit adjacent plants (Frey et al., 2009).

Benzoxazinoids function when the glucoside form of the compound changes into the aglucon through a hydrolysis reaction that is catalysed by a beta-glucosidase enzyme (Frey et al., 2009; Oikawa et al., 2001). The aglucon version of the molecule is toxic to pathogens and has strong antifungal and antifeedant properties against leaf eating pests (Oikawa et al., 2001). In order to prevent autotoxicity the glucoside is located in the vacuole while the glucosidase is located in the plastid and the two will only meet upon disintegration of the cell due to pathogen and

pest attack (Frey et al., 2009). They are consequently classified as a non-specific reaction (Oikawa et al., 2001).

The benzoxazinoid glucosides found in maize are; 2,4-dihydroxy-7methoxy-2h-1,4-benzoxazin-3(4H)-one (DIMBOA), 2,4-dihydroxy-2H-1,4-benzoxazin-3(4H)-one (DIBOA) and 2-droxy-4,7-dimethoxy-1,4-benzoxazin-3-one (HDMBOA) but the main one found in maize is DIMBOA (Frey et al., 2009). The aglucans exist as DIMBOA-Glc and this is their stable form. The level of active benzoxazinoids in maize is controlled by the *Bx* genes; *Bx1*, *Bx2*, *Bx3*, *Bx4* and *Bx5*. These genes code for monooxygenase enzymes whose role is to convert indole –the precursor molecule – into DIMBOA in a step-wise manner (Ahmad et al., 2011; Frey et al., 2009).

While phytoanticipins are generally present at basal levels in a maize pant, phytoalexins are synthesised from scratch in response to biotic factors (Meyer et al., 2015) and they complement each other. Phytoalexins are also synthesised in response to abiotic stresses such as heavy metals, salt stress and UV radiation (Pedras et al., 2011).

Phytoalexins were first discovered by Muller and Borger in 1940 in potato tubers that were infected with *Phytophtora infestans* (Daniel & Purkayastha, 1995; Echeverri et al., 2012; Pedras et al., 2011). Since then much more has been discovered about their biosynthesis and mode of action and many more have been characterised in many plant species. This section looks at the biochemical structures, classification, mode of action and examples of phytoalexins in different plants.

Phytoalexins from different plant species can be classified according to the genus of the species from which they are produced –including but not limited to brassicaceae, poaceae, solanaceae, fabaceae and vitaceae (Ahuja et al., 2012). Plants produce a wide array of phytoalexins with more than ten thousand structures elucidated for the diterpenes alone (Hammerschmidt, 1999). Maize, *Oryza sativa* (rice) and *Triticum aestivum* (wheat) produce antimicrobial phytoalexins, and *Nicotiana tobacum* and *N. attenuata* (tobacco species) produce antiherbivore diterpenes glycosides and antimicrobial phytoalexins (Ahuja et al., 2012).

Phytoalexins are diverse in terms of their biochemical structures. They can be grouped into isoflavonoids, terpenoids and others (Ahuja et al., 2012; Meyer et al., 2015). The isoflavonoids

are formed in the phenylpropanoid pathway. Isoflavonoid phytoalexins are mostly found in the legume family Fabaceae and one example is phaseollin found in the bean plant (Bailey & Ingham, 1971). The others group is a mixed bag of compounds that do not qualify either as the large groups of isoflavonoids or terpenoids but are still phytoalexins by definition. This others group includes compounds that are acetate poly-malonate derivatives and shikimate poly-malonate derivatives (Dey & Harborne, 1997).

Classification of the terpenoids group includes but is not limited to sesquiterpenoids, diterpenoids and triterpenoids. Terpenoids (also referred to as isoprenoids) are compounds derived from the five carbon unit structure called terpene (Dey & Harborne, 1997; Goodwin & Mercer, 1983) shown in Figure 1.3 below. The terpene structure is made up of five carbon atoms with the first three carbon atoms in a linear arrangement and the last two carbon atoms branching outwards from C_3. The head of the terpene is the branched side while the tail is the side where the atoms linked in a straight line.

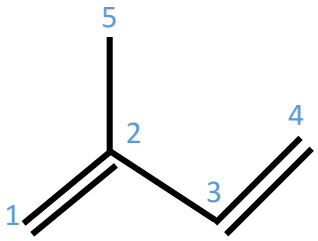

Figure 1.3: Terpene molecule structure. Terpene also known as isoprene is a five carbon molecule which represents the basic terpene structure. The head is the branched side with the carbon 1 and the tail is the linear side with carbon 4.

The nomenclature of terpenoids is based on the number of carbon atoms, in multiples of 10. Monoterpenes such as geraniol have 10 carbon atoms while hemiterpenes, sesquiterpenes, diterpenes and sesterpenes have 5, 15, 20 and 25 carbon atoms respectively (Goodwin & Mercer, 1983). Polyterpenes are terpenoid molecules with more than 20 carbon atoms, for example rubber. The arrangement of carbon atoms can be in various forms, the terpene groups can join together in a head to tail arrangement that forms a continuous linear chain,

they can also be joined backwards, or on different planes giving rise to various structures such as hexagonal rings. A good example is the monocyclic monoterpene called limonene that has one 10 carbon atoms forming a hexagonal ring and it is produced by citrus species (Goodwin & Mercer, 1983).

The maize phytoalexins, kauralexins and zealexins are tetracyclic diterpenoids and sesquiterpenoids respectively, which means they have a four ring structure and these biochemical structures are shown in Figure 1.4 below. Zealexins were discovered in maize infected with *Fusarium graminearum* (Huffaker et al., 2011) and are also reported to be produced in response to the European corn borer *Ostrinia nubilalis* and the combined effect of the plant hormones jasmonic acid (JA) and ethylene (Huffaker et al., 2011). The kauralexins have also been found to be expressed under the same conditions (Schmelz et al., 2011) and localised in the area around the infection or damage.

The activity of zealexins and kauralexins are not necessarily identical as seen in the case of *C. graminicola* in maize, where this pathogen induced kauralexin accumulation (Schmelz et al., 2011) but failed to induce zealexin accumulation above levels similar to the controls (Huffaker et al., 2011). Kauralexins were reported to be induced by both fungal pathogens including *R. microsporus*, *F. graminearum* and *C. graminicola*, and insect herbivory by *O. nubilalis* (Schmelz et al., 2011). Zealexins were strongly induced by the majority of the inoculations done except for *C. graminicola* and these included *F. graminearum*, *U. maydis*, *Cochliobolus heterosporus*, *C. sublineolum* and *A. flavus* (Huffaker et al., 2011). The differential response of the two maize phytoalexin groups shows that their functions are not necessarily identical.

Kauralexins have a variation where two of the tetracyclic groups are located on different directional planes from the main atoms, and these variants are named kaurene and *ent*-kaurene (Goodwin & Mercer, 1983), as shown in Figure 1.4 below for Kauralexin A1 and B1 *versus* Zealexin A1 and B1. Figure 1.4 below also shows the biochemical structures of some phytoalexins produced by plants in the grass family Poaceae (Ahuja et al., 2012); Maize has kauralexins and zealexins, rice has momilactone, phytocassane A and sakuranetin (Kanno & Hasegawa, 2012) and oats have avenanthramide A and luteolin.

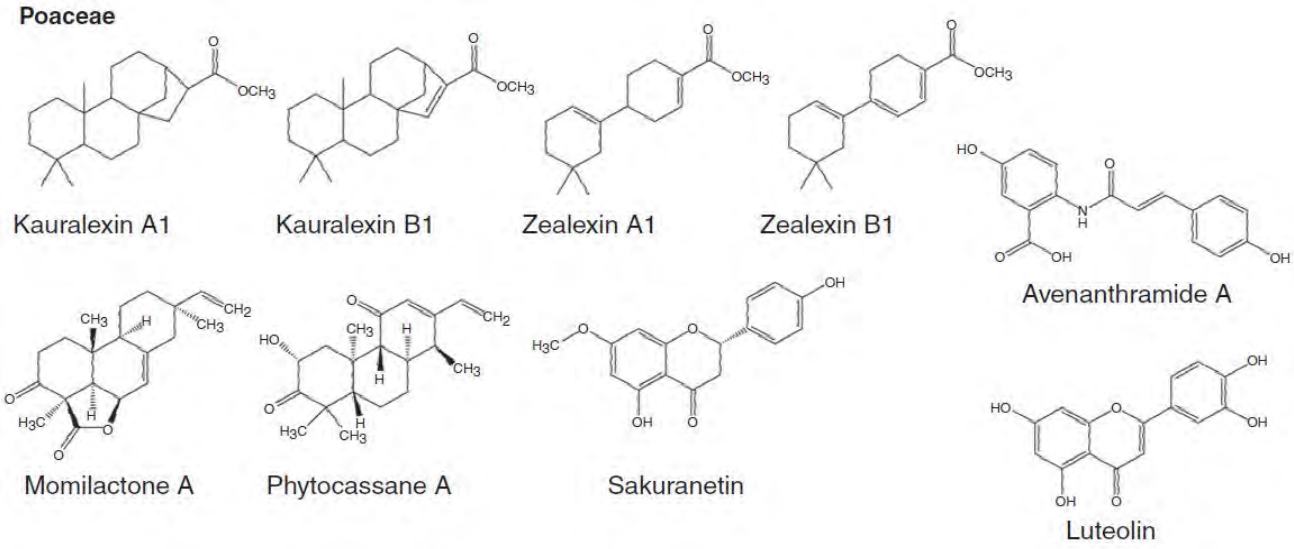

Figure 1.4: Biochemical structures of phytoalexins of the grass family Poaceae – adapted from Ahuja *et al* 2012

These compounds are inducible (Schmelz et al., 2011) and are produced in response to stimuli. The known elicitors of phytoalexins include microbial biopolymers like oligosaccharides and polypeptides or chitosan and metal salts such as copper II chloride ($CuCl_2$) and silver chloride (AgCl) (Pedras et al., 2011). Related volatile terpenoid compounds (linalool, β-caryophyllene and nerolidol) are released by plants to reduce pest attack indirectly by attracting parasitoids to attack the pests (Turlings et al., 1990). In the same manner, plants attract entomopathogenic nematodes to come and attack and therefore slow down the growth of below ground pests (Degen et al., 2012).

The ability of a pathogen to detoxify phytoalexins through metabolism is positively correlated to virulence (Hammerschmidt, 1999; Pedras et al., 2011). The mode of action of phytoalexins against pathogens has different targets as they have unique and diverse biochemical structures (Pedras & Sarma-mamillapalle, 2012), however in general phytoalexins cause plasma membrane disruption and inhibit respiration of invading pathogens (Pedras et al., 2011). Phytoalexins are also phytotoxic and this may explain why they are locally produced and short lived (Echeverri et al., 2012; Pedras et al., 2011).

The oat phytoalexins avenathramides, were found to accumulate in mesophyll cells of plants infected by the fungal pathogen *Puccinia coronata* at the time of haustoria formation during a hypersensitive response (R Hammerschmidt, 2011). This indicates that phytoalexins are part of the hypersensitive response in which cell death is targeted at concurrent pathogen death and therefore reduced disease progression (Uchihashi et al., 2011).

Examples of the phytoalexin repertoire in different plants contributing to resistance are; in rice momilactone is responsible for resistance to *Sarocladiun oryzae*, in soybean (*Glycine max*) plants glyceollin is responsible for resistance to *Macrophomina phaseolina*, *Colletotrichum demtium* var. *truncate* and *Myrothecium roridum* and in groundnuts (*Arachis hypogea*) cis-3, 5-dimethoxy stillbene is responsible for resistance to *M. phaseolina* (Pedras et al., 2011). Studies reveal that each plant species has a suite of phytoalexins not just a single one. Phytoalexins form a large diverse family found in many plants and this forms a strong base that is unpredictable for the invading pathogens (Pedras et al., 2011).

Maize phytoalexins: biosynthetic pathways

The biosynthesis of terpenoid phytochemicals occurs in the smooth endoplasmic reticulum of the cell, together with other lipids, steroids and cell membranes according to the requirements of the plant (Agrios, 2004). This section will discuss general terpenoid biosynthesis followed by the zealexin and kauralexin biosynthesis pathways. They are made and released in the localised area surrounding the site of infection (Schmelz et al., 2011). Terpenoid biosynthesis starts from mevalonic acid (MVA) then branches into the specialised subgroups of terpenoids (Dey & Harborne, 1997).

MVA is formed from acetyl coenzyme A (Acetyl-CoA) in a multiple step conversion with the following intermediate molecules; acetyl-CoA, acetoacetyl-CoA, hydroxymethylglutaryl-CoA (HMG-CoA) and MVA (Dey & Harborne, 1997) as illustrated in Figure 1.5. To initiate terpenoid biosynthesis MVP is converted to isopentyl pyrophosphate (IPP) by addition of a phosphate group. The IPP is then converted to dimethylallyl pyrophosphate (DMAPP) in a reversible reaction. Both IPP and DMAPP give rise to geranyl pyrophosphate (GPP) as shown in Figure 1.5 below by the arrows. The reactions in the main pathway can be described as successively increasing the number of isoprene units in a head to tail condensation reaction by means of prenyl transferase enzymes (Dey & Harborne, 1997).

The pathway branches at GPP to form monoterpenoids that have 10 carbon atoms for example menthol from mint plants (*Mentha* species). GPP is converted to farnesyl pyrophosphate (FPP) and this is where the pathway branches to form sesquiterpenoids with 15 carbon molecules. The zealexin phytoalexins are sesquiterpenoid molecules. FPP is also converted to squalene which is in turn converted to the sterols which includes the steroid hormones. The next step in the terpenoid biosynthesis is conversion of FPP to geranyl geranyl pyrophosphate (GGPP) from which the pathway branches out to form the diterpenoids with 20 carbon atoms and also the carotenoids (Dey & Harborne, 1997) whose function is pigmentation of the leaves and fruits. The kauralexin phytoalexins of maize are found in the diterpenoid group.

Downstream from this point are sesterpenoids (C_{20}) such as the gibberellins and polyprenoids ($C_{n>20}$) which have very long chains of the five carbon isoprenoid units. (Dey and Harborne 1997). Figure 1.5 below shows the pathway of terpenoid/isoprenoid biosynthesis starting with HMG-CoA.

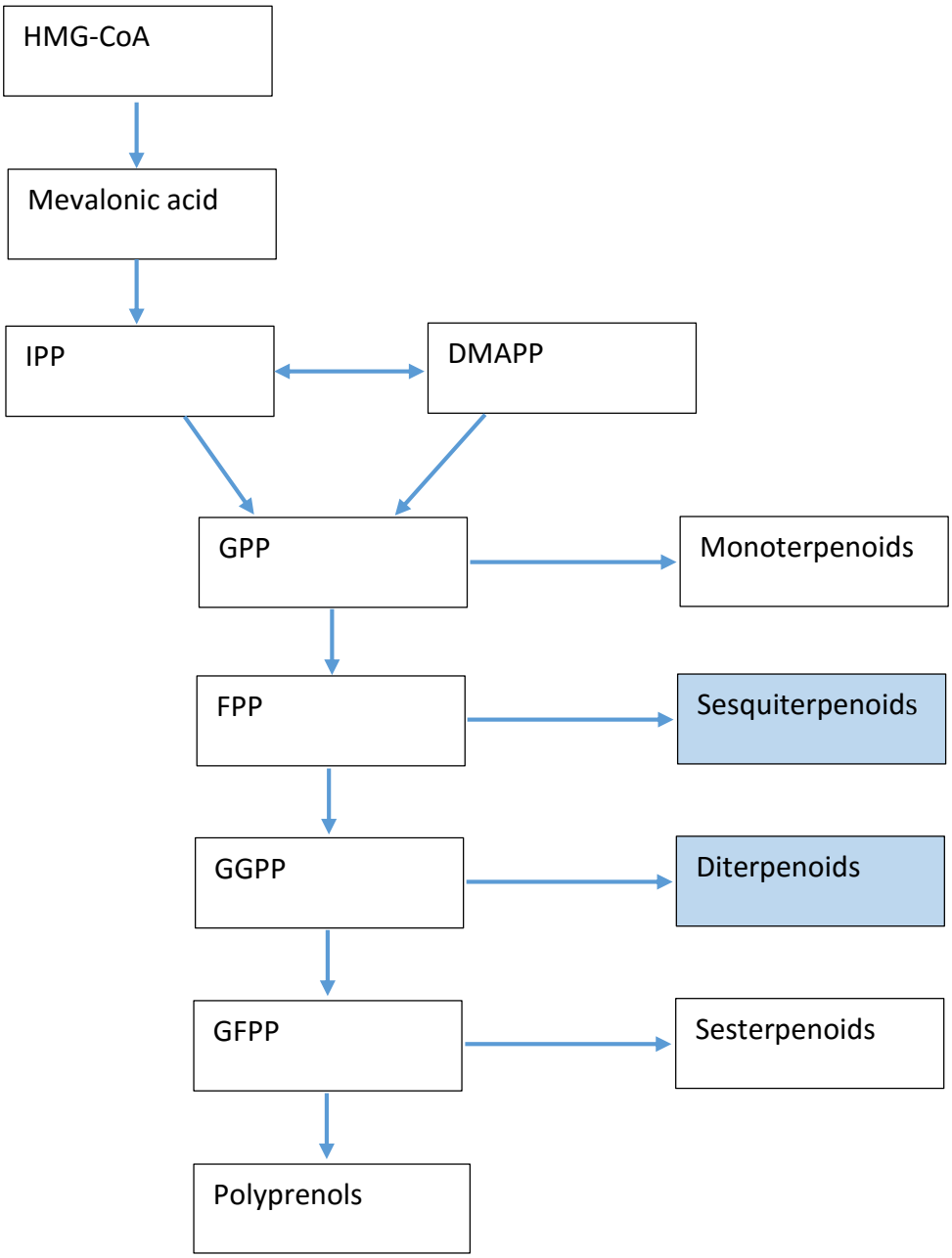

Figure 1.5: Isoprenoid biosynthesis pathway.

Hydroxymethylglutaryl-CoA (HMG-CoA) is first converted to mevalonic acid and a chain of reactions leads to farnesyl pyrophosphate (FPP) and geranyl geranyl pyrophosphate (GGPP), the parent molecules for kauralexin (diterpenoid) and zealexin (sesquiterpenoid) biosynthesis respectively.

The diterpenoid phytoalexins of maize arise from geranyl geranyl pyrophosphate. Figure 1.6 below shows the predicted biosynthesis pathway for maize zealexins. FPP is converted to beta-bisabolene by the *TPS6/11* enzyme. This is the converted to beta-marcrocarpene by the same enzyme. Zealexin A1 is made after a series of enzyme controlled steps then it is the converted into two groups with zealexin A2 and A3 in the first group and B1 in the second group (Huffaker et al., 2011; Schmelz et al., 2011).

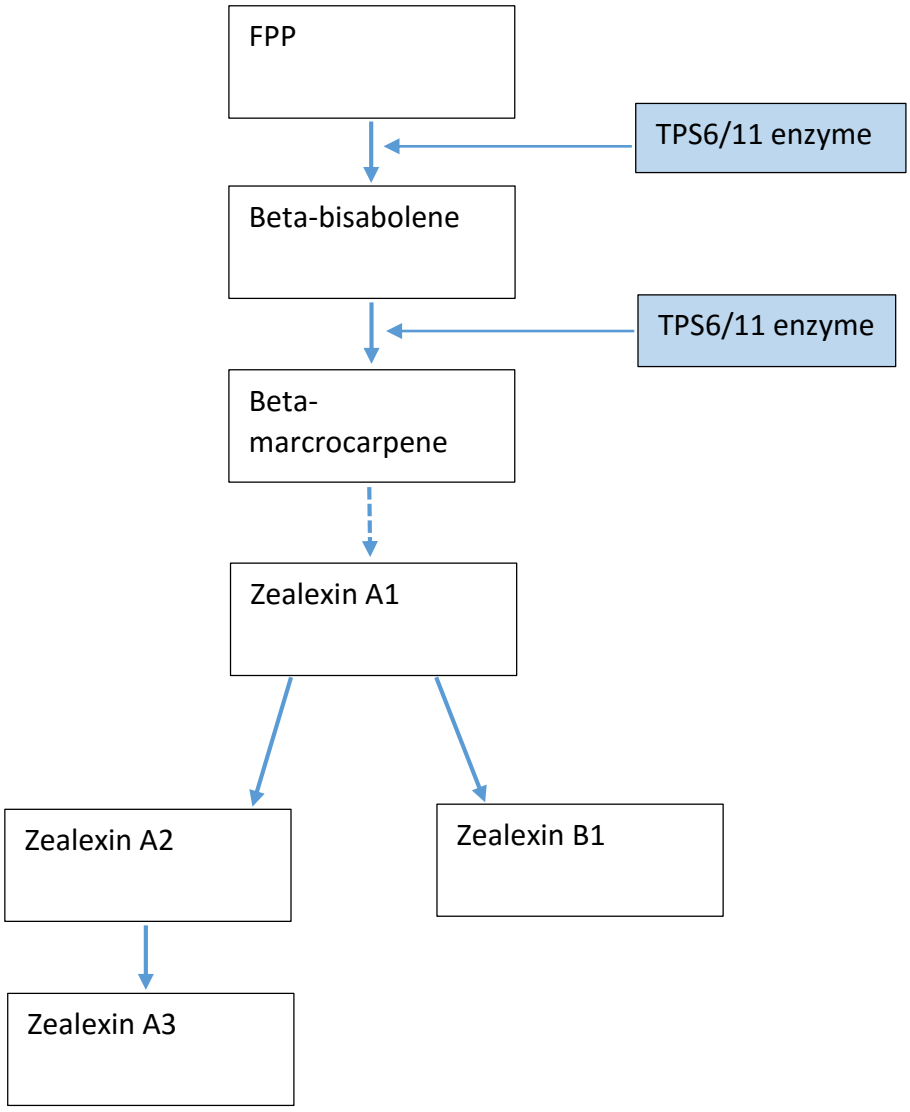

Figure 1.6: Zealexin biosynthesis pathway in maize

Figure 1.7 below outlines the biosynthesis of kauralexin phytoalexins. GPP is converted to ent-copalyl diphosphate by the *ent*-copalyl diphosphate synthase 2 (CPPS2) enzyme. This compound is then converted to ent-kaurene and ent-isokaurene. *Ent*-kaurene is converted to kauralexin A1, A2, and A3 while *ent*-isokaurene is converted to kauralexin B1, B2 and B3.

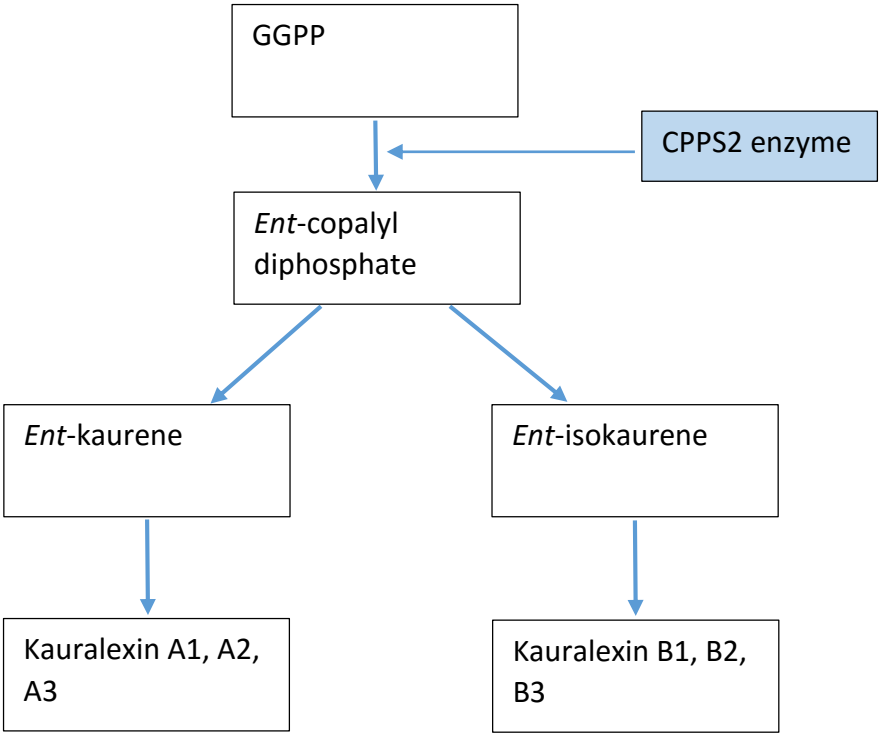

Figure 1.7: Kauralexin biosynthesis pathway in maize.

Cercospora zeina

Grey leaf spot is an important disease to southern Africa because of its wide spread distribution or epidemiology and large extent of damage. It can reduce the expected yield by 20% to 60% (Korsman et al., 2011; Latterell & Rossi, 1983; Ward et al., 1999) in a field. GLS causes characteristic elongated lesions on the leaves that follow the leaf venation shown in Figure 1.8 below. The lesions are parallel to the leaf veins at first then the infection degenerates into blighting of the entire leaf at the peak of infection. The fungus cannot penetrate the sclerenchyma tissue in leaf veins. Inter-vein distance (IVD) has been linked to quantitative resistance to GLS (Benson et al., 2015). Wider IVD is associated with suspectibility

while maize with narrower IVD is more resistant to GLS due to smaller lesions formed and lower amount of inoculum for secondary infections (Benson et al., 2015).

Figure 1.8: GLS lesions on maize leaf. Source - University of Pretoria Maize Greenhouse.

The major damage caused by GLS is the loss of photosynthetic area particularly important at the grain filling stage of development, where photosynthesis is required to make sugars directly for filling the kernels. Chlorosis and lodging are characteristic symptoms of GLS after tassel formation (CIMMYT maizedoctor.org). Lodging is caused by translocation of sugars from the lower levels of the plant to the new cobs for grain filling leading to weaker stems, thus the plant falls over. It is a problem in machine harvesting where up to 100% crop losses were recorded in the USA (Beckman & Payne, 1982; Crous et al., 2006). The infection is considered severe when leaves above the ear display symptoms and the other leaves are blighted. These losses amount to large financial losses for the farmer and food security losses for a nation.

GLS is caused by two biologically similar species. Initially *C. zea-maydis* was considered the sole cause of GLS. Subsequently *C. zeina* was found to be a morphologically similar but genetically different cause of GLS (Crous et al., 2006). The conidia and conidiophores were indistinguishable for both species. The conidia are spores borne on the conidiophores and the general Cercospora species structures are shown in Figure 1.9. The conidia are 5 – 10 µm in width to 30 – 100 µm in length and are hyaline (clear), obclavate, slightly curved and several celled (CMMYT maizedoctor.org). Both species can be grown on V8 agar producing either

black dome shaped structures that sporulate highly or a white cotton-like sterile growth of mycelium (Beckman & Payne, 1982).

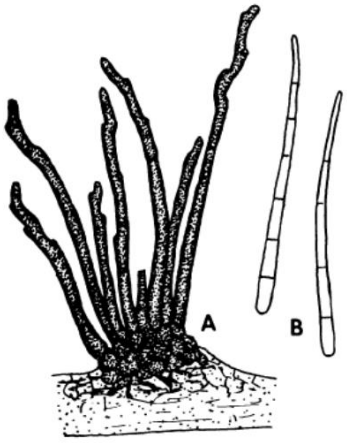

Figure 1.9 Cercospora Conidiophores and conidia. Cercospora conidiophores (A) and conidia (B) Source - (Barnett & Hunter, 1998)

While *C. zea-maydis* produces a toxin called cercosporin which is seen as a pink pigment in culture, *C. zeina* does not. A PCR assay was developed to distinguish the two species genetically(Korsman et al., 2011). It is rare for both species to be found in one epidemic (Korsman et al., 2011). The two species are also geographically separated with *C. zea maydis* being the predominant cause of GLS in USA and Canada while *C. zeina* is more extensive in Brazil and the sub-Saharan Africa (Crous et al., 2006; Korsman et al., 2011; Meisel et al., 2009). Both species are hemi biotrophic fungal pathogens. This means that it is initially biotrophic when the plant is alive and it becomes necrotrophic and continues to thrive off the dead tissues.

The ideal conditions for growth of GLS are climates with high humidity and high temperatures ranging from 22˚C to 30˚C. Heavy rains and winds promote the spread of disease. Field conditions that promote GLS are overcrowding, poor airflow, poor drainage, and zero tillage. However it is important to note that while conventional tillage reduces the disease, it increases soil erosion (CMMYT maizedoctor.org).

The life cycle and reproduction of *C. zeina* starts with the primary inoculum as shown in Figure 1.10 below. These are spores and mycelium that overwintered in plant debris on the soil

surface. As the new season begins with higher temperatures and humidity levels with increased rainfall, the fungus in the debris begins sporulating (CMMYT maizedoctor.org). Conidia are asexual spores and they are dispersed by the wind and rain splash to infect the newly planted maize plants (Korsman et al., 2011).

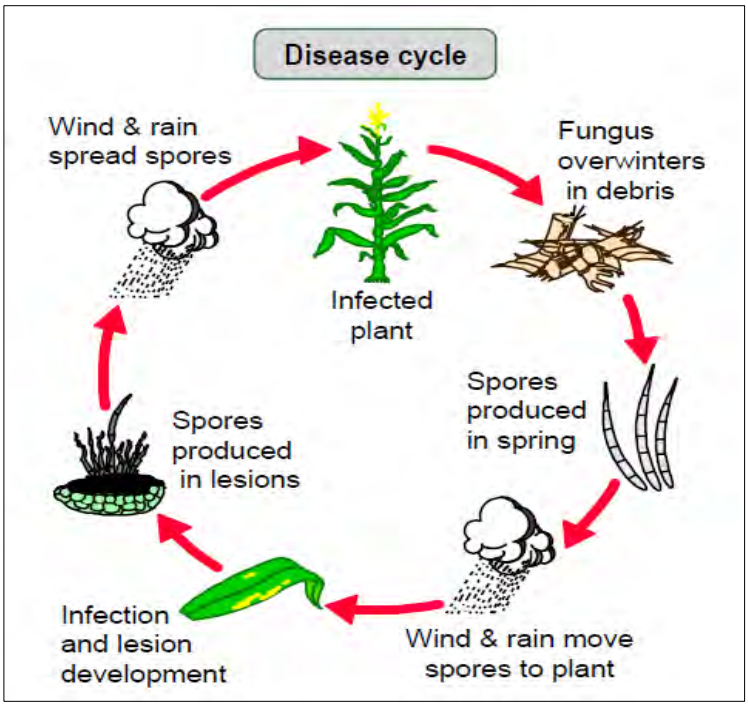

Figure 1.10: life cycle of the GLS disease in maize

Source: Pioneer Agronomy Sciences

Once the spores land on the maize plant, there is a latent phase of 10 to 100 days (Beckman & Payne, 1982; Korsman et al., 2011) before germination into a germ tube and then appresorium which penetrates the plant. However, for field experiments a long latent period of 100 – 120 days may be the result of spores landing onto the maize plant at an unknown time between planting and observing the lesions. The germ tubes can grow towards the stomata under high humidity conditions in response to tropistic attraction. The stomata are a major entry point of the fungus (Beckman & Payne, 1982) as evidenced by mycelial growth being more extensive on the underside of the leaf. The disease starts at the bottom and moves upwards, so that lower leaves show more severe symptoms than upper leaves. This pattern may also be due to higher levels of humidity provided by the plants own canopy and the high amount of inoculum re-circulating (Beckman & Payne, 1982).

In terms of the resistance of maize to GLS many QTL have been defined for GLS resistance in maize (Benson et al., 2015; Berger et al., 2014). QTLs for other physiological processes have also been identified in other studies and interestingly three GLS QTLs overlap with the vein formation QTL (Benson et al., 2015).

The maize gene ontology terms associated with GLS QTLs show that genes involved in a wide range of functions also make up in QDR (Benson et al., 2015). These are genes that are involved in the following; structural components, secondary metabolites, primary metabolites, pathogen defence genes, membrane transporter, development, cellular energy, cell signalling, and cell cycle (Benson et al., 2015).

AIMS AND OBJECTIVES

The aim of this project is to investigate the phytoalexin defence response in maize inoculated with *C. zeina*, and to further analyse how phytoalexin accumulation in maize is controlled.

The objectives are

1. To measure both expression of the genes identified in literature as coding for enzymes that catalyse the first step of phytoalexin biosynthesis in zealexins (– *TPS6* and *TPS11*) and kauralexins (– *CPPS2*) (Huffaker et al., 2011; Schmelz et al., 2011) and phytoalexin accumulation in maize samples inoculated with *C. zeina* at four stages in disease development (T0, T1, T2 and T3). Gene expression will be measured by reverse transcriptase quantitative PCR (RT-qPCR) and phytoalexin accumulation will be measured by gas chromatography mass spectrometry (GC: MS).
2. To measure biosynthetic gene expression and phytoalexin accumulation in maize samples infiltrated with the synthetic elicitor chitosan. Chitosan will be used to mimic fungal infection. It is similar to chitin, the major component of fungal cell walls which is a pathogen associated molecular pattern (PAMP) that is recognised by the plant (Agrawal et al., 2002; Ahmad et al., 2011) and triggers plant defence.
3. To measure biosynthetic gene expression and phytoalexin accumulation in six diverse maize lines that are representative of maize grown by farmers in the southern African region. This would be carried out on maize seedlings grown to the vegetative growth stage of emergence, designated VE. Maize plants produce phytoalexins as a preventive defence mechanism only at this developmental stage, but not in subsequent developmental stages.
4. To uncover any other diseases, insect pests or abiotic factors that cause an increase in the gene expression of the maize phytoalexin biosynthetic genes for zealexins (*TPS6/11*) and kauralexins (*CPPS2*). This will be carried out by analysing gene expression patterns in various microarray experiments that have been uploaded onto the online database Genevestigator.
5. To identify the *cis*-acting regulatory elements present in the 1kb promoter regions of the two phytoalexin biosynthetic genes. Online bioinformatics tools will be used to obtain candidate element sequences, positions and functions.

Chapter 2 : Materials and Methods

Maize Growth Conditions

Maize plants were grown in two locations; the first group of plants were grown at the University of Pretoria where a greenhouse was set up for *Cercospora zeina* inoculations. The second group of maize plants were grown at the University of Cape Town (UCT) in the Molecular and Cell Biology (MCB) Department and these consisted of the diverse maize lines that were studied at seedling stage and B73 maize plants that were treated using the synthetic elicitor chitosan.

To inoculate the plants, a suspension of *C. zeina* conidiophores – ex-type culture CBS 117757 (Meisel et al., 2009) was diluted to 3 X 10^{-4} conidia per ml in 0.01% (v/v) Tween 20 and painted onto the leaf surface using a small brush. This was carried out and leaves were sampled by Dr Bridget Crampton. Maize samples grown at the University of Pretoria were transported on dry ice to UCT via courier.

To plant at UCT, the maize seeds were first rinsed in 10 % (v/v) ethanol for 5 seconds then soaked in 10 % (v/v) JIK solution for 10 minutes to sterilise them, followed by sterile water for another 10 minutes. The soil mixture was made up of a 1: 1 ratio of peat and vermiculite. Equal amounts of dolomitic lime and fertiliser (N: P: K = 2: 3: 2) were added in the soil mixture. Four maize seeds were planted per pot, spaced equidistant from each other. Plastic flower pots of 10cm diameter were used and set on trays for drainage. The moisture levels were kept well drained by watering every two days. The growth-room temperature range was between 21 and 28 °C. The humidity level in the growth room was set to between 20 and 50 %. Fluorescent lights were on a 16 hour light/ 8 hour dark cycle for the duration of the growing stage.

In the diverse maize lines seedlings experiment, plants were harvested at growth stage VE (Abendroth et al., 2011). These are codes for the plant age based on the vegetative stage and number of leaves, where VE is emergence, V1 is when the first is leaf fully developed and V3 is when three leaves are fully developed. Table 3.3 (Characterisation of the six diverse maize lines) in the results section gives the background and origins of the six diverse maize lines that were analysed.

Chitosan Treatment

Infiltration of maize leaves of 14 day old V3 maize plants was carried out using a 1ml needleless syringe. The solutions used were water, 0.2 % (v/v) acetic acid and 0.1 % (v/v) chitosan (Sigma Aldrich, Missouri USA) prepared in 0.2% acetic acid, as described by Ahmad et al 2011. A 5 cm length of leaf 2 of each plant was marked off using a ruler and black marker. Pressure was applied to the needleless syringe to push the liquid through the stomata on the underside of the leaf into the spongy mesophyll cell layer. Four maize plants represented four biological replicates in each treatment.

Maize leaves were harvested by cutting off the leaf using a new sterile blade or scissors soaked in 70 % ethanol. The leaf was quickly folded and placed in a foil packet that has been pre-folded and labelled. The packet was immediately placed into liquid nitrogen to snap freeze the sample.

The frozen leaf samples were then stored at -80°C until required or used immediately in their respective experiments.

Callose Assay

For callose extraction (Korsman et al., 2011; Voigt et al., 2006), the maize leaf samples were ground up in liquid nitrogen and quickly weighed. To remove the chlorophyll, 1.2 ml of 96 – 100 % ethanol (EtOH) was added to a sample of 50 mg maize leaf tissue and incubated for 10 minutes at 50°C. Each sample was centrifuged at 400 X *g* for 5 minutes at room temperature and the supernatant was discarded. To wash, 600 µl of 96 – 100 % of EtOH was added and the sample was centrifuged at the same speed for 1 minute. The supernatant was removed and a second wash was carried out. The supernatant was removed.

To solubilise the callose in the remaining pellet, 200 µl of 1 N sodium hydroxide was added to the sample and it was incubated at 80°C for 15 minutes. During this time, the micro tube was lifted out of the heating block and shaken by hand three times. The sample was centrifuged at 400 X *g* for 5 minutes. The supernatant was carefully decanted into a new tube and stored at 4°C short term and -20°C long term.

Fluorescence quantification (Shedletzky et al., 1997) of the extracted callose was carried out with three technical replicates for each biological replicate. A black 96 well plate was used

and 10 µl of sample was added to each well. 120 µl of the aniline blue dye mix was added to each well to activate the fluorescence. The aniline blue dye mix was made up by adding 40 volumes of 0.1 % aniline blue dye in water, 21 volumes of 1 N hydrochloric acid and 59 volumes of 1 m glycine at pH 9.5 .The plate was shaken briefly to mix then incubated at 50˚C for 30 minutes with shaking in a Multiskan FC Photometer (Thermo scientific, Massachusetts USA) plate reader. The plate was incubated at room temperature with shaking for 30 minutes in a Promega Glomax Fluorescent plate reader (Promega, Wisconsin USA). Following this, fluorescent readings in the UV range with the excitation filter of 368 nm and emission filter of 410 – 460 nm were recorded for a period of 5 seconds.

RNA Extraction

Maize leaf material was ground up in liquid nitrogen using autoclaved and baked pestle and mortar. Pre-cooled micro tubes and spatulas were used to prevent thawing of the samples as this could lead to RNA degradation. The RNA extraction guidelines outlined in the MCB Honours Techniques course manual were followed.

Two RNA extraction protocols were followed in this project. These were either using Trizol based Qiazol reagent[2] followed by subsequent RNA clean-up using Qiagen columns (Qiagen, Hilden Germany) or using the Purelink Plant RNA reagent (Thermo scientific, Massachusetts USA).

In the first method, one ml of Qiazol was added to 100 µg of finely ground-up leaf tissue in a 1.5 ml Eppendorf micro-tube in the fume hood. This was incubated at 55˚C for five minutes on a heating block then centrifuged for ten minutes at 12,000 X *g* at 4˚C in a cooling centrifuge. The supernatant was decanted into a new micro tube. 200 µl of chloroform was added, then vortexed for 20 seconds and left at room temperature for five minutes. The sample was centrifuged for fifteen minutes at 12,000 X *g* at 4˚C and the supernatant was decanted into a new tube. Half volumes each of pre-chilled Isopropanol and 5 M sodium chloride, equal to the volume of decanted supernatant were added and mixed well by inverting the tube several times. The tube was incubated for 10 minutes at room temperature. The tube was centrifuged at 10,000 X *g* at 4˚C for 10 minutes and the supernatant was discarded. At this point the RNA

[2] https://www.qiagen.com/za/shop/lab-basics/buffers-and-reagents/qiazol-lysis-reagent#resources

pellet was visible at the bottom of the tube. One ml of 75 % ice-cold ethanol was added and the tube was centrifuged at 10,000 X *g* at 4˚C for five minutes to wash the pellet. The ethanol was aspirated off using a pipette the tube was briefly centrifuged for 10 seconds to collect any remaining ethanol. This was removed using a smaller filter tipped pipette and the pellet was left to dry for 10 minutes in the fume hood with the micro tube lid open 30 µl of DEPC treated water were added to resuspend the pellet.

RNA clean-up was done using the Qiagen RNeasy clean-up kit[3]. The protocol was followed with alterations at the elution step. In summary 2.5 µl of DNAse I stock solution and 10 µl of buffer RDD were added to the sample and nuclease fee water was added to make up 100 µl. The sample was incubated at room temperature (20 – 25˚C) for 10 minutes. For the clean-up 350 µl of buffer RLT were added to the sample and mixed well. 250 µl of 96 – 100 % ethanol were added and mixed by pipetting. The now 700 µl sample was transferred onto an RNeasy MinElute spin column and collection tube and centrifuged at 8000 X *g* for 15 sec. The flow through was discarded and 500 µl of buffer RPE was added to the column and centrifuged as above. 500 µl of ethanol was added to the column and centrifuged at 8000 X *g* for 2 minutes to wash. The column was placed in a new collection tube and centrifuged at full speed for 5 minutes to remove any residual ethanol. The spin column was placed in a new 1.5 µl tube with lid. 30 µl of nuclease free water was added onto the column and centrifuged at full speed for 1 minute to elute the RNA. The same elute was reloaded onto the column and the centrifuged as above to maximise RNA concentration.

In the second RNA extraction method, Purelink plant RNA reagent was purchased from Life Technologies Applied Bio Systems (California, USA) and the protocol was followed according to the manufacturer's instructions. In summary, 0.5 ml of cold Purelink plant RNA reagent was added to 1.0 grams of frozen ground maize leaf tissue and mixed well by flicking the bottom of the tube and using the vortex, then incubated at room temperature for 5 min while laying horizontally on the lab benchtop to increase the surface area. The tubes were centrifuged for two minutes at 12,000 X *g* at room temperature. The supernatant was carefully aspirated using a filter tipped pipette and transferred to a new RNase-free micro tube. 0.1 ml of 5 M sodium chloride was added to the supernatant and mixed well by tapping the tube. Following

[3] https://www.qiagen.com/za/resources/resourcedetail?id=06f3d3ff-5926-4915-bffe-4adcf99266aa&lang=en

this, 0.3 ml of chloroform was added to the tube and mixed thoroughly by inverting the tube. The tube was centrifuged for ten minutes at 12,000 X *g* at 4°C and the upper aqueous phase was carefully aspirated using a pipette and transferred into a new tube. An equal volume of isopropanol was added to the aqueous phase and mixed well by inverting the micro tube several times then incubated for 10 minutes at room temperature on the benchtop. The sample was centrifuged for 10 minutes at 12,000 X *g* at 4°C. The supernatant was carefully decanted off, in order to keep the translucent RNA pellet at the bottom of the tube. One millilitre of 75 % cold ethanol was added to the pellet and the tube was centrifuged for one minute at 12,000 X *g* at room temperature to wash the pellet. The supernatant was decanted off taking care not to lose the pellet. The sample was centrifuged for 10 seconds to collect any residual liquid at the bottom of the tube, which was aspirated using a smaller filter tipped pipette. The pellet was left to dry for 10 minutes in the fume hood with the micro tube lid open 30 µl of RNAse free water were added to the dry pellet and was gently pipetted up and down around the pellet until it resuspended.

Nanodrop readings of the extracted RNA were taken to determine the RNA concentration and any phenolic or protein contamination. Each sample was divided into aliquots of 10 µl and stored at -80°C. Quality was further checked using the RNA Nano assay on a bio-analyser (Agilent Technologies, Waldbronn, Germany) to check that the RNA was not degraded. RNA integrity (RIN) numbers are used to rate the RNA quality on a scale of 1 – 10 and generally samples that are above 7 are considered to be intact RNA suitable for downstream applications like cDNA synthesis. The RNA quality control data are presented in the supplementary table xix.

Synthesis of cDNA

The synthesis of cDNA was done using two different kits. The first one was the Maxima H minus First Strand cDNA synthesis kit with ds DNase[4] (Thermo scientific, Massachusetts USA). Two µg of total RNA was used per sample. The volume was calculated from the RNA concentrations and pipetted into a PCR tube. Master mixes were used due to the small volumes of reagents. To each tube 0.25 µl of oligo $(dT)_{18}$ primers and 0.25 µl of random

[4] https://www.thermofisher.com/order/catalog/product/K1681

hexamer primers were added at final concentrations of 25 pmol each. One microlitre of 10mM dNTPs was also added at a final concentration of 0.5 mM and the volume was brought up to 15 µl with nuclease free water. Samples were mixed and then incubated at 65˚C for 5 minutes in a PCR machine, then mixed again, centrifuged and placed on ice for 10 minutes. A mixture of 4 µl 5 X RT buffer and 1 µl Maxima H minus enzyme mix was added bringing the total reaction volume to 20 µl. Each sample was mixed gently then centrifuged briefly. The tubes were incubated at 25˚C for 10 minutes, then at 50°C for 10 minutes, followed by 85°C for 5 minutes to terminate the reaction. A 1/10 dilution was made for the cDNA and 1 µl was used in a single RT-qPCR reaction.

The second kit was the High Capacity cDNA Reverse Transcription kit (Applied Biosystems, California USA). Reverse transcriptase (RT) master mix was added to each tube. The RT master mix for a single reaction consisted of 2.0 µl of 10X RT buffer, 0.8 µl of 100 mM dNTP's, 2.0 µl of 10X random primers and 1.0 µl of 10X MultiScribe Reverse Transcriptase enzyme. 2 µg of the RNA template was added and the total reaction volume was brought up to 20 µl with nuclease free water. The tubes were centrifuged briefly to mix the reagents and eliminate water bubbles. The samples were incubated in a PCR machine at 25°C for 10 min, 37°C for 120 min, 85°C for 5 min and 4°C for 10 min. A 1/10 dilution was made and samples were stored at -20°C.

Primers

The three genes analysed by RT-qPCR were *Terpene synthase 6* (*TPS6*), *Terpene synthase 11* (*TPS11*), and *Ent-copalyl diphosphate synthase 2* (*CPPS2*) also known as *Anther ear 2* (*AN2*) (Schmelz et al 2011; Huffaker et al 2011). The details of each gene are listed in Table (xx) in the supplementary data section.

The primers for the reference genes that were used to calculate the relative expression were published by Manoli et al (2011) and they were selected for their stable expression across the growth cycle of a maize plant. The reference genes were *membrane protein PB1A10.07c* (*MEP*), *ubiquitin carrier protein* (*UBCP*), *leunig* (*LUG*) and *RNA Polymerase 1* (*Rpol1*). Their gene names and primer sequences are also listed in the Table (xx) in the supplementary data tables.

To ensure that each primer pair amplified the unique transcript corresponding to the relevant gene, all the primers underwent specificity analysis using the basic logarithmic alignment search tool (BLAST) on the NCBI database. They were checked against the maize genome to ensure that they were only hybridizing with the target gene within the maize genome and against the human and rat genomes since they could cause a false positive result if the samples became contaminated. Specificity to the gene of interest was checked and by doing a multiple sequence alignment of the primer sequence and the gene sequence in using DNAMAN software.

RT-qPCR

Gene expression was analysed using reverse transcriptase quantitative polymerase chain reaction (RT-q PCR).

A standard curve was made by pooling the biological samples' cDNA being analysed and making a twofold serial dilution. The pooled cDNA was initially diluted to 1 in 5 and this was considered as the neat sample. The dilution series was; neat, 1 in 2, 1 in 4, 1 in 8, 1 in 16, 1 in 32, 1 in 64, 1 in 128 and this corresponded to 20 ng/ µl, 10 ng/ µl, 5 ng/ µl, 1.25 ng/ µl, 0.625 ng/ µl, 0.3125 ng/ µl, 0.3125 ng/ µl and 0.15625 ng/ µl total RNA (Manoli et al., 2011). The amount of RNA used was 2000 ng in a reaction volume of 20 µl therefore the concentration was 100 ng / µl. 1 µl of cDNA was added to each qPCR reaction tube and this corresponded to the absolute amount of DNA calculated in the dilution series. No template control (NTC) and no reverse transcriptase (no RT) controls were also included. The standard curve and experimental samples for the same gene were placed together in a single run without splitting them up. Each biological sample was repeated in triplicate technical replicates according to the minimum information for publication of quantitative real time PCR experiments (MIQE) guidelines (Bustin et al., 2009).

The Kapa SYBR Fast qPCR master mix (Kapa Biosystems, Cape Town, South Africa) was used in all the RT-qPCR reactions. A single 10 µl reaction contained 5 µl of 2 X Kapa master mix at a final concentration of 1 X, 0.2 µl each of the Forward and Reverse primers from a stock solution of 10 mM at a final concentration of 200 nM, 1 µl of nucleotide template and 3.6 µl of nuclease free water.

The two RT-PCR instruments that were used in different experiments were the ABI 7500 (Applied Biosystems, California USA) at CPGR and the Rotor Gene 6000 (Qiagen formerly Corbett Life Sciences, Hilden, Germany) at MCB. Whole experiments were carried out on a single machine. The light cycler (at CPGR) was used in the "Analysis of Phytoalexin Accumulation and Gene Expression in B73 Maize during the Development of GLS Disease" experiment, while the remaining experiments "Analysis of Chitosan as an Elicitor of Phytoalexin Accumulation in Maize" and "Comparison of early phytoalexin accumulation in six diverse maize lines and B73 at seedling stage" were done using the Rotorgene (at the MCB department, UCT). The ABI 7500 run profile was set at 95°C for 10 minutes followed by 40 cycles of 95°C for 15 sec, 60°C for 1 min and the melt stage was switched on (selected) for melt analysis. The Rotor Gene 6000 run profile was 95°C for 3 min followed by 40 cycles of 95°C for 3 sec denaturation, 60°C for 20 sec annealing and 72°C for 1 sec elongation. The cycle ended with a melt curve analysis from 35°C to 99°C.

The slope for each standard curve was checked to be within the range -3.2 to -3.6 according to MIQE guidelines (Bustin et al., 2009). The R^2 values of technical reps were checked to be greater or equal to 0.99. Each biological replicate had three technical replicates whose Cq values were within 0.5 Cq's of each other. Each gene or target was checked to have a single product shown by a single peak in the melt analysis. All these quality control steps were done using the instrument software for the two RT-qPCR machines used.

The data output from both the ABI and Rotorgene qPCR machines were analysed using the Biogazelle qbase plus software (Gent, Belgium). The software recognises both formats and calculates the relative gene expression based on the stability of the reference genes. It uses an algorithm based on geNorm (qbase plus manual[5]) to determine expression stability of reference genes from the cycle threshold (Cq) values. Multiple runs are combined in a single experiment for analysis and the output is given as calibrated normalized relative quantities (CNRQ). These were imported into excel for statistical analysis and histograms. Statistica was used to calculate ANOVA and post hoc Fishers tests.

[5] https://www.biogazelle.com/qbaseplus

TPS6/11 Distinction Using Restriction Enzyme Digest

Restriction enzyme digestion was done using the Ajil/ BmgBI restriction enzyme from Thermo Scientific code #ER1941. It is a blunt end cutter that recognises the following palindromic sequence 5'CACGTC3' where it cleaves between C and G in both DNA strands with no overhang. The digestion protocol was incubation for 4 hours at 37˚C in a water bath. After digestion samples were loaded onto a 2 % agarose gel to visualise bands and band sizes were estimated using the Thermo Scientific Gene ruler 1 kb and 100 bp DNA ladders that were run concurrently on the same gel.

Prior to digestion the DNA amplification was done by PCR using the *TPS6* and *TPS11* primers (Huffaker et al., 2011) described above, on T3 inoculated maize tissue. The Supertherm TAQ DNA polymerase enzyme (Roche, Basel Switzerland) was used with annealing temperatures of 55˚C and 54˚C respectively for each PCR. The PCR thermal cycling conditions were; initial denaturation 94˚C for 5 minutes, denaturation 94˚C for 30 seconds, annealing primer annealing temperature for 30 seconds, elongation 72˚C for 30 seconds and these three stages were repeated in 40 cycles. The final elongation step was 72˚C for 10 minutes and 4˚C for 10 minutes to hold the sample. The PCR product was stored at -20˚C.

An aliquot of the PCR product was loaded into a well on a 2 % agarose gel made up with 1 % TAE buffer with ethidium bromide added to each sample. The gel was run at 70 – 100 volts for 30 minutes to 1 hour and the DNA bands were visualised under UV light.

TPS6 (294nt) and *TPS11* (398nt) are alternative splice variations of the same gene separated at gene expression. This experiment was done to distinguish the *TPS6* and *TPS11* gene products in end point PCR. The restriction enzyme Agil/ BmgBI recognises a single nucleotide polymorphism that is present in the *TPS6* transcript but not the *TPS11*.

Fungal Quantification

DNA was extracted from inoculated leaf samples at the four time points (T0, T1, T2 and T3) using the CTAB method. DNA concentration and purity was checked using a Nanodrop spectrometer and integrity was checked by running DNA on a 0.1 % agarose gel and visualising the bands. The reference maize gene *glutathione S-transferase III* (*gst3*) and *C. zeina* gene

cytochrome P450 reductase 1 (*cpr1*) were used to amplify DNA from the respective organisms (Korsman et al., 2011). The published primer sequences (Korsman et al., 2011) that were used are; gst3F – 5'GGAGCCCTGAGTCGAATAAAAG3', gst3R – 5'AACACACACGAAAGGCAACAGT3', cpr1F – 5'TGAACTACGCGCTCAATG3' and cpr1R – 5'TCTCTCTTGGACGAAACC3'. Quantitative PCR was done in triplicate per sample. Each tube contained 5 µl of Kapa SYBR Fast qPCR master mix, 200 nM of the forward and reverse primers and 1 µl of the DNA template in a total reaction volume of 10 µl. Samples and the serial dilutions (for the standard curve) were run on a light cycler (Applied Biosystems, California USA) at 95°C for 10 min then 40 cycles of 95°C for 15 sec and 60°C for 1 min. The mean Cq was calculated from the three technical replicates. The amount of DNA in nanograms for each sample was calculated based on the slope of the standard curve. To normalise, amount fungal DNA was divided by amount of maize DNA.

Phytoalexin Analysis

Maize phytoalexins consisting of zealexins and kauralexins were extracted from various maize leaf tissue samples. Two methods were used in the study. Samples that were analysed according to the protocol described by Schmelz et al 2004 were sent to the USDA (Florida, USA) on dry ice for GC: MS analysis. Maize leaf samples were ground up in liquid nitrogen and 100 µg were placed in screw cap micro tubes. Extraction was done by adding 300 µl of 1-propanol: H2O: HCl (2:1:0.005) to each sample and shaking for 30 sec in a tissue homogenizer. To this, 1 ml of $MeCl_2$ was added and the sample was shaken for 5 sec, then centrifuged at 11 000 X *g* for 30 sec. The bottom layer of $MeCl_2$ was pipetted carefully into a new tube.

Derivatization of the compounds to form methyl esters was done by adding 2 µl of 2.0 M trimethylsyldiazomethane in hexane to the samples. The tubes were vortexed and incubated at room temperature for 30 minutes. To quench the excess trimethylsyldiazomethane, 4 µl of 2.0 M acetic acid was added to each sample. Surplus solvent was removed under a N_2 stream and samples were re-dissolved in 100 µl of $MeCl_2$.

Chemical ionization gas chromatography mass spectrometry was used to analyse the phytoalexin compounds. This was done using a gas chromatograph HP 6890 interfaced to a mass spectrometer HP 5973 (Hewlett-Packard, Palo Alto, CA, USA) (Schmelz et al., 2004). Isobutane was the ionisation gas at a reaction pressure of 1.0×10^{-4} torrent and helium was

the carrier gas at 0.7 ml per minute. Separation was done on a column of dimensions 30m X 0.25 mm X 0.25 mm at a temperature of 70°C for 1 minute, then increased by 15°C per minute to 300°C and held for 7 minutes (Huffaker et al., 2011; Schmelz et al., 2011). The selected ion mass units (SIM) and retention times for each compound were measured. The internal control standard used was $^{13}C_{18}$ linolenic acid.

In an effort to establish a local protocol, the second group of samples were analysed at the Central Analytical Facility (CAF) at Stellenbosch University. To extract the metabolites, the leaf tissue was ground finely in liquid nitrogen and 100 mg was placed in a micro tube. To this 900 µl of 2: 1 methylene chloride ($MeCl_2$): 1-propanol was added and samples were incubated at room temperature with shaking for 4 hours. The tubes were centrifuged at 11,300 X *g* for 30 seconds and the liquid phase was transferred to a new tube leaving the leaf debris behind. The centrifuge step was repeated and the bottom organic liquid layer was carefully transferred into a new tube. The samples were dried down overnight using a vacuum centrifuge Speed Vac (Savant, Thermo Scientific, Massachusetts, USA) and stored at 4°C before being transported to the CAF.

The GC-MS protocol applied at CAF was slightly different. Electronic ionization using a gas chromatograph (Thermo Trace 1300) linked to a mass spectrometer (TSQ8000) (Thermo Scientific, Massachusetts, USA) was carried out. One µl of the derivatized sample mixture was injected onto a Restek Rxi5Sil MS column with dimensions 15m x 0.25 mm id x 0.25 µm film thickness. The instrument settings were inlet temperature of 250°C, split flow of 30 ml/ min, surge pressure of 300 kPa/ min, carrier gas flow was 1.2 ml/ min. Temperature was at 100°C for 2 min then increased by 10°C per minute to 300°C and held for 5 minutes. The mass spectrometer was set in scan mode and software used to extract ions of the relevant m/z from the raw chromatograms was XCalibur 2.0. No internal control was used.

Genevestigator Analysis

GENEVESTIGATOR is an online resource for microarray data and RNA-seq data (Zimmermann et al., 2005). This resource was used to identify expression levels of the phytoalexin biosynthesis genes *TPS6/11* (GRMZM2G127087) and *CPPS2* (GRMZM2G044481) in other maize lines and in different biotic and abiotic stresses including fungal pathogens, nematodes, pests and drought. The accession numbers (GRMZM2G127087 and GRMZM2G044481) were

used to identify existing experiments in Genevestigator. The biotic and abiotic perturbations were selected and the gene expression output for each sample and technical replicates in each experiment was given in a scatterplot in a range from low medium and high. The interquartile range was used based on the signal intensity on Affymetrix Maize Genome Array.

Promoter Region Analysis

In order to analyse the promoter regions of the phytoalexin biosynthetic genes, the type and number of *cis* acting regulatory elements and their functions were studied. A 1 kb length of DNA sequence upstream of the transcription start site (TSS) (Li et al., 2014; Sharma et al., 2011) of the *TPS6/11* and *CPPS2* genes were downloaded from the grass plants promoter database grasspromdb [6] using their accession numbers GRMZM2G127087 and GRMZM2G044481 respectively. This sequence was entered into two online databases for plant cis acting regulatory elements which are; Plant cis acting regulatory DNA elements (PLACE) (Higo etal., 1999) database and Plant Cis Acting Regulatory Elements (PLANTCARE) (Lescot et al., 2002). The consensus output of the *cis*-acting regulatory elements from both databases was presented in the results.

[6] http://grassius.org/grasspromdb.html

Chapter 3 : Results

This chapter consists of five sections of experiments that consist of wet lab and bioinformatics. The first section is 'Analysis of phytoalexin accumulation and gene expression in B73 maize during the development of GLS disease' followed by the 'Analysis of chitosan as an elicitor by measuring the callose deposition, metabolite accumulation and gene expression' section and the 'Comparison of early phytoalexin accumulation in maize seedlings in five diverse African maize lines and B73' section. In the bioinformatics experiments, there is 'Analysis of the expression of the phytoalexin biosynthetic genes in various biotic and abiotic stresses using Genevestigator' section and the '*Cis*-acting regulatory elements found in the promoter of the phytoalexin biosynthetic genes' section. Each section seeks to fulfil the aims described in Chapter one.

Analysis of Phytoalexin Accumulation and Gene Expression in B73 Maize during the Development of GLS Disease

In this section, induction of phytoalexin accumulation and expression of phytoalexin biosynthetic genes was investigated in the maize cultivar B73 following inoculation with *C. zeina*. It has recently been shown that zealexins and kauralexins (the two classes of maize terpenoid phytoalexins) accumulate as a defence response to fungal pathogens and that the genes *TPS6*, *TPS11* as well as *CPPS2* are upregulated preceding this (Huffaker et al., 2011; Schmelz et al., 2011). In addition a recent unpublished microarray study showed that gene expression of *TPS6/11* and *CPPS2* was upregulated in *C. zeina* inoculated maize (Crampton and Murray, pers com). Therefore the experiments described in this section aimed to validate the microarray study and expand on it further by looking at both phytoalexin accumulation and expression of phytoalexin biosynthetic genes at different stages of GLS lesion development.

In this study, B73 maize plants were grown in a greenhouse at the University of Pretoria and inoculated with a 1 X 10^5 spores/ ml suspension of *Cercospora zeina* conidiophores (Meisel et al., 2009) by our associate Dr Bridget Crampton. Samples of the maize leaves were harvested at four stages designated T0, T1, T2 and T3 during the course of the disease progression during which the characteristic symptoms of GLS changed, as shown in Table 3.1 and Figure 3.1.

As indicated in Table 3.1, a long lag phase was observed from the date of inoculation to symptom development (first seen at 17dpi), which corresponds to the slow initial growth pattern of *Cercospora* species (Beckman & Payne, 1982) after which development of disease symptoms progressed rapidly. A 15 cm length of the leaf (equivalent to a CD cover) was measured to demarcate the area around the inoculation point (Figure 3.1). This tissue was harvested and couriered to UCT for further analysis. Three plants representing three biological replicates were harvested per time point.

Table 3.1: Symptoms of GLS on maize leaves

Time-point	T0	T1	T2	T3
Days post inoculation	0	17	18	24
Age of plants in days[α]	49	66	67	81
Description	No symptoms	Chlorotic flecks	Elongation	Fully developed

[α] Days after sowing

Photographs of the GLS leaf symptoms were taken and these are shown in Figure 3.1 below to give a visual representation of the symptoms of GLS obtained in the experiment. Figure 3.1 a) was taken at T0 and there were no visible symptoms of GLS as shown in the image. (The stripes of green were due to fertilizer limitations in the greenhouse and are not symptoms of disease). Figure 3.1 b) was taken at T1 and shows the formation of chlorotic flecks on the leaf surface. These are seen as independent irregular shaped yellowing lesions on the leaf surface. Figure 3.1 c) was taken at the start of lesion elongation (T2). The lesions are confined to the inter-veinal region of the leaf veins. Figure 3.1 d) was taken at the final stage of disease development designated T3. The lesions had joined together to cover most of the leaf.

a) No Symptoms

b) Chlorotic Flecks

c) Lesion elongation

d) Lesion coalescence

Figure 3.1: Symptoms of GLS on maize leaves. Leaf samples were harvested at the four stages of GLS disease progression. The figure shows a) leaves with no symptoms that were harvested at zero days post inoculation (dpi), b) chlorotic flecks 17 dpi c) lesion elongation 18 dpi and d) fully developed GLS at 24 dpi (Photo credit: Maryke Carstens).

In order to determine the disease progression at the molecular level, the amount of fungal growth was measured using a quantitative PCR method previously described for *C. zeina* (Meisel et al., 2009). The abundance of fungal DNA was expressed in relation to the amount of maize DNA. Figure 3.2 below shows the quantification of *C. zeina* DNA at each of the four stages of disease progression. Three biological and three technical replicates were used. The data show a general trend of increasing amounts of the fungal DNA as the GLS symptoms expand. At T0 there is a larger fungal quantity than at T1, most likely due to the *C. zeina* inoculum added to the samples immediately before sampling. It increases at T2 relative to T1

and then furthermore at T3. No statistically significant differences were detected using ANOVA (supplementary data table i).

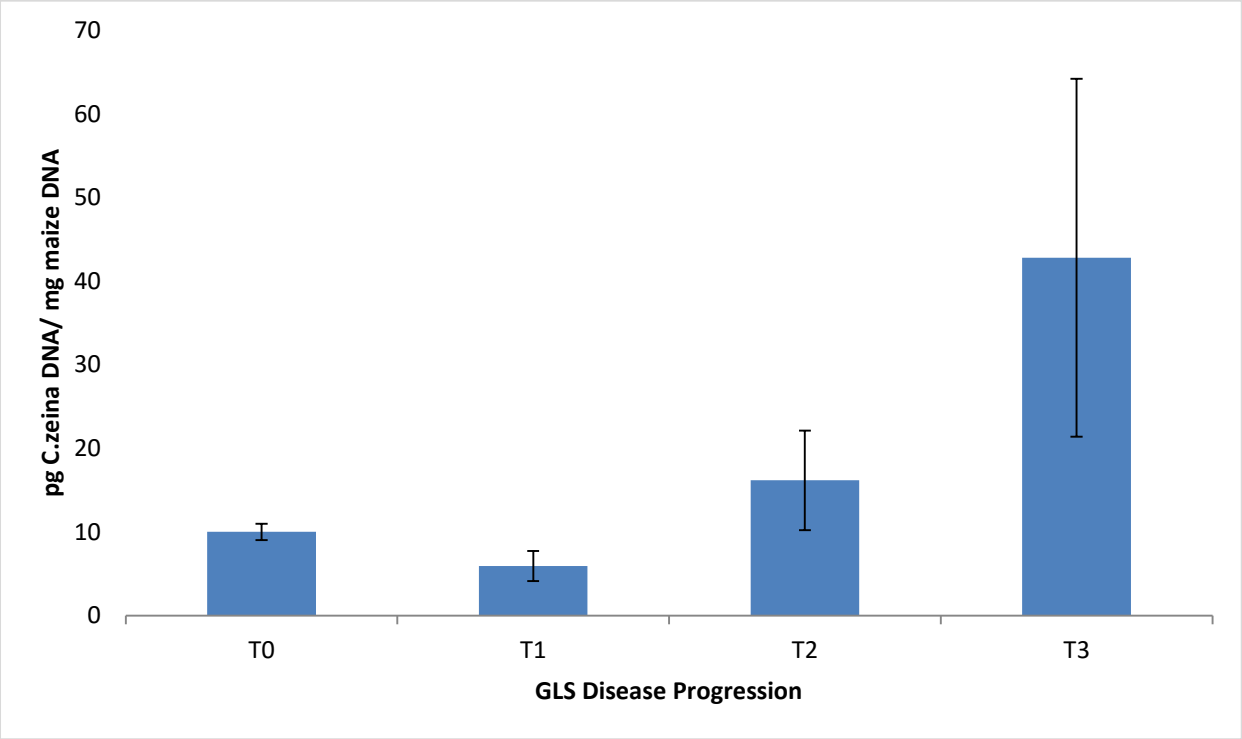

Figure 3.2: Quantity of *C. zeina* DNA per unit of maize DNA. The histogram shows the quantity of *C. zeina* DNA in picograms (pg) per unit in milligrams (mg) of maize DNA, at T0, T1, T2 and T3 time-points of GLS disease. The trend is increasing amounts of fungal DNA as the disease progressed but ANOVA showed no significant differences (n=3; SD; $p<0.05$).

The phytoalexin accumulation in maize plants inoculated with *C. zeina* was analysed at the four stages of disease development described above: T0, T1, T2 and T3. At each time point the phytoalexin metabolites were extracted and quantified using GC: MS following isobutene chemical ionization with helium as the carrier gas (Schmelz et al 2011). Several zealexin and kauralexin signatures were identified at each harvested time point (see supplementary table iv). One zealexin (zealexin B2) that we expected to see, was missing and this could be due to differences in the type of maize tissue analysed. We used leaf tissue while the Huffaker et al (2011) reported results using maize stem tissue. The combined total amounts for each phytoalexin group (zealexins and kauralexins) were plotted on a histogram as shown in Figure 3.3. The general trend of phytoalexin accumulation across the time points was increased

amounts as the disease progressed from T0 up to T2 then a reduced level at the last time point T3. In the infected maize samples the kauralexins accumulated in larger quantities than the zealexins as shown at each time point in Figure 3.3 below, with the exception of the first time point where the quantity of zealexins was higher than the kauralexins. This time point (T0) was taken on the day of inoculation therefore it is considered to be the baseline representing the normal metabolite levels in the maize plants. This indicates that the zealexin baseline levels are higher than kauralexins in the B73 line. The nutrient deficiency due to fertiliser limitations could not be ruled out as a factor influencing the high baseline levels of zealexins observed.

The ANOVA statistical analysis showed that for the category of zealexins there were no significant differences in accumulation of this class of phytoalexin across all the time points (supplementary data table ii). In the kauralexins shown in red in Figure 3.3 below, there were significant differences between T0 and T2 (supplementary data table iii), which corresponds to the highest and lowest levels of kauralexin.

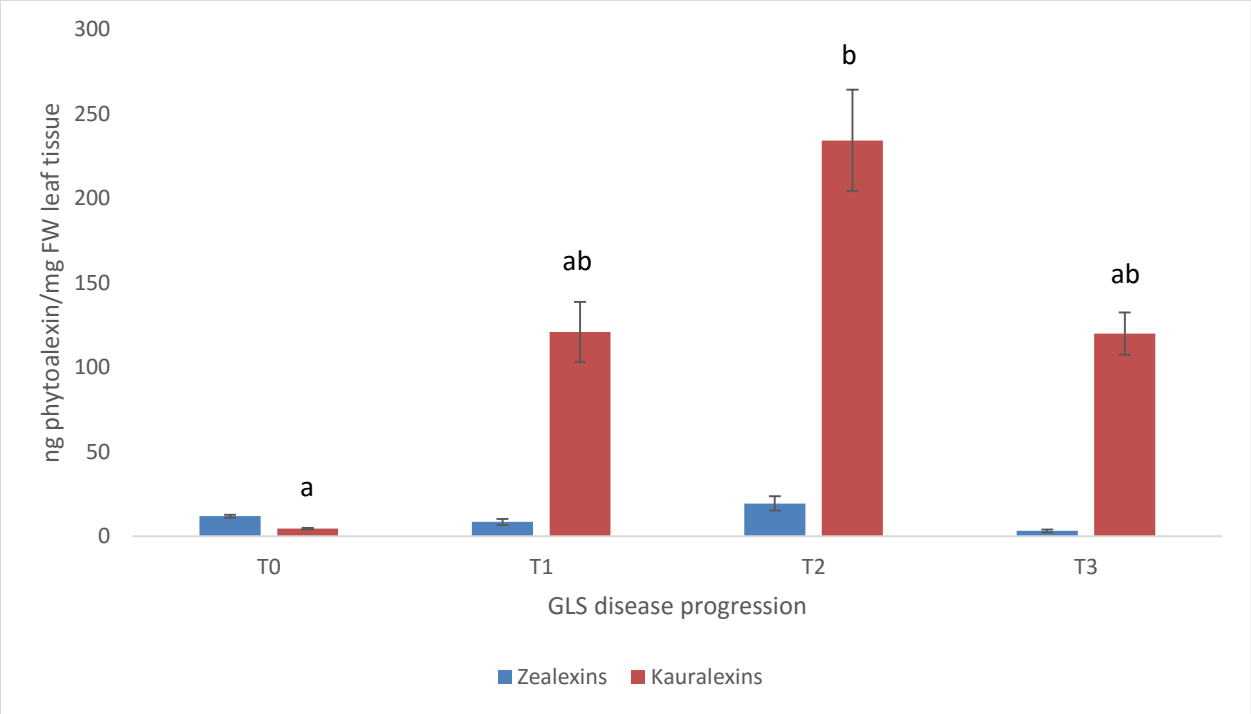

Figure 3.3: Phytoalexin analysis in B73 during GLS disease development. Average total zealexin and kauralexin compounds (n=3; ±SD) detected at the four time-points T0, T1, T2 and T3 following *C. zeina* inoculation. ANOVA showed no significant differences in accumulation

of zealexins between the different time points. However kauralexin accumulation at T0 was significantly different to T2 ($p<0.05$).

Gene expression analysis of the phytoalexin biosynthesis genes encoding ent-copalyl diphosphate synthase (*CPPS2*) and terpene synthase 6/11 (*TPS6/11*) was carried out. These genes have previously been identified as biosynthetic genes leading to kauralexin (*CPPS2*; (Schmelz et al., 2011)) and zealexin (*TPS6/11*; (Huffaker et al., 2011)) accumulation. Previously *TPS6* and *TPS11* were thought to be tandemly duplicated genes (Huffaker et al., 2011), however BLAST analysis using the current annotation of the maize genome indicates that the primer pairs that were used to define *TPS6* and *TPS11* align to the same gene (GRMZM2G127087). The gene has three alternative transcripts, two of which correspond to the primer pairs used for detection of *TPS6* (RefSeq: NM_001112204) and *TPS11* (RefSeq: NM_001112480) expression. Protein analysis using Uniprot indicated that both transcripts encode proteins with two putative terpene synthase domains, which could explain why previous authors assumed it that they corresponded to two tandemly repeated genes. The third transcript was not included in this study because it does not have a reference sequence (RefSeq) number[7] and not much is known about its activity in plant defence or otherwise. Figure 3.4 below is an illustration of the distribution of the transcripts along the main gene locus.

[7] RefSeq is a comprehensive non redundant compilation of genomic sequences of organisms administered by the national centre for biotechnology information (NCBI)

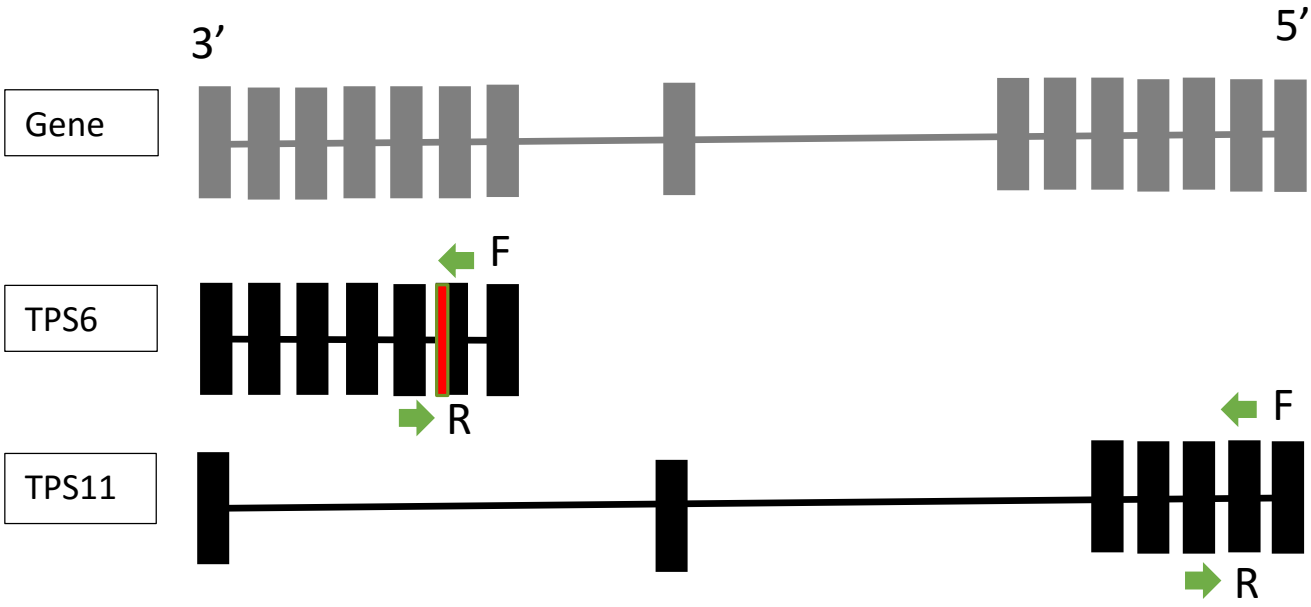

Figure 3.4: Location of TPS6 and TPS11. The figure shows the positions of the exons (blocks) and introns (lines) that are differentially spliced to make up the *TPS6* and *TPS11* transcripts. The arrows show the positions of the forward and reverse primers and the red line indicates the location of the restriction enzyme *AgiI*/ *BmgBI* digestion site, used to confirm the presence of TPS6 (Huffaker et al 2011).

In order to confirm that the *TPS6* primers amplified the *TPS6* transcript and not the *TPS11* transcript, the PCR products were digested by the restriction enzyme *AgiI/BmgBI*. The restriction recognition site (CACGTC) is present only in *TPS6* at position 338 from the transcription start site but not in *TPS11* (Huffaker et al., 2011).

Figure 3.5 shows a 2% acrylamide gel image with the post PCR products and the post restriction enzyme digest products. The PCR products were of different sizes of 294 nucleotide units for *TPS6* and 398 bp for *TPS11*, and to confirm that each primer pair was amplifying the correct gene restriction enzyme digestion was carried out. The restriction enzyme digestion showed the two bands of the cleaved *TPS6* gene product while *TPS11* remained uncut. Gene expression analysis could then be carried out once it was confirmed that the primers were amplifying the correct transcript.

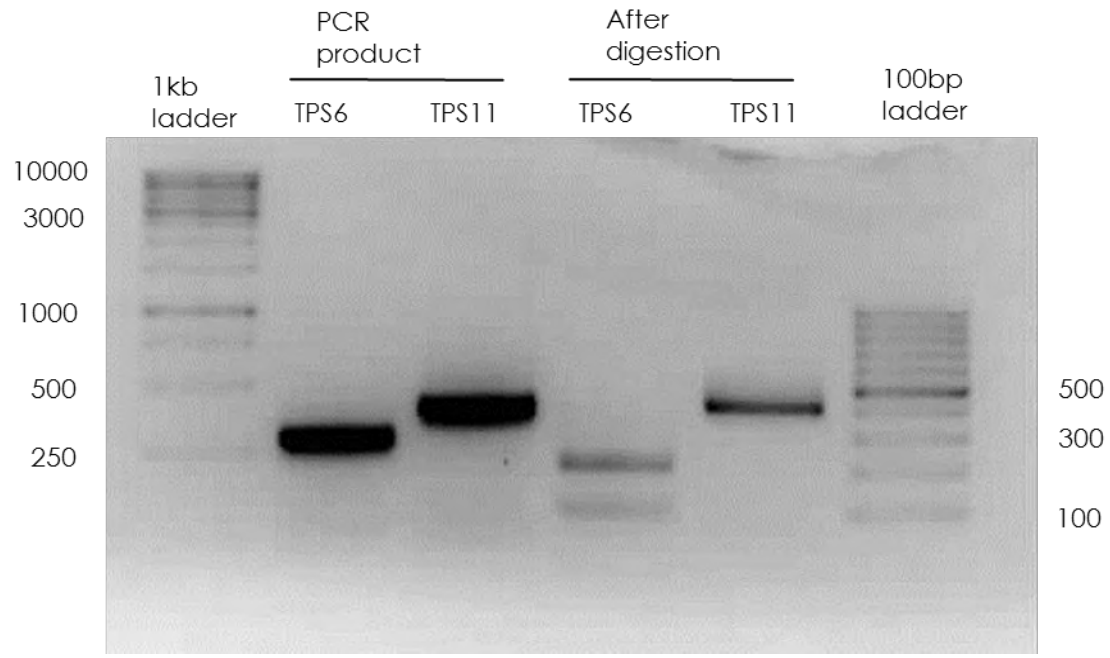

Figure 3.5: *TPS6/TPS11* differentiation Gel. The gel image above shows the PCR products (before and after digestion with *AgiI/BmgBI*) generated using the *TPS6* and *TPS11* primers. Digestion with the restriction enzyme cleaved *TPS6* only at position 338 from the TSS.

The relative gene expression was plotted at each time point for each gene in Figure 3.6 below. Relative expression for each gene was normalised using three reference genes, according to the MIQE guidelines. All three genes were upregulated in response to *C. zeina* inoculation and have a general trend of increased relative gene expression as the disease progressed. Statistical analysis was done for each gene using ANOVA. For *TPS6* and *CPPS2* each time point was significantly different from the other time points as shown by the letters on the graphs below. For *TPS11* all time points except for T2 and T3 are significantly different from each other (supplementary data tables v to vii).

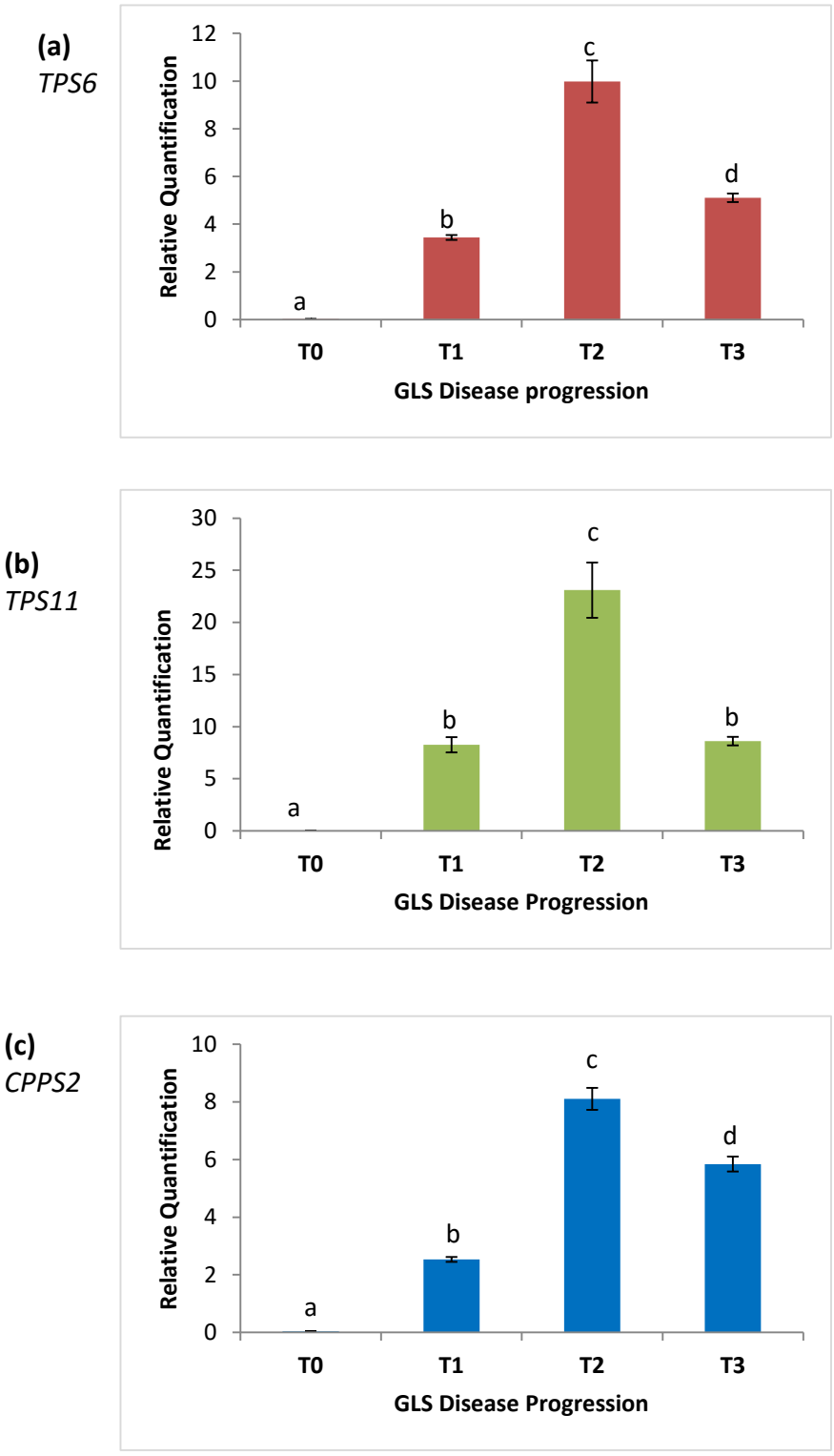

Figure 3.6: Gene Expression of (a) *CPPS2*, (b) *TPS6* and (c) *TPS11* in response to *C. zeina* inoculation. The compound figure above shows average gene expression of the three phytoalexin biosynthetic genes of maize a) ent-copalyl-diphosphate synthase 2 (*CPPS2*) b) terpene synthase 6 (*TPS6*) c) terpene synthase 11 (*TPS11*) (n=3 ± SD). ANOVA showed

significant differences at all time points for *TPS6* and *CPPS2*. For *TPS11* there were significant differences at all time points except between T2 and T3 ($p<0.05$).

The table below shows the correlation coefficients calculated for a gene and its corresponding phytoalexin group comparing *TPS6* vs Zealexin accumulation, *TPS11* vs Zealexin accumulation and *CPPS2* vs Kauralexin accumulation across all four time points. Kauralexin accumulation correlates very well (0.924) with expression of *CPPS2*, the biosynthetic gene. Zealexin accumulation did not have a significant difference across the four time points even though the gene expression analysis showed significant increases as the disease developed, and the correlation of TPS6 and TPS11 with zealexin accumulation was lower (0.474 and 0.593 respectively).

Table 3.2: Correlation of gene expression and phytoalexin accumulation

Categories	**Correlation coefficient**
***TPS6* vs Zealexins**	0.474
***TPS11* vs Zealexins**	0.593
***CPPS2* vs Kauralexins**	0.924

Analysis of Chitosan as an Elicitor of Phytoalexin Accumulation in Maize

B73 maize plants were infiltrated with chitosan in order to mimic the activity of the fungal elicitor chitin that may play a role in the establishment of a *Cercospora zeina* defence. It was established in related literature that in rice, the terpenoid phytoalexins sakuranentin and momilactone accumulated following chitosan treatment and this also resulted in lesion formation on the leaves (Agrawal et al., 2002). A number of other defence related changes including the production of defence proteins OsPR5 and OsPR10 were also observed. Since these defence responses were mounted in rice in response to chitosan, it would be interesting to see if the same applies for phytoalexins in maize.

A callose assay was used to measure the amount of callose formed as a defence response to chitosan infiltration (Agrios, 2004; Ahmad et al., 2010). Callose accumulation was measured using aniline blue dye which binds to callose and emits fluorescence (Annegret Kohler, 2000). Fluorescence was visualised at excitation 368 nm and emission 410 – 460 nm using a UV filter in a fluorescent plate reader.

In order to establish the incubation time with the highest callose response post inoculation, maize leaves were harvested at 12, 24, 36 and 48 hours post infiltration. Figure 3.7 below shows the fluorescence levels for two sets of samples infiltrated with either 0.2% acetic acid or 0.1% chitosan. Statistical analysis carried out using ANOVA showed that the chitosan 48 hours sample was significantly different to all four acetic acid treatments and the other chitosan treatments except for the chitosan 36 hours only (Figure 3.7, supplementary data tables viii a. and b.).

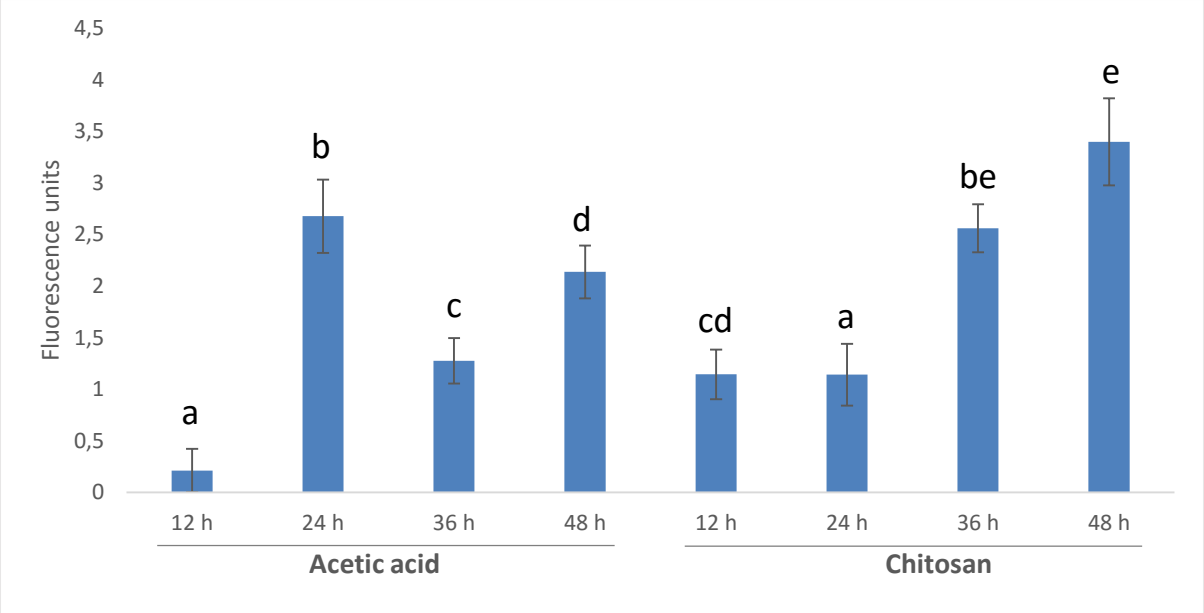

Figure 3.7: Optimisation of the callose assay. The figure shows average fluorescence levels for the samples infiltrated with 0.1% acetic acid and 0.2% chitosan solution (n=4; ± SD). The samples of leaves from V3 maize plants were harvested at different times post infiltration; at 12, 24, 36 and 48 hours. ANOVA showed significant differences as indicated on the graph with letters and the highest callose deposition was observed at 48 hours ($p<0.05$).

As the highest fluorescence was observed at 48 hours post chitosan treatment, it was decided that this time point should be used in a subsequent experiment aimed at investigating the effect of chitosan treatment on phytoalexin accumulation. Leaves from maize plants at growth stage V3 were infiltrated with the same four treatments (No treatment, water, 0.2 % acetic acid and 0.1% chitosan) and harvested at 48 hours post infiltration only. The control for infiltration was the water and the control for dilution of chitosan was the acetic acid.

Four biological replicates, corresponding to four plants, were used. Figure 3.8 shows the fluorescence units of each treatment and these correspond to callose formation in the infiltrated leaf. Statistical analysis using ANOVA showed that No treatment and Water were not significantly different from each other. Acetic acid was significantly different from No treatment but not water. Finally Chitosan was significantly different from all three controls ($P<0.05$; supplementary data table ix a. and b.). This confirmed that the callose deposition

that occurred in the chitosan infiltrated samples was significantly higher than in the control samples and this could indicate a greater defence response.

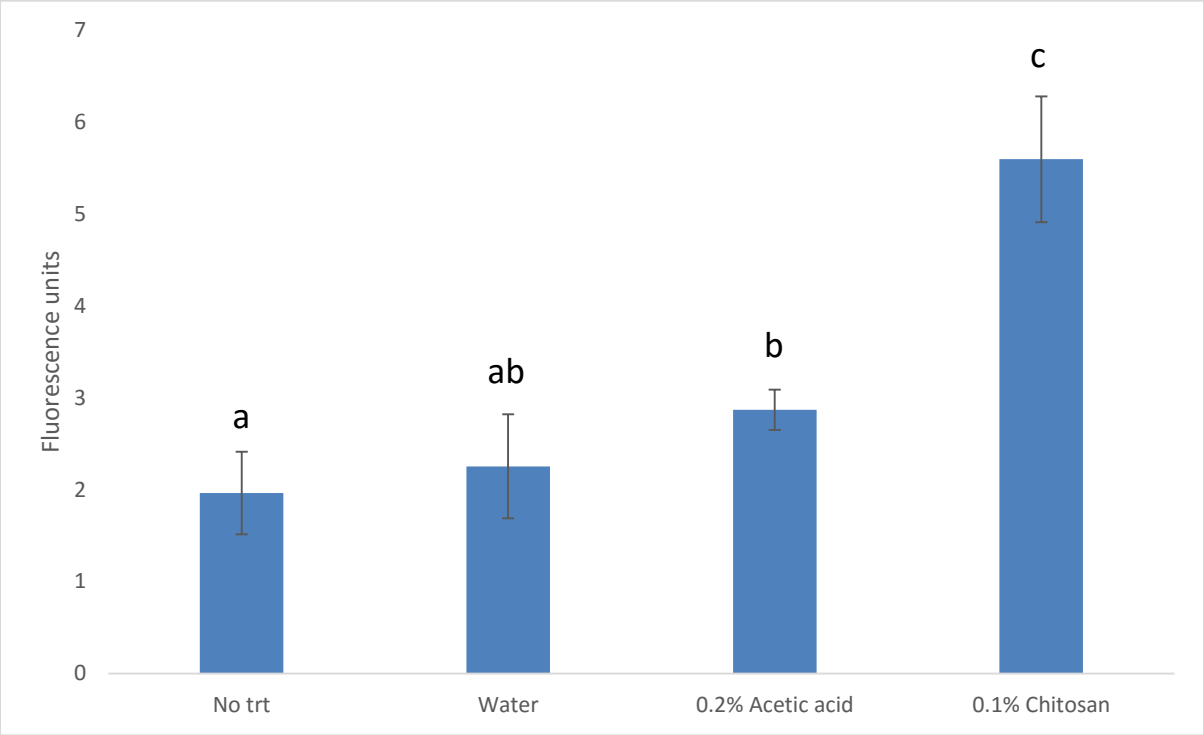

Figure 3.8: Callose assay. The figure above shows average fluorescence readings which correlate to callose deposition levels from leaf samples harvested at 48 hours post infiltration with chitosan (n=4; ±SD; $p<0.05$). The controls were no treatment (No trt), sterile distilled water and 0.2% acetic acid which served as a carrier. 0.1% chitosan was dissolved in 0.2% acetic acid.

Phytoalexin metabolites were extracted from maize leaf samples analysed in Figure 3.9 and analysed using GC: MS electronic ionization[8]. Figure 3.9 shows the total zealexins and kauralexins for each treatment. For the constituent phytoalexins see supplementary table iv. Not all the phytoalexins observed in previous studies (Huffaker et al., 2011; Schmelz et al., 2011) were observed here, most likely due to differences in sensitivity between the chemical and electronic ionisation methods in the GC: MS methods used. Nevertheless, total zealexins and kauralexins were analysed further. The trend shows that zealexins are more abundant

[8] Electronic ionization was used in the samples analysed locally in South Africa, a slightly different method to the chemical ionization used in the samples (Section 1: B73 GLS Experiment) that were analysed in the USA.

than the kauralexins in young seedlings. Furthermore, the zealexin and kauralexin groups show similar levels of phytoalexins in the controls as in the plants infiltrated with chitosan. Statistical analysis using ANOVA showed that for the zealexins there were no significant differences amongst the four treatments and same applies for the kauralexins (supplementary data tables from x and xi).

Therefore, while chitosan can act as a PAMP to induce callose formation in maize, it does not act to induce phytoalexin accumulation. In rice (Agrawal et al., 2002) chitosan infiltration caused chlorotic leaf symptoms, phytoalexins and defence related proteins. This is in contrast to another elicitor, pectinase - that was isolated from *R. microsporus* – which resulted in a phytoalexin accumulation response in maize (Schmelz et al., 2011).

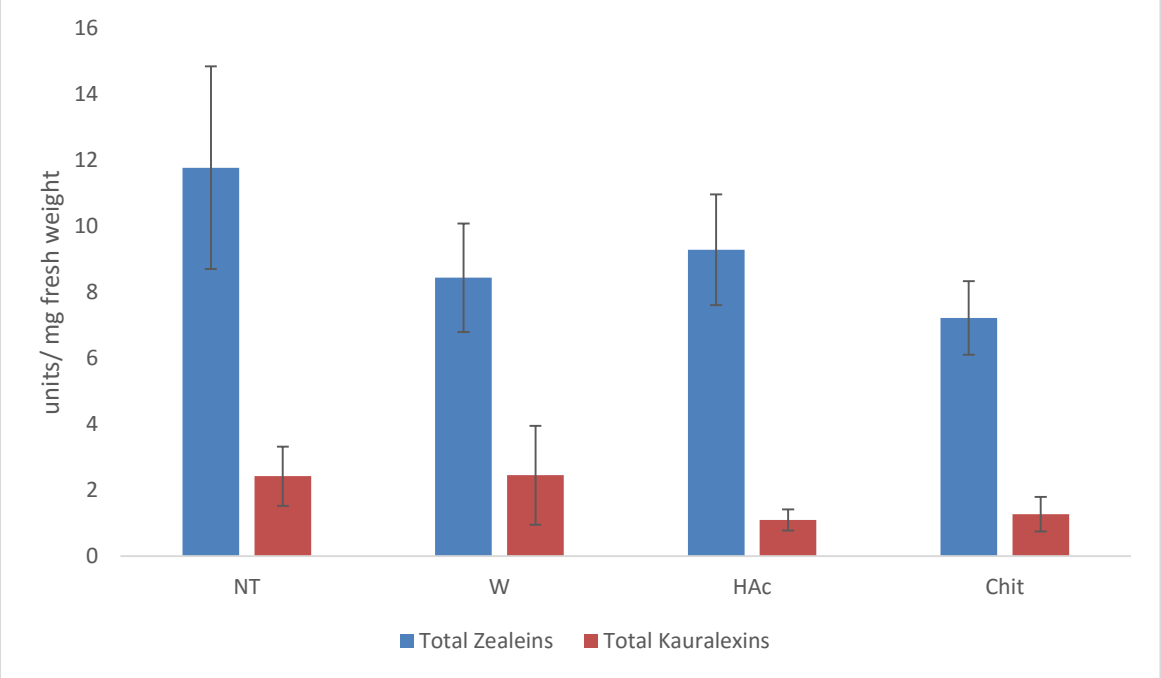

Figure 3.9: Average accumulation of total zealexins and kauralexins in response to chitosan treatment. (n=4; ± SD). NT – no treatment, W – water, HAc – 0.2 % acetic acid and Chit – 0.1 % chitosan suspended in 0.2 % acetic acid. The first three are controls while the last one is the test treatment. ANOVA statistical analysis showed no significant differences ($p<0.05$).

Leaf samples from the same experiment were used for RNA extractions, in order to establish if chitosan treatment increased the expression of phytoalexin biosynthetic genes. The aim was to determine whether the phytoalexin biosynthesis pathway was activated by treatment

with the chitosan elicitor. The genes used were *TPS6*, *TPS11* (the zealexin biosynthesis genes) and *CPPS2* (the kauralexin biosynthesis gene).

The results are shown in Figure 3.10 below. The relative gene expression of *TPS6* was low for the first two controls (No treatment and water), was significantly higher in the 0.2 % acetic acid control – possibly due to an outlier in one of the replicates or an acid response – and low in the 0.1 % chitosan treatment. *TPS11* expression remained unchanged in all four treatments, while *CPPS2* expression showed no significant differences between the four treatments (supplementary data tables from xii to xiv) which is in line with the fact that no changes are seen in the phytoalexin levels.

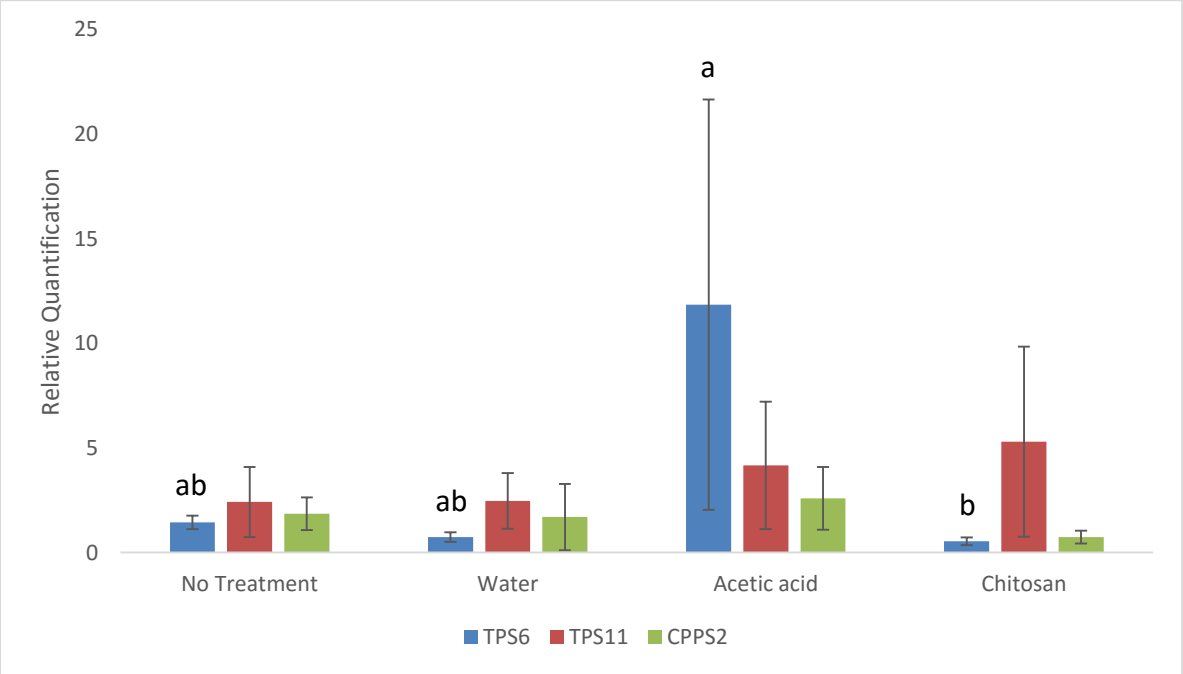

Figure 3.10: Analysis of the phytoalexin biosynthetic gene expression following chitosan treatment. The figure above shows average relative gene expression for *TPS6*, *TPS11* and *CPPS2* after infiltration with the following treatments; No treatment, Water, 0.2% Acetic Acid and 0.1% Chitosan (n=3, ± SD; $p<0.05$). Statistical analysis using ANOVA showed significant differences in *TPS6* expression and no significant differences for *TPS11* and *CPPS2* gene expression.

Comparison of early phytoalexin accumulation in six diverse maize lines and B73 at seedling stage

The aim was to select a group of maize lines with diverse genotypes and a range of disease resistance and to compare their phytoalexin accumulation and gene expression at seedling stage. Six different maize were grown up to the vegetative emergence stage (VE) and the differences in their phytoalexin accumulation and gene expression were measured. We looked at six maize lines to see if they also had any differences in their early defence response.

The VE stage of growth was chosen based on various data. Firstly Schmelz and Huffaker reported phytoalexin accumulation in the 10 day old scutellum or cotyledon of germinating seedlings (Huffaker et al., 2011; Schmelz et al., 2011). Secondly, in Genevestigator (Zimmermann et al., 2005) a scatterplot of the expression of each gene in different anatomical parts of the maize plant showed that the juvenile leaf had higher expression levels than the foliar leaf, leaf blade (lamina) and adult leaf for both genes (see supplementary Figure iii). The maize expression atlas on the maize genome database (Sekhon et al., 2011) was used to analyse the expression of the two phytoalexin biosynthesis genes *TPS11* (GRMZM2G127087) and *CPPS2* (GRMZM2G044481) across the developmental stages of the maize plant life cycle.

Figure 3.12 below shows an anatomy and development plot of the gene expression levels for (a) *TPS11* and (b) *CPPS2* on a scale ranging from pale yellow for the lowest to deep red for highest amounts. It is interesting to note that for both genes, the first leaf at stage V3 has the highest expression levels. The other anatomical parts had low to moderate expression shown in various shades of yellow as shown by the images below. The first leaf was therefore a good candidate for laboratory experiments. At this stage in the research project *TPS11* was the transcript chosen to represent the zealexin biosynthesis genes. In a separate study *TPS6* (GRMZM2G127087) expression was not observed in an African maize line (data not shown). In this study *TPS6* gene expression runs gave no amplification (data not shown), so it was decided to exclude *TPS6* from this experiment.

(a) *TPS6/11*

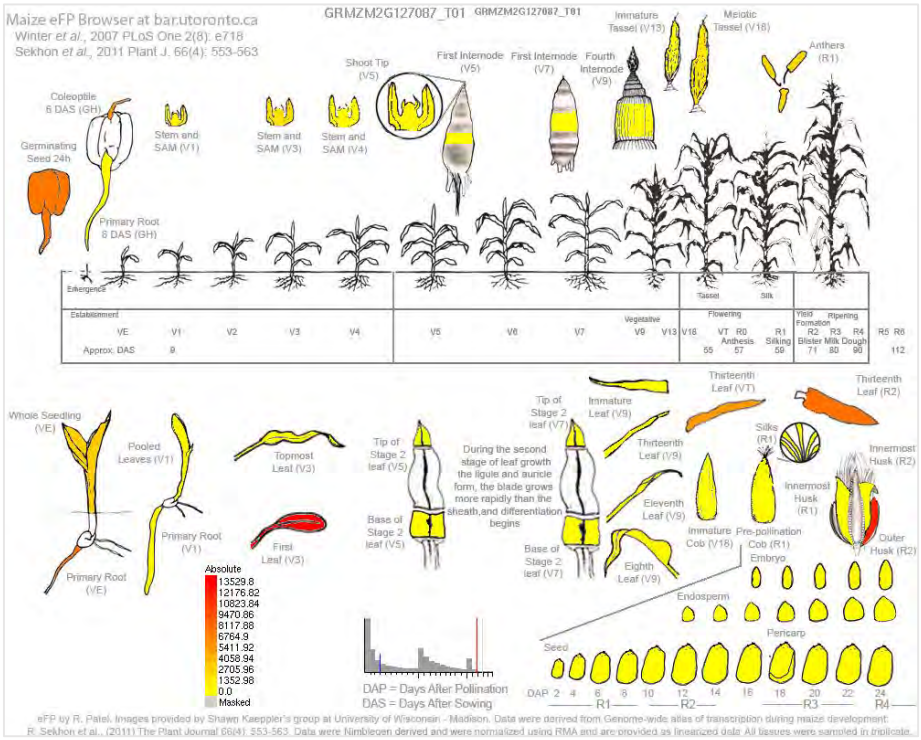

(b) *CPPS2*

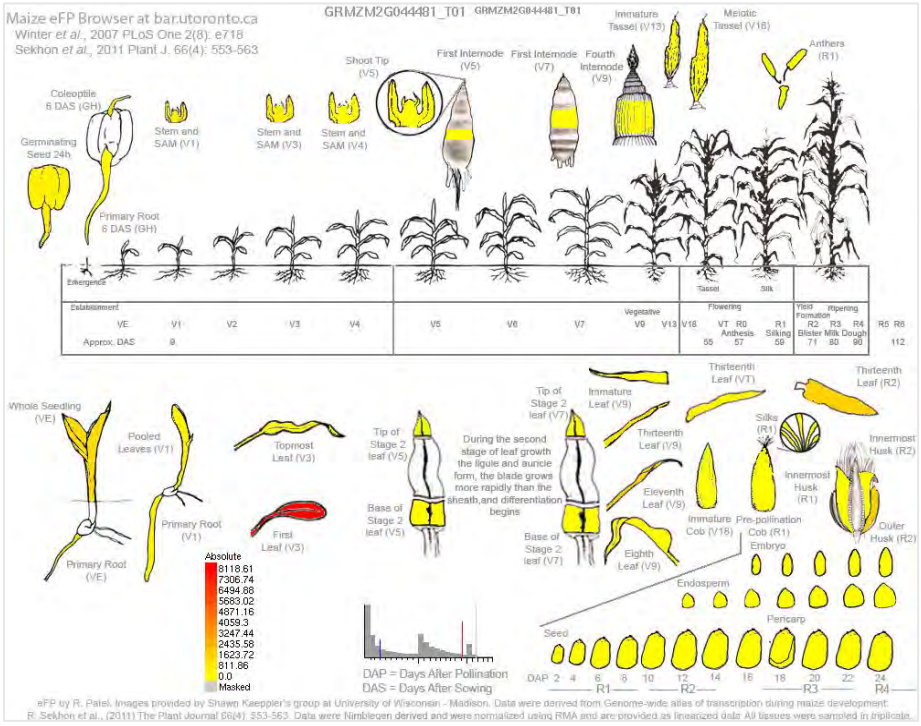

Figure 3.12: Developmental gene expression generated using data from a genome wide atlas of transcription during maize development. (Maize GDB, Sekhon et al., 2011) The figure above shows pictographs of the developmental and anatomic locations of the expression of (a) *TPS6/11* and (b) *CPPS2* obtained from the maize genetic database. The colour intensification form pale yellow to deep red represents increasing expression levels.

The six maize lines were selected, which represent local white maize lines that are grown in the southern African region, sweet corn lines and B73 (a temperate maize line). Table 3.3 below shows the full names of the six maize lines and gives their important characteristics. The maize cultivars ranged from good specific resistance to GLS in the Zimbabwean maize lines to moderate general disease resistance in the international white maize line and the South African hybrid sweetcorn. The two main groups were white maize and sweetcorn which are further subdivided to include open pollinated and hybrid sweetcorn respectively. The full name, genetic type of maize, country of origin and disease resistance are given for each cultivar.

Table 3.3: Characteristics of the six diverse maize lines

Maize line	Full name	Type	Country	Disease resistance
Star	Star7754	Hybrid Sweetcorn	South Africa	Moderate
GB	Golden Bantam	Sweetcorn	South Africa	Unknown
KEP	Kalahari Early Pearl	White maize	South Africa	Unknown
B73	B73	White maize	International	Moderate
ZM4	ZM401	OPV White maize	Zimbabwe	Good (GLS)
ZM5	ZM521	OPV White maize	Zimbabwe	Good (GLS)

In order to quantify the total phytoalexins in the six diverse maize lines, the metabolites were extracted and analysed using GC: MS[9]. The individual phytoalexins identified are summarised

[9] Electronic ionisation method.

in supplementary table iv and include two new unidentified terpenoid metabolite species[10]. Figure 3.13 shows the total zealexins and total kauralexins for each maize line. The zealexins were accumulated in larger amounts than the kauralexins for all the six maize lines. This shows that the zealexins may be playing a role as a phytoanticipin in the early defence of young seedlings, possibly against soil borne pathogens.

Statistical analysis using ANOVA showed that for zealexin accumulation there was a significant difference between B73 and KEP and no significant differences among the remaining maize lines. For kauralexin accumulation there were significant differences between Star and GB, also between GB and ZM4 and between B73 and ZM4 as shown in the ANOVA tables in the supplementary data tables xv and xvi. The units of phytoalexin per milligram fresh weight are defined as the area under the spectral peak and no internal standard was used.

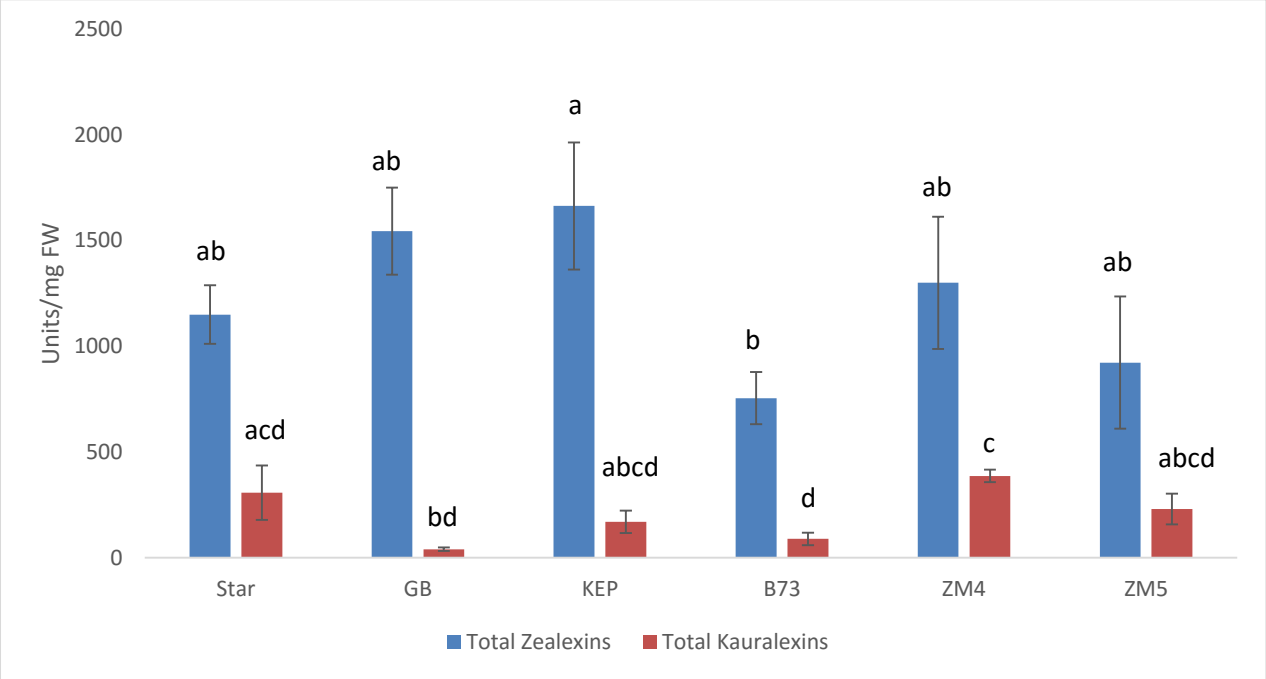

Figure 3.13: Total Phytoalexin accumulation in the six diverse maize lines. The figure above shows average phytoalexin accumulation in units per milligram of fresh weight of maize leaf sample (n=3, ± SD, $p<0.05$). Six different maize lines were analysed and the results for each cultivar are displayed as total zealexins and total kauralexins. The letters above each bar are

[10] The two unidentified kauralexin species were excluded from any calculations pending confirmation of their identity in future work.

limited to the data series i.e. only comparing amongst the zealexins or amongst the kauralexins. Three biological replicates were analysed for each sample.

The harvested diverse maize seedlings samples were analysed for their expression of the phytoalexin biosynthesis genes. The relative quantification for both *TPS11* and *CPPS2* gene expression was varied across the six maize lines as shown in Figure 3.14 below. Statistical analyses showed no significant differences across the six cultivars for *TPS11* and *CPPS2* as shown in the supplementary data ANOVA tables xvii and xviii. For *TPS11* the highest relative quantities were observed in the B73 and ZM5 cultivars while the remaining cultivars were very low. For *CPPS2* the cultivars that had the highest gene expression were Star, GB and ZM4 while KEP, B73 and ZM5 had low expression levels. There seemed to be an inverse relationship in the relative expression values of the two genes as shown by either high *CPPS2* with low *TPS11* in Star, GB and ZM4 or low *CPPS2* with high *TPS11* in B73 and ZM5. Only KEP had low relative expression of both genes.

(a)
TPS11

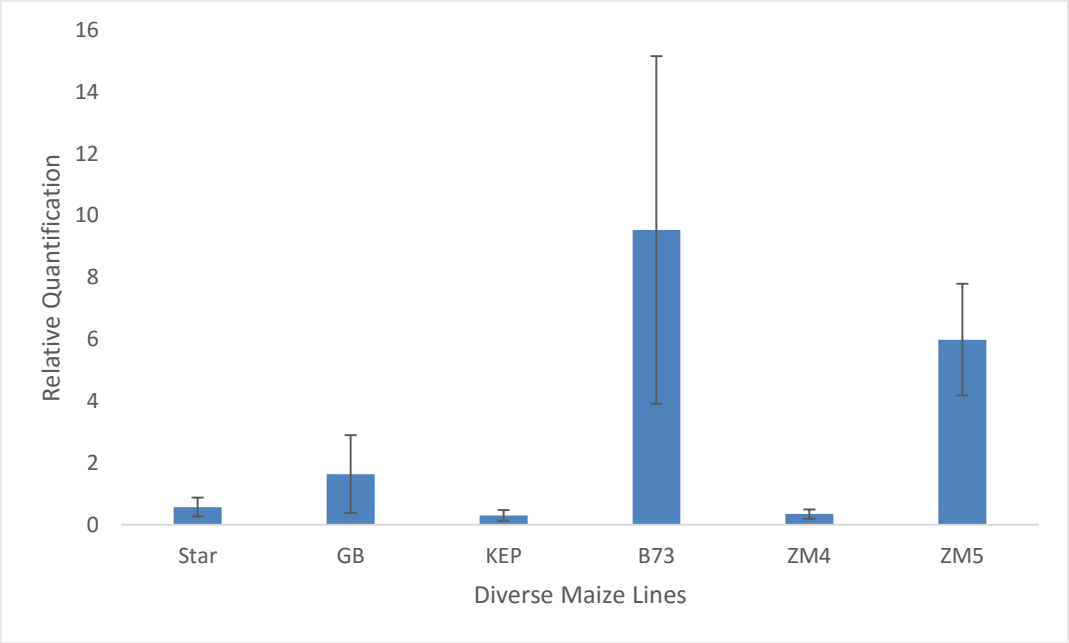

(b)
CPPS2

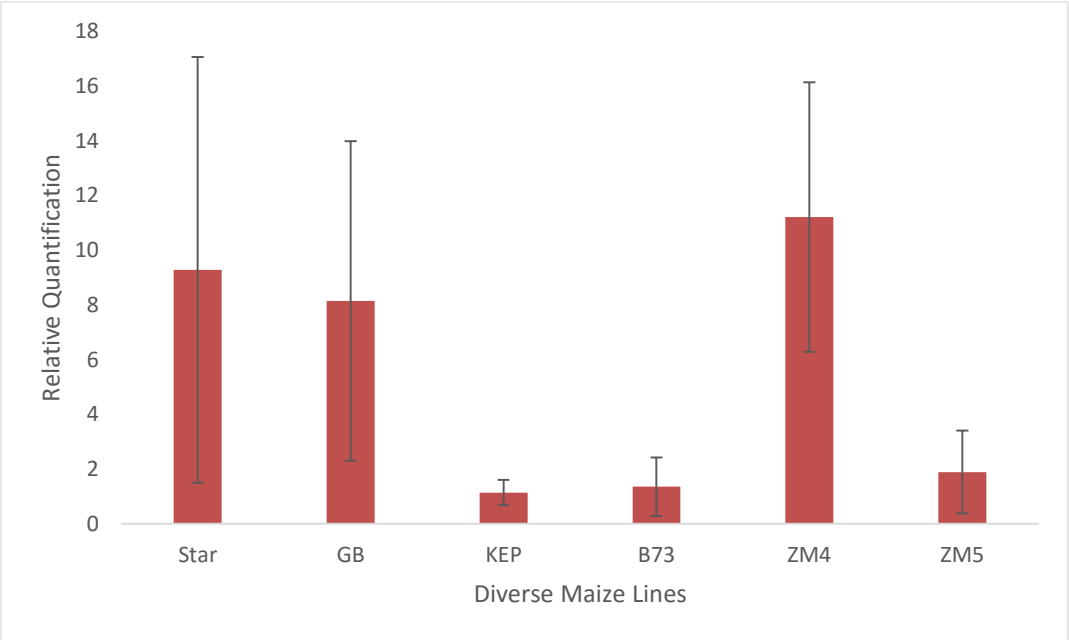

Figure 3.14: Gene Expression for (a) *TPS11* and (b) *CPPS2* in six diverse lines. The figure above shows the relative quantification of the gene expression of *TPS11* and *CPPS2* the zealexin and kauralexin biosynthesis genes. There were no statistically significant differences for both genes across the six cultivars in an ANOVA analysis (n=3; SD; $p<0.05$).

Table 3.4 shows the correlation coefficients calculated for the diverse maize lines seedlings experiment of *TPS11* vs Zealexin accumulation and *CPPS2* vs Kauralexin accumulation. Zealexin accumulation is closer to a negative (inverse) correlation with a coefficient of -0.8. *CPPS2* and kauralexin accumulation is positively correlated (0.513).

Table 3.4: Correlation of gene expression and phytoalexin accumulation

Categories	**Correlation coefficient**
***TPS11* vs Zealexins**	-0.831
***CPPS2* vs Kauralexins**	0.514

Analysis of the expression of the phytoalexin biosynthetic genes in response to various biotic and abiotic stresses using Genevestigator

The results shown in the next two sections were generated from the bioinformatics based experiments. The first experiment was to check whether the maize phytoalexin biosynthesis genes (*TPS6/11* and *CPPS2*) were upregulated in various microarray experiments that were uploaded by various scientists worldwide on the online platform called Genevestigator. The importance of this experiment was that it allowed us to see other biotic and abiotic conditions where these genes are highly expressed.

In the Genevestigator bioinformatics experiment, the expression of *TPS6/11* (GRMZM2G127087) and *CPPS2* (GRMZM2G044481) were analysed in various experiments. The tables below shows the extent of gene expression for each experimental condition, which included various fungal diseases, nematode infection, waterlogging and drought stress, on a scale of low, medium and high compared to the maximal expression of that gene. The first table displays biotic interactions while the second table looks at abiotic stresses.

High gene expression for both genes was found in the following individual experiments; *Phytophthora cinnamomi* at 6 hours post infection (hpi); *Fusarium moniliforme* strains Ye478 and BTI at 4 days post infection (dpi) in two reps each; *Colletotrichum graminicola* at 36 hpi and 96 hpi in three reps each; *Sporisorium reilianum* at 28 dpi in three reps; insect pest *Ostrinia nubilalis* in Golden Queen maize at 48 hpi and *Ustilago maydis* strains SG200 and SG200tin2 at 4 dpi in three reps each (Table 3.5). The nematode *Meloidogyne incognita* infection in the maize line A188XB73 progeny suppressed both genes at 14 dpi and 21 dpi. The abiotic conditions with high expression of both genes were waterlogging in two maize cultivars HKI1105 and V372 at 7 days recovery and at 7 days waterlogged for HKI1105 and drought in two maize cultivars HKI1532 and PC3 at 5 days in two reps each. This similarity in being highly expressed under the same conditions shows that both zealexins and kauralexins are working in the plant defence system in response to the same condition. The lowly expressed conditions include the negative controls or un-induced samples (i.e. uninfected or not subjected to the stress) (data not shown). The fact that the pattern of expression is very similar for the two genes overall suggests that they are activated together or by the same type of stimuli.

Table 3.5: Gene expression in experiments of Biotic Perturbations

Experiment name in Genevestigator	***TPS6/11***	***CPPS2***
P. cinnamomi 6hpi rep 2		
P. cinnamomi 6hpi rep 1		
P. cinnamomi 6hpi rep 3		
Control 24hpi rep 1		
P. cinnamomi 24hpi rep 2		
P. cinnamomi 24hpi rep 1		
Control 24hpi rep 3		
Control 6hpi rep 2		
Control 6hpi rep 3		
Control 24hpi rep 2		
Control 6hpi rep 1		
F. moniliforme Ye478 4dpi rep 1		
F. moniliforme BT-1 4dpi rep 2		
F. moniliforme Ye478 4dpi rep 2		
F. moniliforme BT-1 4dpi rep 1		
Control Ye478 con 4d rep 2		
Control BT-1 4d rep 2		
Control Ye478 4d rep 1		
Control BT-1 4d rep 1		
C. graminicola 96hpi 4th leaf rep 2		
C. graminicola 96hpi 4th leaf rep 1		
C. graminicola 96hpi 4th leaf rep 3		
C. graminicola 36hpi 4th leaf rep 2		
C. graminicola 36hpi 4th leaf rep 3		
C. graminicola 36hpi 4th leaf rep 1		
Control 96hpi 4th leaf rep 1		

Control 96hpi 4th leaf rep 2		
Control 36hpi 4th lea rep 3		
Control 96hpi 4th lea rep 3		
Control 36hpi 4th lea rep 1		
Control 36hpi 4th lea rep 2		
S. reilianum 28dpi ear 1-2cm rep 2		
S. reilianum 28dpi ear 1-2cm rep 3		
S. reilianum 28dpi ear 1-2cm rep 1		
Control 28dpi ear 1-2cm rep 2		
Control 28dpi ear 1-2cm rep 1		
Control 28dpi ear 1-2cm rep 3		
Control 21dpi rcel rep 3		
Control 14dpi rcel rep 3		
Control 14dpi rcel rep 2		
M. incognita 14dpi gcel rep 1		
M. incognita 14dpi gcel rep 2		
M. incognita 21dpi gcel rep 2		
M. incognita 21dpi gcel rep 3		
M. incognita 21dpi gcel rep 1		
Control 21dpi rcel rep 2		
Control 14dpi rcel rep 1		
Control 21dpi rcel rep 1		
M. incognita 14dpi gcel rep 3		
O. nubilalis 48h rep 2		
O. nubilalis 48h rep 3		
O. nubilalis 48h rep 1		
Control untreat. 48h rep 2		

Control untreat. 48h rep 3		
Control untreat. 48h rep 1		
U. maydis (SG200tin2) 4dpi rep 2		
U. maydis (SG200tin2) 4dpi rep 1		
U. maydis (SG200tin2) 4dpi rep 3		
U. maydis (SG200) 4dpi rep 1		
U. maydis (SG200) 4dpi rep 3		
U. maydis (SG200) 4dpi rep 2		
Control 4dpi rep 1		
Control 4dpi rep 2		
Control 4dpi rep 3		

Low	Medium	High

Level of expression (signal intensity on Affymetrix Maize Genome Array)

Table 3.6: Abiotic Perturbations

Experiment name in Genevestigator	***TPS11***	***CPPS2***
Waterlogged HKI1105 7d rep 1		
Waterlogged HKI1105 7d rep 2		
Waterlogged V372 7d recov. 7d rep 2		
Waterlogged V372 7d recov. 7d rep 1		
Waterlogged HKI1105 7d recov. 7d rep 1		
Waterlogged HKI1105 7d recov. 7d rep 2		
Waterlogged V372 4d rep 2		
Waterlogged V372 4d rep 1		
Control HKI1105 untreated rep 1		
Control V372 untreated rep 1		
Control V372 untreated rep 2		
Waterlogged V372 7d rep 1		

Control HKI1105 untreated rep 2		
Waterlogged V372 7d rep 2		
Waterlogged HKI1105 4d rep 2		
Waterlogged HKI1105 4d rep 1		
Drought PC3 5d leaf rep 2		
Drought PC3 5d leaf rep 1		
Drought HKI1532 5d leaf rep2		
Drought HKI1532 5d leaf rep 1		
Control HKI1532 leaf rep 2		
Control HKI1532 leaf rep 1		
Control PC3 leaf rep 2		
Control PC3 leaf rep 1		

Low	Medium	High

Level of expression (signal intensity on Affymetrix Maize Genome Array)

Cis-acting regulatory elements found in the promoter of the phytoalexin biosynthetic genes

This section looks at the analysis of *cis*-acting regulatory elements located in the promoter region of the two phytoalexin biosynthetic genes in the B73 maize genome. B73 was used because it is the cultivar of maize that had its entire genome sequenced and this is available online. This experiment was useful because it would show us previously identified *cis*-regulatory elements that might inform how expression of the phytoalexin biosynthesis genes is controlled under varying conditions and perhaps in different maize cultivars and sweetcorn.

A one kilo base sequence directly upstream of the transcription start site (TSS) was obtained from Ensembl plants (formerly maizesequence.org) for each phytoalexin biosynthesis gene. Two different online databases for *cis*-acting regulatory elements in plants were used to analyse the promoter sequences. These are (PLACE) (Higo et al., 1999) and plant cis acting regulatory element (PLANTCARE) (Lescot et al., 2002). PLACE is mostly based on algorithms that calculate the probability of an element being present in the DNA sequence. PLANTCARE however gives results based on research findings and also gives the organism and reference where it was previously found.

Table 3.7 and 3.8 show the combined results of the elements that were only found in both databases at the same position for *TPS11* and *CPPS2* respectively. The properties shown are name of the element, the element sequence, the strand (+ or –) on which the sequence was found and its position when counting upstream from the transcription start site (TSS) designated zero. The final column gives a description of the function of the element.

Table 3.7: *Cis*-acting regulatory elements in the 1 kb upstream of *TPS11* promoter

Element name	Sequence	Strand	PLANTCARE position and organism	PLACE position and accession no	Function
CAAT box 1	CAAT	+	-132 *Glycine max*	-131 [S000028]	Common in promoter and enhancer regions
CAAT box 1	CAAT	-	-409 *Hordeum vulgare*	-708 [S000203]	Common in promoter and enhancer regions
CAAT box 1	CAAT	-	-428 *Arabidopsis thaliana*	-427 [S000203]	Common in promoter and enhancer regions
CAAT box 1	CAAT	-	-187 *Hordeum vulgare*	-186 [S000203]	Common in promoter and enhancer regions
TATA box 3	TATTAAT	+	-680 *Glycine max*	-679 [S000110]	Core promoter element ahead of TSS
TATA box 5	TTATTT/ TTTTA	-	-825 *Lycopersicon esculentum*	-822 [S000203]	Core promoter element ahead of TSS
TATA box 5	TTATTT/ TTTTA	-	-364 *Lycopersicon esculentum*	-366 [S000203]	Core promoter element ahead of TSS

(+) denotes the forward strand and (-) denotes the reverse strand.

Table 3.8: *Cis*-acting regulatory elements in the 1 kb upstream of *CPPS2* promoter

Element name	Sequence	Strand	PLANTCARE position	PLACE position	Function
ABRE/ ABRELATERD1	(T)ACGT(G)	+	-827 *Arabidopsis thaliana*	-825 [S000414]	Abscisic acid responsiveness
ABRE/ ABRELATERD1	(T)ACGT(G)	-	-435 *Arabidopsis thaliana*	-434 [S000414]	Abscisic acid responsiveness
CAAT box 1	CAAT	+	-960 *Glycine max*	-959 [S00028]	Common in promoter and enhancer regions
CAAT box 1	CAAT	+	-733 *Hordeum vulgare*	-732 [S000028]	Common in promoter and enhancer regions
CAAT box 1	CAAT	+	-573 *Hordeum vulgare*	-572 [S000028]	Common in promoter and enhancer regions
CAAT box 1	CAAT	-	-812 *Hordeum vulgare*	-811 [S000028]	Common in promoter and enhancer regions
CAAT box 1	CAAT	-	-646 *Hordeum vulgare*	-645 [S000028]	Common in promoter and enhancer regions
CAAT box 1	CAAT	-	-53 *Hordeum vulgare*	-52 [S000028]	Common in promoter and enhancer regions
W box/ WRKYHVISO1	TTGAC	+	-915 *Arabidopsis thaliana*	-914 [S000390]	General defence
TATA box 4	TATATAA	-	-421 *Arabidopsis thaliana*	-421	Core promoter element ahead of TSS

(+) denotes the forward strand and (-) denotes the reverse strand

While this method gives the consensus of the two resources, it leaves out some potentially interesting elements in both genes that were present in only one database, such as the Skn_1 motif (both), MBS box (*CPPS2*), Box W1 (*CPPS2*) and TC rich repeats (*CPPS2*), found only on PLANTCARE whose functions are endosperm expression, drought inducibility, fungal elicitor

response and defence and stress responsiveness respectively. The elements found on PLACE only (in both genes) were POLLEN1LELAT52 (Filichkin et al 2004), DOFCOREZM (Yanagisawa et al 1999), CACTFTPPCA1 (Gowik et al 2004) and W boxes (WBOXNTERF3 and WBOXHVISO1) (Nishiuchi et al 2004; Li Junhua et al 2012) whose functions are, pollen specific activation, Dof proteins (promoter regulation) target site, C4 plants phosphoenol pyruvate (PEP) carboxylase gene expression and response to wounding and sugar, respectively.

The data above was used to draw a visual representation of the *cis*-acting regulatory elements for *TPS11* and *CPPS2*. Figure 3.15 below summarises the *cis*-acting regulatory elements found in the 1 kb region upstream of the promoter. The CAAT is described as common in promoter and enhancer regions, the TATA box is a core promoter element found ahead of the TSS. The W box is for general defence response including wounding and lastly the ARE box is for abscisic acid responsiveness. It was unusual to observe the TATA motifs in positions other than the conserved region of between -25 and -35. The observation of multiple motifs was also unusual.

(a) *TPS11*

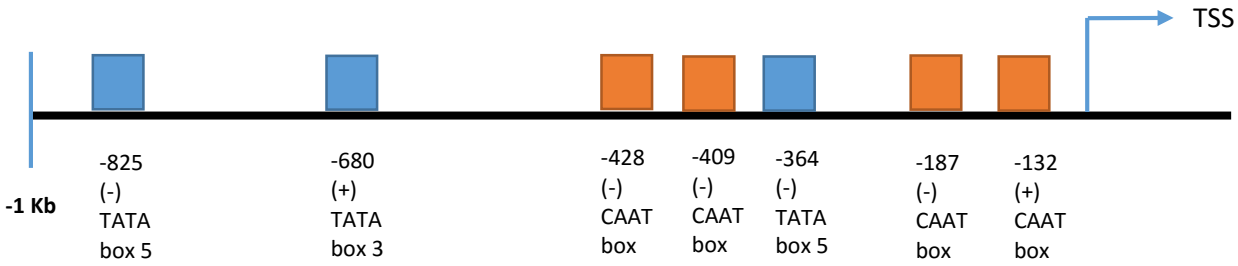

(b) *CPPS2*

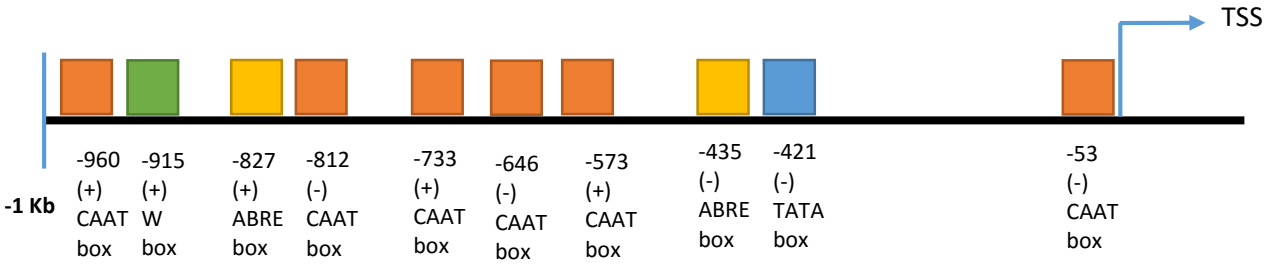

Figure 3.15: Positions of *cis*-acting regulatory elements in 1 kb upstream of the TSS for (a) *TPS6/11* and (b) *CPPS2* The elements are colour coded and the position of each one is given relative to the TSS designated zero.

Chapter 4 : Discussion and Conclusion

The development of GLS disease symptoms on maize

The experiments where B73 maize was inoculated with *C. zeina* looked at the symptoms at molecular and phenotypic level. The images of inoculated maize leaves that are presented in the results section (Figure 3.1) show how the *C. zeina* lesions can completely consume the entire leaf making it unable to photosynthesise. The four distinct stages of *C. zeina* disease development that we observed were; no symptoms – while the fungus was growing on the leaf surface; chlorotic flecks – these are yellowing spots on the leaves; lesion elongation – this is the typical symptom that is used to identify GLS disease in a maize field by farmers; and lastly lesion coalescence – the lesions join together and cover the entire leaf surface (Crous et al., 2006).

The infection time frame life cycle of *C. zeina* was approximately 24 days from inoculation to totally engulfing the leaf and there was a long lag phase of 17 days, before any GLS symptoms appeared on the maize leaves followed by a growth spurt where the pathogen quickly overtook the plant (Table 3.1). The long lag phase between inoculation and symptom development for *Cercospora* species has been reported in literature as typically ranging between 16 and 120 days and is attributed mainly to the ability of the fungus to sustain mycelial growth before penetration occurs (Beckman & Payne, 1982; Korsman et al., 2011). However, for field experiments a long latent period of 100 – 120 days may be the result of spores landing onto the maize plant at an unknown time between planting and observing the lesions. This length of time can be influenced by various factors such as high humidity, absence of water on the leaf surface and moderate to high ambient temperature. The 17 day lag phase observed in this study was relatively short due to high humidity maintained in the green house. Germ tubes grew towards the stomata through tropistic attraction and formed appresorium which penetrated the plant (Beckman & Payne, 1982). This lag phase could influence infection of the plant because the growth of the fungus can be paused before penetration occurs. For example the presence of free water on the surface of the leaf prevents appresorium formation and results in a longer lag phase during which plant growth is undisturbed (Beckman and Payne 1982).

The fungal quantification experiment showed the ratio of the cytochrome P450 reductase (*cpr1*) gene that represented the amount of *C. zeina* DNA to the glutathione S-transferase III (*gst3*) gene that represented the amount of maize DNA (Korsman et al., 2011). In the inoculated maize samples, the ratio started out high at T0, then reduced at T1 before increasing steadily at T2 and T3 up to its maximum value at T3 at the end of the experiment. The ANOVA statistical analysis showed no significant differences across the four time points despite the pattern of increasing ratio of *C. zeina* DNA to maize DNA. In order to improve this type of experiment in future, more biological replicates should be used in order to obtain a statistically more robust result.

Metabolite Accumulation

The metabolite analysis findings in the GLS experiment were that kauralexins were produced in much larger quantities than zealexins, there was no significant difference in zealexin accumulation across the four harvesting time points (T0, T1, T2 and T3) and the kauralexin accumulation increased markedly at each time point until reaching the maximum levels at T2, before declining at the final time point T3.

At T0, at the start of the experiment, the amount of zealexins was higher than kauralexins. This may be because zealexins may exist normally at higher baseline levels in the maize plant than kauralexins. The kauralexin increase showed that the kauralexins were accumulating in the plants due to GLS disease growth. The decrease at T3 at the end may have been the result of a negative feedback loop where excess amount of kauralexins led to switching off one of the crucial compounds in the biosynthetic pathway, thereby shutting down their biosynthesis. This has been shown to occur where the expression of a suite of five *Bx* genes reduced due to accumulation of DIMBOA –the active glucoside, forming a negative transcriptional feedback loop (Ahmad et al., 2010). Alternatively this could have been due to extensive tissue death and disintegration at the final stages of the infection therefore fewer cells remained that were still producing the kauralexins as normal and this was measured as a lower accumulation level. Phytoalexins accumulate in the cells in and around infection sites (Agrawal et al., 2002).

Callose is a high molecular weight amorphous heterogeneous polymer made up of 1, 3 β-glucan (Annegret Kohler, 2000; Luna et al., 2011). It forms a matrix on the plant cell wall called appositions or papillae which from physical barriers to pathogen entry (Annegret Kohler,

2000) and also block the pathogen thereby establishing a targeted location for concentration of the plant defences (Luna et al., 2011).

The induction of callose is a reliable chemical marker of an activated defence response (Annegret Kohler, 2000). Callose can be extracted from various plant tissues with sodium hydroxide (NaOH). It can be measured under ultraviolet (UV) light following reaction with a specific fluorochrome that is present in aniline blue dye (Annegret Kohler, 2000). The intensity of the fluorescence can be used to calculate the quantity of callose in the plant. In this study the chitosan elicitor and callose assay were important tools to use as a proxy for induction of defence responses in the absence of the pathogen. It allowed us to ask the question of whether chitosan is a recognised PAMP leading to phytoalexin accumulation in maize.

In the chitosan elicitor experiment there were no significant differences for either group of phytoalexins across the four treatments (NT, W, HAc and Chit) (Figure 3.10). This indicates that there was no increase in the amount of the zealexins or kauralexins due to infiltration with chitosan. This leads to the conclusion that chitosan is not the effective elicitor for the phytoalexin defence response in maize. In a study of benzoxazinoid phytoanticipins (Ahmad et al., 2010) chitosan elicitor resulted in the accumulation of DIMBOA in the apoplast only, and not in whole leaf extracts. The apoplast is the non-living part of plant tissue between cells and adjacent to the cellulose cell wall. Apoplast specific extractions may have shown a statistically significant increase in phytoalexin accumulation compared to whole leaf extraction performed in this study.

In a rice study the same concentration of chitosan used in this study (0.1 % chitosan) resulted in the formation of brownish necrotic spots on the leaves caused by oxidative stress (Agrawal et al., 2002) that are similar to the early stages of a fungal infection. This may be a hypersensitive response. Chitosan also resulted in the accumulation of two phytoalexins of rice namely, sakuranetin a flavonoid and momilactone a diterpenoid.

A study on zealexin accumulation used pectinase obtained from the fungal pathogen *Rhizopus microsporus* as an elicitor to induce the metabolite accumulation (Huffaker et al., 2011). The pathogen *R. microsporus* causes cob rots in maize. The pectinase actually showed a weak response that was similar to the control (inoculated with H_2O) and weaker than samples infected with *R. microsporus* spores (Huffaker et al., 2011). Therefore pectinase may not be

useful as a potential candidate elicitor to model the phytoalexin response of *C. zeina* infection in maize.

In the diverse lines seedlings experiment, there were a lot of differences in the metabolite accumulation amongst the maize lines (Figure 3.14), with B73 being the most dissimilar and Star and ZM5 were the most alike. In terms of zealexin accumulation, Star, GB, ZM4 and ZM5 were not significantly different from each other and from KEP and B73. KEP and B73 were significantly different from each other and all other cultivars. In the kauralexin accumulation Star, KEP and ZM5 were not significantly different from each other and the other cultivars while B73 and ZM4 were each different from the rest. GB was significantly different to ZM4 only and similar to the rest. These differences demonstrate the inherent diversity that was expected from a varied cohort of maize cultivars. The accumulation of either phytoalexin group did not necessarily correspond i.e. having one group accumulating highly did not mean the other would follow suit, for example B73 had the lowest zealexin accumulation but GB had the lowest kauralexin accumulation.

The zealexins were the dominant group above the kauralexins in all six maize lines. All the plants had higher zealexin levels and this may be because un-induced maize plants have high endogenous zealexin levels and not kauralexins. The zealexins may be playing a role in protecting the newly germinated plants from soil borne pathogens and nematodes (Huffaker et al., 2011).

The definition of what qualifies to be a phytoalexin or phytoanticipin blurs when considering compounds that are synthesised *de novo* on the onset of an infection, but are also present at baseline levels in the plant. Phytoanticipins are compounds that are constitutively expressed in plants and are involved in defence (Meyer et al., 2015). The zealexins observed in this study may be acting as phytoanticipins. In the diverse maize lines seedlings experiment (Figure 3.14) the amount of zealexins was higher in all the six maize lines in the absence of an external inducer. In the chitosan elicitor experiment (Figure 3.10) the amount of zealexins was higher than kauralexins and this may be because chitosan had no effect and the observation made was of the basal levels.

For the data presented here (Figures 3.3, 3.10 and 3.14), it appears that the kauralexins are more active during an active fungal infection, and in the absence of such an inducer, the

zealexins dominate. This is clear when comparing the GLS inoculated samples in which kauralexin accumulation was higher than zealexin accumulation, with the diverse lines seedlings experiment where the opposite trend occurred. In the chitosan elicitor experiment, the zealexins dominated in baseline samples.

Physiologically relevant concentrations that were reported for phytoalexins to have a negative effect of pathogen growth are as low as 10 µg/ ml for Kauralexin B3 (Schmelz et al., 2011). The concentration of zealexin A1 that was able to cause a decline in the growth of fungal pathogens was 100 µg/ ml (Huffaker et al., 2011). The amount of zealexins in maize tissue infected with *Fusarium graminearum* was in the range of 230 – 290 µg/ g fresh weight (Huffaker et al., 2011). The highest phytoalexin accumulation in the GLS B73 experiment was total kauralexins at approximately 240 µg/ g fresh weight. The GLS B73 experiment is suitable to use in making a comparison with the work of Schmelz et al because the ionization method used to determine the concentration of phytoalexins was the same. The level observed in our plants was within the range of reported physiologically relevant phytoalexin concentrations.

There may be maize varieties that retain the ability to produce high concentrations of phytoalexins. In future crop improvement, phytoalexin biosynthesis could be increased to levels that are useful to the plant in defending against fungal pathogens, by increasing the gene expression levels

TPS6/11 Gene Expression

Gel and sequence confusion

TPS6 and *TPS11* were thought to be alternatively spliced forms of the same part of the gene (Huffaker et al., 2011). However this could not be correct since one of them (*TPS6*) had a single nucleotide polymorphism (SNP) that was absent in *TPS11*. If the transcripts were originating from the same position then it would not be possible to have a SNP difference as this is not a post transcriptional modification. To add to the confusion, previous multiple sequence alignment of the two transcript showed that they are very similar, as shown in Figure 4.1 below. However, the restriction enzyme digestion with *AgiI/BmgBI* (Figure 3.6) was able to distinguish between the two transcripts of the zealexin biosynthesis gene

GRMZM2G127087 (*TPS6/11*) and this allowed further analysis of gene expression to be done in the various experiments, with the knowledge that the correct gene was being amplified.

Analysis of the transcripts using Ensembl Plants for maize showed that each transcript was made up of seven exons, and this could have added to the assumption that they were almost identical. However these were not the same exons except for the first exon as shown in Figure 3.4 (results chapter). These exons probably arose from tandem exon duplication events (Morgante et al., 2005) during the evolution of maize for the purposes of selective gene splicing and preservation of gene function in the species.

Figure 4.1: Multiple sequence alignment of *TPS6* and *TPS11* sequences. The two sequences align almost perfectly as if they were transcribed originated from the same gene. (Source Huffaker et al 2011 supplementary data). Primer annealing sites for TPS6 amplicon are shown in blue and the primer annealing sites for TPS11 amplicon in green. The BmgBI recognition site (CACGTC) in TPS6 amplicon is shown in orange and an orange arrow points to the cut site. The site in the TPS11 amplicon is highlighted in dark grey with the T→C change that renders it unrecognizable by BmgBI underlined.

***TPS6/11* Gene expression**

Gene expression of the phytoalexin biosynthetic genes was analysed in samples of maize inoculated with *C. zeina*. In the inoculated samples, *TPS6* gene expression increased significantly from T0 to T1 and from T1 to T2. At T2 *TPS6* expression was at its highest then declined at T3, but was still significantly different from T0 or T1. In the same samples, the gene expression of *TPS11* increased steadily then declined at the last time point T3. T0, T1 and T2 were significantly different from the rest according to ANOVA statistical analysis and T3 was significantly different from T0 and T1 but not T2. This showed us that gene expression of the two zealexin biosynthetic genes was increasing as the disease pressure increased.

In the chitosan elicitor experiment, *TPS6* expression was low in the no treatment (NT) and water (W) samples and high in the samples infiltrated with acetic acid, then intermediate in the samples infiltrated with chitosan. *TPS11* expression remained unchanged across all four treatments. This high level of *TPS11* expression in the acetic acid control may have been a result of an acid response in the plant tissue. Acetic acid causes a chitosan like effect (Valletta et al., 2016) and therefore it may not be the most suitable carrier solvent for chitosan. It acts as a signal molecule for the release of a group of polyphenols called xanthones found in root tissue of *Hypericum perforatum* commonly known as St. John's wort (Valletta et al., 2016). Generally the unchanged levels of gene expression for both genes across the three controls and the chitosan treatment led to the conclusion that chitosan did not act as an elicitor. In rice chitosan induced a defence response (Agrawal et al., 2002), however in this study we measured callose formation, metabolite accumulation and gene expression. It is likely that the chitosan caused changes that we did not measure such as changes in the expression of pathogenesis related proteins found in the rice study.

In the diverse seedlings experiment investigating early phytoalexin accumulation, only *TPS11* gene expression data was presented for the zealexin biosynthesis because *TPS6* was shown to be very lowly expressed in an African maize line in a separate unpublished study done by our collaborators at the CPGR. The *TPS11* gene expression resulted in no significant

differences across the six maize cultivars, however B73 and ZM5 had the highest expression levels. The high inherent variation in the samples resulted in no significant differences.

When the expression of the *TPS6/11* was silenced using virus induced gene silencing (VIGS) in maize plants, they became more susceptible to *U. maydis* infection showing earlier symptom (Van Der Linde et al., 2011)development and general chlorosis. This provides further evidence that this gene is not only induced in a defence response but it is also active in reducing the virulence of the infection.

Genevestigator analysis showed that *TPS11* was differentially expressed in infection with *U. maydis*, *P. cinnamomi*, *F. moniliforme*, *S. reilianum* and pest attack by *O. nubilalis*, *M. incognita* as well as under the abiotic stresses drought and waterlogging. This paints a picture of the wide range of conditions during which *TPS11* expression and subsequent zealexin accumulation may occur in the maize plant.

CPPS2 Gene Expression

Ent-copalyl diphosphate synthase 2 is a gene that encodes an enzyme of the same name. It catalyses the first dedicated step of kauralexin biosynthesis (Figure 1.4). Gene expression of *CPPS2* in the GLS inoculation experiment increased steadily at each successive time point. ANOVA analysis showed that each of the four time points (T0, T1 T2 and T3) were significantly different from the rest. The trend on the graph shows an increase that peaks at T2 then declines at T3 but still being higher than T0 and T1. This shows that *CPPS2* gene expression was increasing in response to the GLS infection as this was the only condition changing. Expression declined slightly at the end either due to a negative feedback loop or extensive cell death.

In the chitosan elicitor experiment *CPPS2* gene expression was not significantly different in the four treatments (Figure 3.11). This shows that there was no change in gene expression due to the presence of chitosan. In the diverse lines seedlings experiment, the expression of *CPPS2* was not significantly different in the six maize cultivars. The cultivars that had the highest expression were Star, GB and ZM4 while KEP, B73 and ZM5 had the lowest expression. The lack of significant differences among the cultivars was not because the plants had similar amounts of *CPP2*, but rather been due to high inherent variation in some of the cultivars. This

skewed the statistical analysis since it takes into account the variation in each group of samples.

The *CPPS2* gene is well annotated on the maize plant cycles online resource as described earlier in the literature review under the biosynthesis pathways section. This gene codes for ent-copalyl diphosphate synthase and it also functions during anther ear formation and is known as anther ear 2 (*AN2*) (Schmelz et al., 2011) The expression of *CPPS2* occurs in maize after inoculation with the following fungal pathogens; *R. microsporus*, *F. graminearum* and *C. graminicola*, and insect herbivory by *O. nubilalis* (Schmelz et al., 2011) and its function is to increase the quantity of precursors to kauralexin formation (Harris et al., 2005; Schmelz et al., 2011).

The Genevestigator analysis (Table 3.3) also showed that *CPPS2* was highly expressed during infection with *U. maydis*, *P. cinnamomi*, *F. moniliforme*, *S. reilianum* and pest attack by *O. nubilalis*, *M. incognita* and under the abiotic stresses drought and waterlogging. These are almost the same conditions as the *TPS11* gene expression with slightly less in the *F. moniliforme* and *S. reilianum* samples. In drought stress, the *CPPS2* expression shows a sharp increase where it changes markedly from low in the control samples to high in the moisture stressed samples, while *TPS11* starts from medium to high. A recent study confirmed that kauralexins accumulate in response to drought stress (Vaughan et al., 2015). In some experiments co-expression of both genes was identical, for example in the experiments with *U. maydis* at and *C. graminicola*. The general pattern revealed is that the phytoalexin gene expression is induced or activated in the same way for both zealexins and kauralexins, and the genes are co-expressed.

In order to look more closely at the genes individually and to determine what may be causing some of the observed differences, a promoter analysis was performed.

Promoter Analysis

Gene expression in eukaryotic cells is regulated by the activities of the DNA binding domains of transcription factors interacting with the specific *cis*-acting regulatory elements that are associated with the gene being expressed (Li et al., 2014). These elements control transcription firstly by their mere presence and secondly by the number of duplicates that

exists, with more duplicates resulting in more gene transcription. The 1kb promoter region upstream of the transcription start site was analysed for *TPS11* and *CPPS2*. The online databases PLACE and PLANTCARE were used in this analysis. The combined results showed that both genes had similar *cis*-acting regulatory elements namely CAAT and TATA boxes and in addition, the *CPPS2* promoter had an ABRE box and W box (Tables 3.4 and 3.5).

The CAAT and TATA boxes are common general regulatory elements with important functions in transcription so it is not surprising that these would be present in the promoters of both genes. The CAAT box is common in promoter and enhancer regions, it is important for tissue specific promoter activity of a pea legumin gene (Li et al., 2014). The TATA box is a core promoter element found ahead of the TSS and it is important in initiating the transcription of a gene. The function of the ABRE box is in abscisic acid responsiveness (Simpson et al., 2003) while the W box is a general defence related element (Li et al., 2014; Nishiuchi et al., 2004; Sharma et al., 2011; Zhang et al., 2004).

There were other notable *cis*-acting regulatory elements that were identified using either search method but not both. This disparity resulted from the differences in the databases algorithms or search methods and whether the results were based on wet lab references or the existence of theoretical sequences that may or may not actually be acting as *cis*-acting regulatory elements. Generally PLACE had references to the wet lab experiments to support the element and its given function in a plant, while PLANTCARE gave a brief description of the function and plant name. There were a large number of elements identified and those discussed below were chosen based on high abundance and relevance in plant defence.

For *TPS11* element found only on PLANTCARE was the GC motif and Skn-1. The elements for *TPS11* found on PLACE and their functions were; CACTFTPPCA1 – responsible for mesophyll layer cells specific expression of phosphoenol pyruvate carboxylase, this specificity is important for the compartmentalisation of the carbon dioxide assimilatory process found in *O. sativa* and *Flaveria trinervia* (Gowik et al., 2004; Li et al., 2014; Sharma et al., 2011); DOFCOREZM – a binding site for a large family of Dof transcription factors that are found in maize plants and regulate various processes such as expression of phosphoenol pyruvate in C4 plants and also active in the endosperm (Li et al., 2014; Yanagisawa & Schmidt, 1999) and thus are expressed in seedlings; GTGANTG10 – binding site for GT-1 proteins found in plant nuclear genes expressed throughout the plant and influence complex regulation of diverse

plant genes for example the late pollen genes of tobacco (*g10*) and tomato (*lat56*) plants (Sharma et al., 2011); TAAAGSTKST1 – target site of stomatal cells specific gene expression to maintain their function specificity (Li et al., 2014; Plesch et al., 2001); WBOXNTERF3 – a wounding responsive element combining a WRKY transcription factor and an ethylene response factor DNA element, identified in *Nicotiana tobacum* (Nishiuchi et al., 2004), WRKY71OS – binding site for WRKY71 a transcriptional repressor of the gibberellin signalling pathway in rice (Li et al., 2014; Sharma et al., 2011; Y. Zhang & Wang, 2005) and WBOXHVISO1 – abscisic acid signalling in rice aleurone cells (Sharma et al., 2011).

The notable *CPPS2* elements found only on PLANTCARE and their functions were; 5UTR Py-rich stretch, Box W1, MBS box, Skn-1 motif and TC rich repeats. The elements for *CPPS2* found on PLACE were; ACGTATERD1 – element for early response to dehydration that was found in the promoter of the *erd1* gene that is induced by dehydration stress and dark induced senescence (Simpson et al., 2003), CACTFTPPCA1, CURECORECR – part of a copper response element and also regulates the oxygen response (Sharma et al., 2011); DOFCOREZM, GATABOX – responsible for light dependent and nitrate dependent gene expression in specific tissues (Li et al., 2014; Sharma et al., 2011), MARTBOX, MYCCONSENSUSAT – responsiveness to cold (Li et al., 2014; Sharma et al., 2011) and to abscisic acid during dehydration or drought stress (Abe et al., 2003) found in the promoter of *rd22* the dehydration responsiveness gene of *A. thaliana* (Sharma et al., 2011); and POLLEN1LELAT52 – pollen tissue specific activation of genes, found in the promoter of the *LAT52* gene in *Lycopersicon esculentum* during late stages of anther development (Filichkin, Leonard, Monteros, Liu, & Nonogaki, 2004; Li et al., 2014). These elements are driving the expression of the *TPS11* and *CPPS2* genes and may be activated under a wide range of conditions and to different expression levels depending on the element present, the number of copies of the element, the type of plant tissue and abundance of transcription factors.

CONCLUSION

The original hypotheses were that GLS infection causes phytoalexin accumulation as a defence response, that chitosan is an elicitor for the phytoalexin defence system, that diverse maize lines would have different basal phytoalexin accumulation levels according to their genotypes, that Genevestigator analysis will show similar expression patterns for both the zealexin and kauralexin biosynthesis gene if the induction pattern is the same and that promoter regions of the phytoalexin biosynthesis genes are controlled by the same *cis*-acting regulatory elements.

Maize leaves inoculated with *C. zeina* did show both phytoalexin accumulation and gene expression that was directly in response to GLS development. Chitosan may not be the elicitor for initiating phytoalexin defence during GLS infection in maize. The pectinase elicitor that was tested by Huffaker et al 2011 resulted in low gene expression and phytoalexin accumulation that was similar to the controls. The diverse maize seedlings had varying levels of phytoalexin accumulation according to their genotypes and this showed that research outcomes for one cultivar e.g. B73 could not be assumed as the default for all maize lines, especially of different origins. Genevestigator analysis showed co-expression of the phytoalexin biosynthesis genes suggesting that they often work together. The promoter analysis revealed that the maize phytoalexins have the genetic potential to be involved in both biotic and abiotic defence responses. The scope of maize phytoalexins is broader than defending the plant against fungal pathogens and also includes insect pests, in addition to a possible role in drought stress. This supports the view that maize phytoalexins would be useful as a defence mechanism with a wide range of defence functions for bio-engineered plants of the future.

Future work for this research project would be looking at the other genes in the phytoalexin biosynthesis pathway downstream of the genes analysed in this study. Other genes that may be co-expressed with the *TPS6/11* and *CPPS2* that may or may not be directly in the phytoalexin pathway can be found by looking at RNA-seq data and microarray data. This can be followed up by carrying out knock out mutant analysis of the *TPS11* and *CPPS2* phytoalexin biosynthetic genes using virus induced gene silencing (VIGS). Study of other possible elicitors may also help to fully understand the defence response of maize to GLS.

REFERENCES

Abe, H., Urao, T., Ito, T., Seki, M., Shinozaki, K., & Yamaguchi-Shinozaki, K. (2003). *Arabidopsis* AtMYC2 (bHLH) and AtMYB2 (MYB) Function as Transcriptional Activators in Abscisic Acid Signaling. *The Plant Cell*, *15*: 63–78.

Abendroth, L. J., Elmore, R. W., Boyer, M. J., & Marlay, S. K. (2011). *Corn Growth and Development*. Iowa State University.

Agrawal, G. K., Rakwal, R., Tamogami, S., Yonekura, M., Akihiro, K., & Saji, H. (2002). Chitosan activates defense/ stress response (s) in the leaves of *Oryza sativa* seedlings *Plant Physiology and Biochemistry*, *40*: 1061–1069.

Agrios, G. N. (2004). *Plant Pathology* (5th ed.).

Ahmad, S., Gordon-weeks, R., Pickett, J., & Ton, J. (2010). Natural variation in priming of basal resistance: from evolutionary origin to agricultural exploitation. *Molecular Plant Pathology*, *11*: 817–827.

Ahmad, S., Veyrat, N., Gordon-weeks, R., Zhang, Y., Martin, J., Smart, L., Ton, J. (2011). Benzoxazinoid Metabolites Regulate Innate Immunity against Aphids and Fungi in Maize. *Plant Physiology*, *157*: 317–327.

Ahuja, I., Kissen, R., & Bones, A. M. (2012). Phytoalexins in defense against pathogens. *Trends in Plant Science*, *17* (2): 73–90.

Annegret Kohler, S. (2000). Extraction and Quanti- tative Determination of Callose from Arabidopsis Leaves. *BioTechniques*, *28* (6): 1084–1086.

Bailey, J. A., & Ingham, J. L. (1971). Phaseollin accumulation in bean (*Phaseolus vulgaris*) in response to infection by tobacco necrosis virus and the rust *Uromyces appendiculatus*. *Physiological Plant Pathology*, *1* (4): 451–456.

Barnett, H. L., & Hunter, B. B. (1998). *Illustrated Genera of Imperfect Fungi* (4th ed.). APS Press.

Beckman, P. M., & Payne, G. A. (1982). Cultural Techniques and Conditions Influencing Growth and Sporulation of *Cercospora zeae-maydi*s and Lesion Development in Corn. *Phytopathology*. 73: 286-289

Benson, J. M., Poland, J. A., Benson, B. M., Stromberg, E. L., & Nelson, R. J. (2015). Resistance to Gray Leaf Spot of Maize: Genetic Architecture and Mechanisms Elucidated through Nested Association Mapping and Near-Isogenic Line Analysis. *PLOS Genetics*, 1–23.

Berger, D. K., Carstens, M., Korsman, J. N., Middleton, F., Kloppers, F. J., Tongoona, P., & Myburg, A. (2014). Mapping QTL conferring resistance in maize to gray leaf spot disease caused by *Cercospora zeina* Mapping QTL conferring resistance in maize to gray leaf spot disease caused by *Cercospora zeina*. *BioMed Central Genetics*, *15*: 60.

Bustin, S. A., Benes, V., Garson, J. A., Hellemans, J., Huggett, J., Kubista, M., Shipley, G. L.

(2009). The MIQE Guidelines: Minimum Information for Publication of Quantitative Real-Time PCR Experiments. *Clinical Chemistry*, *55* (4): 1–12.

Crous, P. W., Groenewald, J. Z., Groenewald, M., Caldwell, P., Braun, U., & Harrington, T. C. (2006). Species of *Cercospora* associated with grey leaf spot of maize. *Studies in Mycology*, *55*: 189–97.

Dangl, J. L., & Jones, J. D. G. (2001). Defence responses to infection. *Nature*, *411*: 826–833.

Daniel, M., & Purkayastha, R. P. (1995). *Handbook of Phytoalexin Metabolism and Action*. (M. Daniel & R. P. Purayastha, Eds.) (1st ed.). New York: Marcel Dekker.

Degen, T., Bakalovic, N., Bergvinson, D., & Turlings, T. C. J. (2012). Differential Performance and Parasitism of Caterpillars on Maize Inbred Lines with Distinctly Different Herbivore-Induced Volatile Emissions. *PLOS One*, *7* (10).

Dey, P. M., & Harborne, J. B. (1997). *Plant Biochemistry*.

Echeverri, F., Torres, F., Quinones, W., Escobar, G., & Archbold, R. (2012). Phenylphenalenone phytoalexins, will they be a new type of fungicide? *Phytochemical Reviews*, *11*: 1-12

Filichkin, S. A., Leonard, J. M., Monteros, A., Liu, P., & Nonogaki, H. (2004). A Novel Endo- b -Mannanase Gene in Tomato LeMAN5 Is Associated with Anther and Pollen Development. *Plant Physiology*, *134*: 1080–1087.

Frey, M., Schullehner, K., Dick, R., Fiesselmann, A., & Gierl, A. (2009). Benzoxazinoid biosynthesis, a model for evolution of secondary metabolic pathways in plants. *Phytochemistry*, *70* (15-16): 1645–51.

Goodwin, T., & Mercer, E. I. (1983). *Plant Phenolics* (2nd ed.). Oxford: Pergamon Press.

Gowik, U., Burscheidt, J., Akyildiz, M., Schlue, U., Koczor, M., Streubel, M., & Westhoff, P. (2004). cis -Regulatory Elements for Mesophyll-Specific Gene Expression in the C 4 Plant Flaveria trinervia , the Promoter of the C4 Phosphoenolpyruvate Carboxylase Gene. *The Plant Cell*, *16*: 1077–1090.

Hadwiger, L. A. (2013). Multiple effects of chitosan on plant systems: Solid science or hype. *Plant Science*, *208*: 42–49.

Hammerschmidt, R. (1999). Phytoalexins: What Have We Learned After 60 Years? *Annual Review in Phytopathology*, 37: 285–306.

Hammerschmidt, R. (2011). Phytoalexins at the right place and time. *Physiological and Molecular Plant Pathology*, *76* (3-4),

Harris, L. J., Saparno, A., Johnston, A., Prisic, S., Xu, M., Allard, S.,Peters, R. J. (2005). The maize An2 gene is induced by Fusarium attack and encodes an ent-copalyl diphosphate synthase. *Plant Molecular Biology*, 59: 881–894.

Higo, K., Ugawa, Y., Iwamoto, M., & Korenanga, T. (1999). Plant cis-acting regulatory DNA elements (PLACE) database. *Nucleic Acid Reserch*, *27* (1): 297–300.

Huffaker, A., Kaplan, F., Vaughan, M. M., Dafoe, N. J., Ni, X., Rocca, J. R., Schmelz, E. A.

(2011). Novel Acidic Sesquiterpenoids Constitute a Dominant Class of Pathogen-Induced Phytoalexins in Maize. *Journal of Plant Physiology*, *156*: 2082–2097.

Jones, J. D. G., & Dangl, J. L. (2006). The plant immune system. *Nature*, *444*: 323–329.

Kanno, H., & Hasegawa, M. (2012). Accumulation of salicylic acid , jasmonic acid and phytoalexins in rice , Oryza sativa , infested by the white-backed planthopper , *Sogatella furcifera* (*Hemiptera: Delphacidae*). *Applied Entomology and Zoology*, 47: 27–34.

Korsman, J., Meisel, B., Kloppers, F. J., Crampton, B. G., & Berger, D. K. (2011). Quantitative phenotyping of grey leaf spot disease in maize using real-time PCR. *European Journal of Plant Pathology*, *133* (2): 461–471.

Latterell, & Rossi. (1983). GRAY Leaf Spot of Corn: A Disease on the Move. *Plant Disease*, 67: 842–847.

Lescot, M., Dehais, P., Moreau, Y., De moor, B., Rouze, P., & Rombouts, S. (2002). PlantCARE: A database of plant cis-acting regulatory elements and a portal to tools for in-silico analysis of promoter sequences. *Nucleic Acid Reserch*, *30* (1): 325–327.

Li, J., Yuan, J., & Li, M. (2014). Characterization of Putative *cis*-Regulatory Elements in Genes Preferentially Expressed in *Arabidopsis* Male Meiocytes. *BioMed Research International*, *2014* (708364).

Luna, E., Pastor, V., Robert, J., Flors, V., Mauch-mani, B., & Ton, J. (2011). Callose Deposition: A Multifaceted Plant Defense Response. *The American Phytopathological Society*, *24* (2): 183–193.

Meisel, B., Korsman, J., Kloppers, F. J., & Berger, D. K. (2009). *Cercospora zeina* is the causal agent of grey leaf spot disease of maize in southern Africa. *European Journal of Plant Pathology*, *124* (4): 577–583.

Meyer, J., Murray, S. L., & Berger, D. K. (2015). Signals that stop the rot: Regulation of secondary metabolite defences in cereals. *Physiological and Molecular Plant Pathology*. http://dx.doi.org/10.1016/j.pmpp.2015.05.011

Morgante, M., Brunner, S., Pea, G., Fengler, K., Zuccolo, A., & Rafalski, A. (2005). Gene duplication and exon shuffling by helitron-like transposons generate intraspecies diversity in maize. *Nature Genetics*, *37* (9): 997–1002.

Nishiuchi, T., Shinshi, H., & Suzuki, K. (2004). Rapid and Transient Activation of Transcription of the *ERF3* Gene. *The Journal of Biological Chemistry*, *279* (53): 55355–55361.

Oikawa, A., Ishihara, A., Hasegawa, M., Kodama, O., & Iwamura, H. (2001). Induced accumulation of 2-hydroxy-4 , 7-dimethoxy- 1 , 4-benzoxazin-3-one glucoside (HDMBOA-Glc) in maize leaves. *Phytochemistry*, *56*: 669–675.

Pedras, M. S. C., & Sarma-mamillapalle, V. K. (2012). The cruciferous phytoalexins rapalexin A, brussalexin A and erucalexin: Chemistry and metabolism in *Leptosphaeria maculans*. *Bioorganic & Medicinal Chemistry*, *20* (13): 3991–3996.

Pedras, M. S. C., Yaya, E., & Glawischnig, E. (2011). The phytoalexins from cultivated and

wild crucifers: Chemistry and biology. *The Royal Society of Chemistry*, 28: 1381–1405.

Plesch, G., Ehrhardt, T., & Mueller-roeber, B. (2001). Involvement of TAAAG elements suggests a role for Dof transcription factors in guard cell-specific gene expression. *The Plant Journal*, *28* (4): 455–464.

Poland, J. a, Balint-Kurti, P. J., Wisser, R. J., Pratt, R. C., & Nelson, R. J. (2009). Shades of gray: the world of quantitative disease resistance. *Trends in Plant Science*, *14* (1): 21–9.

Ray, P. D., Huang, B.-W., & Tsuji, Y. (2013). Reactive oxygen species (ROS) homeostasis and redox regulation in celular signalling. *Cell Signal*, *24* (5): 981–990.

Schmelz, E. A., Engelberth, J., Tumlinson, J. H., Block, A., & Alborn, H. T. (2004). The use of vapor phase extraction in metabolic profiling of phytohormones and other metabolites. *The Plant Journal*, 39: 790–808.

Schmelz, E. A., Kaplan, F., Huffaker, A., Dafoe, N. J., Vaughan, M. M., Ni, X., Teal, P. E. (2011). Identity, regulation, and activity of inducible diterpenoid phytoalexins in maize. *Proceedings of the National Academy of Sciences*, 1–6.

Sekhon, R. S., Lin, H., Childs, K. L., Hansey, C. N., Buell, R. C., de Leon, N., & Kaeppler, S. M. (2011). Genome wide atlas of transcription during maize development. *The Plant Journal*, *66* (4): 553–563.

Sessa, G. (Ed.). (2013). Molecular Basis of Effector Recognition by Plant NB-LRR proteins. In *Molecular Plant Immunity* (1st ed.). John Wiley and Sons.

Sharma, N., Russell, S. D., Bhalla, P. L., & Singh, M. B. (2011). Putative cis-regulatory elements in genes highly expressed in rice sperm cells. *BioMed Centranl Research Notes*, 4: 319–329.

Shedletzky, E., Unger, C., & Delmer, D. P. (1997). A Microtiter-Based Fluorescence Assay for (1, 3)- b-Glucan Synthases. *Analytical Biochemistry*, *93* (249): 88–93.

Simpson, S. D., Nakashima, K., Narusaka, Y., Seki, M., & Shinozaki, K. (2003). Two different novel cis -acting elements of *erd1*, a clpA homologous *Arabidopsis* gene function in induction by dehydration stress and dark-induced senescence. *The Plant Journal*, 33: 259–270.

Tena, G., Asai, T., Chiu, W., & Sheen, J. (2001). Plant mitogen-activated protein kinase signaling cascades. *Current Opinion in Plant Biology*, 4: 392–400.

Turlings, T. C. J., Tumlinson, J. H., & Lewis, W. J. (1990). Exploitation of Herbivore-Induced Plant Odors by Host-Seeking Parasitic Wasps. *Science*, *250* (4985): 1251–1253.

Uchihashi, K., Nakayashiki, H., Okamura, K., Ishihara, A., & Tosa, Y. (2011). In situ localization of avenanthramide A and its biosynthetic enzyme in oat leaves infected with the crown rust fungus, *Puccinia coronata f. sp. avenae*. *Physiological and Molecular Plant Pathology*, *76* (3-4): 173–181.

Valletta, A., Angelis, G. De, Badiali, C., & Brasili, E. (2016). Acetic acid acts as an elicitor exerting a chitosan-like effect on xanthone biosynthesis in *Hypericum perforatum* root cultures. *Plant Cell Reports*.

Van Der Linde, K., Kastner, C., Kumlehn, J., Kahmann, R., & Doehlemann, G. (2011). Systemic virus-induced gene silencing allows functional characterization of maize genes during biotrophic interaction with *Ustilago maydis*. *New Phytologist*, *1*: 471–483.

Vaughan, M. M., Christensen, S., Schmelz, E. A., Huffaker, A., Mcauslane, H. J., Alborn, H. T., Teal, P. E (2015). Accumulation of terpenoid phytoalexins in maize roots is associated with drought tolerance. *Plant, Cell and Environment*, *38*: 2195–2207.

Voigt, C. A., Schäfer, W., & Salomon, S. (2006). A comprehensive view on organ-specific callose synthesis in wheat (*Triticum aestivum*): glucan synthase-like gene expression, callose synthase activity , callose quantification and deposition. *Plant Physiology and Biochemistry*, *44*: 242–247.

Ward, J. M. J., Stromberg, E. L., Nowell, D. C., & Nutter, F. W. J. (1999). Gray Leaf Spot: A Disease of Global Importance in Maize Production. *Plant Disease*, *83* (10): 884–895.

Yanagisawa, S., & Schmidt, R. J. (1999). Diversity and similarity among recognition sequences of Dof transcription factors. *The Plant Journal*, *17* (2): 209–214.

Zhang, Y., & Wang, L. (2005). The WRKY transcription factor superfamily: its origin in eukaryotes and expansion in plants. *BMC Evolutionary Biology*, *5* (1): 1.

Zhang, Z., Xie, Z., Zou, X., Casaretto, J., Ho, T. D., & Shen, Q. J. (2004). A Rice WRKY Gene Encodes a Transcriptional Repressor of the Gibberellin Signaling Pathway in Aleurone Cells. *Plant Physiology*, *134*: 1500–1513.

Zimmermann, P., Hennig, L., & Gruissem, W. (2005). Gene-expression analysis and network discovery using Genevestigator. *Trends in Plant Science*, *10* (9): 9–11.

SUPPLEMENTARY DATA

Table i): Fungal Quantification ANOVA

Effect	Univariate Tests of Significance for Fungal Quant (Spreadsheet1) Sigma-restricted parameterization Effective hypothesis decomposition				
	SS	Degr. of	MS	F	p
Intercept	4212,00	1	4212,001	2,822163	0,131483
Var2	2475,18	3	825,059	0,552813	0,660469
Error	11939,78	8	1492,473		

Table ii) a): B73 GLS Zealexin ANOVA

Effect	Univariate Tests of Significance for GLS B73 Zealexins (Spreadsheet4) Sigma-restricted parameterization Effective hypothesis decomposition				
	SS	Degr. of	MS	F	p
Intercept	1,385633E+09	1	1,385633E+09	13,20038	0,006654
Var2	4,188030E+08	3	1,396010E+08	1,32992	0,330947
Error	8,397536E+08	8	1,049692E+08		

Table ii) b): B73 GLS Zealexin Fishers LSD post hoc test

Cell No.	LSD test; variable GLS B73 Zealexins (Spreadsheet4) Probabilities for Post Hoc Tests Error: Between MS = 1050E5, df = 8,0000				
	Var2	{1}	{2}	{3}	{4}
1	T0		0,688957	0,395855	0,325375
2	T1	0,688957		0,225838	0,544637
3	T2	0,395855	0,225838		0,087686
4	T3	0,325375	0,544637	0,087686	

Table iii) a): B73 GLS Kauralexin ANOVA

Effect	Univariate Tests of Significance for GLS B73 Kauralexins (Spreadsheet7) Sigma-restricted parameterization Effective hypothesis decomposition				
	SS	Degr. of	MS	F	p
Intercept	1,724280E+11	1	1,724280E+11	38,09442	0,000267
Var2	7,918691E+10	3	2,639564E+10	5,83157	0,020637
Error	3,621065E+10	8	4,526332E+09		

Table iii) b): B73 GLS Kauralexin Fishers post hoc test

Cell No.	LSD test; variable GLS B73 Kauralexins (Spreadsheet7) Probabilities for Post Hoc Tests Error: Between MS = 4526E6, df = 8,0000				
	Var2	{1}	{2}	{3}	{4}
1	T0		0,067009	0,003069	0,068721
2	T1	0,067009		0,072869	0,987466
3	T2	0,003069	0,072869		0,071057
4	T3	0,068721	0,987466	0,071057	

Table iv): Table of Phytoalexins identified

Phytoalexin Identified	Code name	GLS B73 Experiment	Chitosan Experiment	Diverse lines seedlings Experiment
Zealexin A1	Z A1	Yes	No	No
Zealexin A2	Z A2	Yes	No	No
Zealexin B1	Z B1	Yes	Yes	Yes
Kauralexin A1	K A1	Yes	No	No
Kauralexin A2	K A2	Yes	No	No
Kauralexin A3	K A3	Yes	Yes	Yes
Kauralexin B1	K B1	Yes	No	Yes
Kauralexin B2	K B2	Yes	Yes	No
Kauralexin B3	K B3	Yes	Yes	No
Terpenoid Unknown	K U1	No	No	Yes

Kauralexin	Unknown	K U2	No	No	Yes

Table v) a): B73 GLS *TPS6* ANOVA

Effect	Univariate Tests of Significance for *TPS6* GLS (Spreadsheet1) Sigma-restricted parameterization Effective hypothesis decomposition				
	SS	Degr. of	MS	F	p
Intercept	275,5508	1	275,5508	374,8675	0,000000
Var2	154,7053	3	51,5684	70,1552	0,000001
Error	6,6156	9	0,7351		

Table v) b): B73 GLS *TPS6* Fishers LSD post hoc test

Cell No.	LSD test; variable *TPS6* GLS (Spreadsheet1) Probabilities for Post Hoc Tests Error: Between MS = ,73506, df = 9,0000				
	Var2	{1}	{2}	{3}	{4}
1	T0		0,000870	0,000000	0,000028
2	T1	0,000870		0,000006	0,031532
3	T2	0,000000	0,000006		0,000039
4	T3	0,000028	0,031532	0,000039	

Table vi) a): B73 GLS *TPS11* AVOVA

Effect	Univariate Tests of Significance for *TPS11* GLS (Spreadsheet4) Sigma-restricted parameterization Effective hypothesis decomposition				
	SS	Degr. of	MS	F	p
Intercept	1278,948	1	1278,948	183,0651	0,000000
Var2	830,386	3	276,795	39,6197	0,000016
Error	62,877	9	6,986		

Table vi) b): B73 GLS *TPS11* Fishers LSD post hoc test

Cell No.	LSD test; variable *TPS11* GLS (Spreadsheet4) Probabilities for Post Hoc Tests Error: Between MS = 6,9863, df = 9,0000				
	Var2	{1}	{2}	{3}	{4}
1	T0		0,004041	0,000002	0,002098
2	T1	0,004041		0,000073	0,867264
3	T2	0,000002	0,000073		0,000052
4	T3	0,002098	0,867264	0,000052	

Table vii) a): B73 GLS *CPPS2* ANOVA

Effect	Univariate Tests of Significance for *CPPS2* GLS (Spreadsheet7) Sigma-restricted parameterization Effective hypothesis decomposition				
	SS	Degr. of	MS	F	p
Intercept	218,1278	1	218,1278	966,1234	0,000000
Var2	116,9427	3	38,9809	172,6527	0,000000
Error	2,0320	9	0,2258		

Table vii) b): B73 GLS *CPPS2* Fishers LSD post hoc test

Cell No.	LSD test; variable *CPPS2* GLS (Spreadsheet7) Probabilities for Post Hoc Tests Error: Between MS = ,22578, df = 9,0000				
	Var2	{1}	{2}	{3}	{4}
1	T0		0,000120	0,000000	0,000000
2	T1	0,000120		0,000000	0,000008
3	T2	0,000000	0,000000		0,000152
4	T3	0,000000	0,000008	0,000152	

Table viii) a): Chitosan Optimisation ANOVA

Effect	Univariate Tests of Significance for Fluorescence (Spreadsheet3) Sigma-restricted parameterization Effective hypothesis decomposition				
	SS	Degr. of	MS	F	p
Intercept	8622,535	1	8622,535	25939,34	0,00
Treatment and Harvest time	65,895	7	9,414	28,32	0,00
Error	29,252	88	0,332		

Table viii) b): Chitosan Optimisation Fishers LSD post hoc test

Cell No.	LSD test; variable Fluorescence (Spreadsheet3) Probabilities for Post Hoc Tests Error: Between MS = ,33241, df = 88,000							
	Treatment and Harvest time	{1}	{2}	{3}	{4}	{5}	{6}	{7}	{8}
1	12h HAc		0,000000	0,000129	0,000001	0,000152	0,114226	0,000000	0,000000
2	24h HAc	0,000000		0,000086	0,005511	0,000072	0,000000	0,182648	0,013664

3	36h HAc	0,000129	0,000086		0,206322	0,962550	0,018003	0,000000	0,000000
4	48h HAc	0,000001	0,005511	0,206322		0,190183	0,000396	0,000066	0,000001
5	12h Chitosan	0,000152	0,000072	0,962550	0,190183		0,020300	0,000000	0,000000
6	24h Chitosan	0,114226	0,000000	0,018003	0,000396	0,020300		0,000000	0,000000
7	36h Chitosan	0,000000	0,182648	0,000000	0,000066	0,000000	0,000000		0,243842
8	48h Chitosan	0,000000	0,013664	0,000000	0,000001	0,000000	0,000000	0,243842	

Table ix) a): Chitosan Callose Assay ANOVA

Effect	Univariate Tests of Significance for Fluorescence (Spreadsheet1 in Workbook1) Sigma-restricted parameterization Effective hypothesis decomposition				
	SS	Degr. of	MS	F	p
Intercept	5778,228	1	5778,228	5557,338	0,000000

Treatment at 48h	99,145	3	33,048	31,785	0,000000
Error	45,749	44	1,040		

Table ix) b): Chitosan Callose Assay Fishers LSD post hoc test

Cell No.	LSD test; variable Fluorescence (Spreadsheet1 in Workbook1) Probabilities for Post Hoc Tests Error: Between MS = 1,0397, df = 44,000				
	Treatment at 48h	{1}	{2}	{3}	{4}
1	No trt		0,489443	0,034888	0,000000
2	Water	0,489443		0,146008	0,000000
3	0.2% Acetic acid	0,034888	0,146008		0,000000
4	0.1% Chitosan	0,000000	0,000000	0,000000	

Table x) a): Chitosan Zealexins ANOVA

Effect	Univariate Tests of Significance for Area (Spreadsheet2) Sigma-restricted parameterization Effective hypothesis decomposition				
	SS	Degr. of	MS	F	p
Intercept	1,245333E+13	1	1,245333E+13	87,43749	0,000001
Trt Zealexins	3,729724E+11	3	1,243241E+11	0,87291	0,484382
Error	1,566680E+12	11	1,424255E+11		

Table x) b): Chitosan Zealexins Fishers LSD post hoc test

Cell No.	LSD test; variable Area (Spreadsheet2) Probabilities for Post Hoc Tests Error: Between MS = 1424E8, df = 11,000				
	Trt Zealexins	{1}	{2}	{3}	{4}
1	NT		0,271852	0,407229	0,142723
2	W	0,271852		0,755901	0,657524
3	HAc	0,407229	0,755901		0,455044
4	Chit	0,142723	0,657524	0,455044	

Table xi) a): Chitosan Kauralexins ANOVA

Effect	Univariate Tests of Significance for Area (Spreadsheet1) Sigma-restricted parameterization Effective hypothesis decomposition				
	SS	Degr. of	MS	F	p
Intercept	5,276068E+11	1	5,276068E+11	15,39312	0,002023
Trt Krlxns	6,324462E+10	3	2,108154E+10	0,61506	0,618280
Error	4,113059E+11	12	3,427549E+10		

Table xi) b): Chitosan Kauralexins Fishers LSD post hoc test

Cell No.	LSD test; variable Area (Spreadsheet1) Probabilities for Post Hoc Tests Error: Between MS = 3428E7, df = 12,000				
	Trt Krlxns	{1}	{2}	{3}	{4}
1	NT		0,981789	0,332003	0,397607
2	W	0,981789		0,321422	0,385574
3	HAc	0,332003	0,321422		0,895827
4	Chit	0,397607	0,385574	0,895827	

Table xii) a): Chitosan *TPS6* ANOVA

Effect	Univariate Tests of Significance for *TPS6* (Spreadsheet1) Sigma-restricted parameterization Effective hypothesis decomposition				
	SS	Degr. of	MS	F	p
Intercept	0,000000	1	0,000000	0,000000	1,000000
Trt 48 hrs	2,668577	3	0,889526	3,061359	0,069346
Error	3,486787	12	0,290566		

Table xii) b): Chitosan *TPS6* Fishers LSD post hoc test

Cell No.	LSD test; variable *TPS6* (Spreadsheet1) Probabilities for Post Hoc Tests Error: Between MS = ,29057, df = 12,000				
	Trt 48 hrs	{1}	{2}	{3}	{4}
1	No Treatment		0,448262	0,232152	0,123595
2	Water	0,448262		0,063716	0,400240
3	Acetic acid	0,232152	0,063716		0,012970
4	Chitosan	0,123595	0,400240	0,012970	

Table xiii): Chitosan *TPS11* ANOVA

Effect	Univariate Tests of Significance for *TPS11* (Spreadsheet1) Sigma-restricted parameterization Effective hypothesis decomposition				
	SS	Degr. of	MS	F	p
Intercept	0,00000	1	0,000000	0,000000	1,000000
Trt 48 hrs	2,88637	3	0,962124	0,681330	0,580236
Error	16,94552	12	1,412126		

Table xiv): Chitosan *CPPS2* ANOVA

Effect	Univariate Tests of Significance for *CPPS2* (Spreadsheet1) Sigma-restricted parameterization Effective hypothesis decomposition				
	SS	Degr. of	MS	F	p
Intercept	0,00000	1	0,000000	0,000000	1,000000
Trt 48 hrs	5,47712	3	1,825706	1,006616	0,423501
Error	21,76447	12	1,813706		

(a) *TPS11*

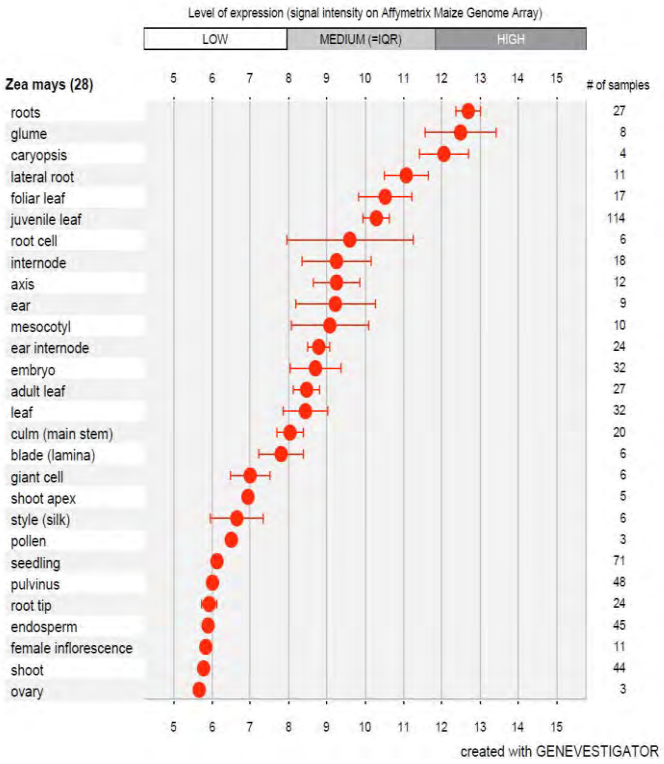

(b) *CPPS2*

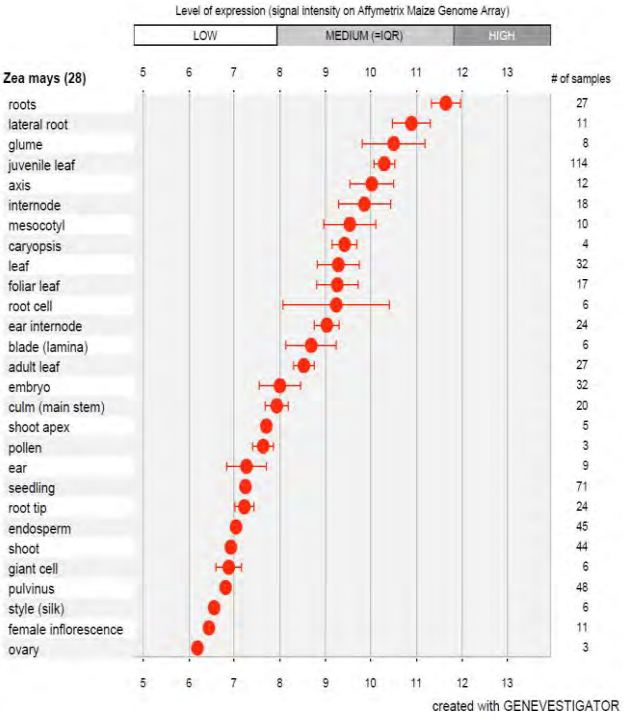

Figure i): Genevestigator Anatomy Scatterplot. The figure above shows pictographs of the anatomic location of the (a) *TPS11* and (b) *CPPS2* genes obtained using Genevestigator. Each maize part is listed at the left side of the image and the corresponding expression level of the gene is plotted ranging from low to high

Table xv) a): Diverse Lines Seedlings Zealexins ANOVA

Effect	Univariate Tests of Significance for ZB1 (Spreadsheet3) Sigma-restricted parameterization Effective hypothesis decomposition				
	SS	Degr. of	MS	F	p
Intercept	2,688330E+13	1	2,688330E+13	111,3876	0,000000
Diverse lines	1,851393E+12	5	3,702786E+11	1,5342	0,251321
Error	2,896190E+12	12	2,413492E+11		

Table xv) b): Diverse Lines Seedlings Zealexin Fishers LSD post hoc test

Cell No.	LSD test; variable ZB1 (Spreadsheet3) Probabilities for Post Hoc Tests Error: Between MS = 2413E8, df = 12,000						
	Diverse lines	{1}	{2}	{3}	{4}	{5}	{6}
1	Star		0,345254	0,224555	0,344447	0,714128	0,582699
2	GB	0,345254		0,770764	0,072778	0,554917	0,147781
3	KEP	0,224555	0,770764		0,042843	0,383057	0,089816
4	B73	0,344447	0,072778	0,042843		0,199048	0,682245
5	ZM4	0,714128	0,554917	0,383057	0,199048		0,365864
6	ZM5	0,582699	0,147781	0,089816	0,682245	0,365864	

Table xvi) a): Diverse Lines Seedlings Kauralexins ANOVA

Effect	Univariate Tests of Significance for Total KA3 and KB1 (Spreadsheet6) Sigma-restricted parameterization Effective hypothesis decomposition				
	SS	Degr. of	MS	F	p
Intercept	7,516455E+11	1	7,516455E+11	42,76919	0,000028
Diverse lines	2,571485E+11	5	5,142969E+10	2,92639	0,059188
Error	2,108935E+11	12	1,757446E+10		

Table xvi) b): Diverse Lines Seedlings Kauralexins Fishers LSD post hoc test

Cell No.	LSD test; variable Total KA3 and KB1 (Spreadsheet6) Probabilities for Post Hoc Tests Error: Between MS = 1758E7, df = 12,000						
	Diverse lines	{1}	{2}	{3}	{4}	{5}	{6}
1	Star		0,029794	0,230079	0,067152	0,477279	0,490993
2	GB	0,029794		0,253283	0,659423	0,007660	0,104907
3	KEP	0,230079	0,253283		0,468771	0,068891	0,589771
4	B73	0,067152	0,659423	0,468771		0,017726	0,217308
5	ZM4	0,477279	0,007660	0,068891	0,017726		0,174317
6	ZM5	0,490993	0,104907	0,589771	0,217308	0,174317	

Table xvii): Diverse Lines Seedlings *TPS11* ANOVA

Effect	Univariate Tests of Significance for DL Zlxns (28082015 DL Zealexins ANOVA.sta) Sigma-restricted parameterization Effective hypothesis decomposition				
	SS	Degr. of	MS	F	p
Intercept	2,688330E+13	1	2,688330E+13	111,3876	0,000000
Cultivar	1,851393E+12	5	3,702786E+11	1,5342	0,251321
Error	2,896190E+12	12	2,413492E+11		

Table xviii): Diverse Lines Seedlings *CPPS2* ANOVA

Effect	Univariate Tests of Significance for DL Krlxns (Spreadsheet4) Sigma-restricted parameterization Effective hypothesis decomposition				
	SS	Degr. of	MS	F	p
Intercept	1,039116E+12	1	1,039116E+12	56,83885	0,000007
Cultivar	1,205156E+11	5	2,410312E+10	1,31842	0,320243
Error	2,193816E+11	12	1,828180E+10		

Table xix: RNA Quality control

Sample	ng/µl	260/280	260/230	RIN*
T0.1	627.7	2.14	2.15	*
T0.2	615.2	2.13	2.21	*
T0.3	721.3	2.12	2.17	*
T1.1	724.6	2.12	2.07	*
T1.2	666.1	2.13	2.09	*
T1.3	853.5	2.15	2.21	*
T2.1	778.4	2.13	2.13	*
T2.2	963.7	2.15	2.21	*
T2.3	936.9	2.14	2.12	*
T3.1	731.4	2.12	2.05	*
T3.2	754.0	2.12	2.16	*
T3.3	974.9	2.13	2.13	*
NT 1	586.36	1.96	1.55	*
NT 2	616.57	2.11	2.26	6.7
NT 3	457.80	2.02	2.31	6.6
NT 4	458.80	2.04	2.26	6.8
W 1	755.33	2.03	1.79	*
W 2	293.7	2.13	2.13	*
W 3	612.88	2.09	2.34	6.6
W 4	549.92	2.07	2.29	6.7
HAc 1	450.62	2.01	2.26	6.6
HAc 2	202.95	2.96	1.17	*
HAc 3	366.75	2.03	2.23	6.6
HAc 4	526.97	2.08	2.19	6.7
Chit 1	313.62	2.03	1.91	3.6
Chit 2	292.80	2.01	2.14	6.7
Chit 3	204.38	2.02	2.17	6.1
Chit 4	444.59	1.93	1.41	*

Star 1	455.20	1.89	2.25	8
Star 2	4683.34	1,84	1.78	*
Star 3	3525.23	2,09	0.36	*
GB 1	231.30	1.97	2.54	7.6
GB 2	857.07	2.14	2.19	*
GB 3	1378.48	2.16	2.19	*
KEP 1	229.22	1.92	2.36	7.7
KEP 2	4792.08	1.63	1.54	*
KEP 3	3456.00	2.1	2.11	*
B73 1	241.03	2.01	2.16	7.8
B73 2	2283.34	2.15	2.22	*
B73 3	1210.42	2.15	2.15	*
ZM4 1	587.1	1.96	2.04	7.5
ZM4 2	4998.18	1.55	1.49	*
ZM4 3	4681.60	1,84	1.42	*
ZM5 1	217.66	1.99	2.42	8
ZM5 2	1527.16	2.17	1.77	*
ZM5 3	2039.47	2.16	2.12	*

*RNA integrity number on a scale from 1 to 10. Due to financial constraints not all samples went through a bio-analyser.

Table xx: Details of genes of interest and reference genes and their primers used in this study

Gene Name	Full name	Type	Source	Accession Number (s)	Amplicon Size	Primer Name	Sequence
TPS6	Terpene synthase 6	Target Gene	Huffaker et al 2011	GRMZM2G127087 T02 NM_001112204	294 bp	TPS6 F	CAAATGAGAGAAAAGGCTGCA
						TPS6 R	AGCCTCAACAAAATTCCCAAG
TPS11	Terpene synthase 11	Target Gene	Huffaker et al 2011	GRMZM2G127087 T03 NM_001112480	398 bp	TPS11 F	GAAATGCGACAAAGGGCTG
						TPS11 R	TCTTGAAGGCATCTCGTAGTA
CPPS2	Ent copalyl diphosphate synthase 2	Target Gene	Schmelz et al 2011	GRMZM2G044481 NM_001111787	236 bp	CPPS2 F	TGTTCTTGTGAAGGCAGTTC
						CPPS2 R	TCATTCGAGCTAAAAGCAGA
MEP	Membrane protein PB1A10.07c	Reference gene	Manoli et al 2011	GRMZM2G018103 T01	203 bp	MEP F MEP R	TGTACTCGGCAATGCTCTTG
							TTTGATGCTCCAGGCTTACC
UBCP	Ubiquitin carrier protein	Reference gene	Manoli et al 2011	GRMZM2G102471 T01	231 bp	UBCP F	CAGGTGGGGTATTCTTGGTG
						UBCP R	ATGTTCGGGTGGAAAACCTT
LUG	Leunig	Reference gene	Manoli et al 2011	GRMZM2G425377 T01	178 bp	LUG F LUG R	TCCAGTGCTACAGGGAAGGT
							GTTAGTTCTTGAGCCCACGC
Rpol1	RNA Polymerase 1	Reference gene	Shane Murray (pers comm)	GRMZM2G007681	301 bp	Rpol1 F	AGCCAAAACGCTAAAGTGGA
						Rpol1 R	TAAGTGACGAGCAAGGCAAA